Mechanistic Studies on Antibiotic Peptides: Lantibiotics and Lipopeptides

by

Alireza Bakhtiary

A thesis submitted in partial fulfillment of the requirements for the degree of

Doctor of Philosophy

Department of Chemistry

University of Alberta

Abstract

Antimicrobial peptides (AMPs) are small protein toxins produced by different bacterial strains to fight against closely related strains in their competitive environment. AMPs have been isolated and studied for their interesting properties, including treatment of pathogenic diseases. In this thesis, results of mechanistic studies on AMPs classified as lantibiotic and lipopeptide are discussed.

In chapter 2, mechanistic studies on lacticin 3147 will be discussed. Lacticin 3147 is a two peptide lantibiotic (LtnA1 and LtnA2) that displays nanomolar activity against many Gram-positive bacteria. Lacticin 3147 may exert its antimicrobial effect by several mechanisms. Isothermal titration calorimetry experiments showed that only LtnA1 binds to the peptidoglycan precursor lipid II, which could inhibit peptidoglycan biosynthesis. An experimentally supported model of the resulting complex suggests the key binding partners are the C-terminus of LtnA1 and pyrophosphate of lipid II. A combination of *in vivo* and *in vitro* assays indicated that LtnA1 and LtnA2 can induce rapid membrane lysis without the need for lipid II binding. However, the presence of lipid II substantially increases the activity of lacticin 3147. Furthermore, studies with synthetic LtnA2 analogues containing either desmethyl- or oxa-lanthionine rings confirm that the precise geometry of these rings is essential for this synergistic activity.

In chapter 3, mechanistic studies on tridecaptin A1 (TriA1) and the synthesis of its analogues will be discussed. Tridecaptin A1 belongs to the lipopeptide class of AMPs with selective activity against Gram-negative bacteria. Our studies showed that

TriA1 exerts its bactericidal effect by interacting with bacterial cell wall precursor lipid II to interrupt the proton motive force.

Preface

Chapter 2 has been published as: Bakhtiary, A.; Cochrane, S. A.; Mercier, P.; McKay, R. T.; Miskolzie, M.; Sit, C. S.; Vederas, J. C. *J. Am. Chem. Soc*. **2017**, 139, 17803–17810. In this work, I was responsible for performing lipid II synthesis, as collaboration with Dr. Stephen Cochrane, and all mechanistic assays. I also prepared the original manuscript, which was edited by Dr. Vederas and Dr. Cochrane. In this chapter, NMR experiments were performed in collaboration with Dr. Ryan McKay and Mark Miskolzie. CYANA simulations were performed in collaboration with Dr. Pascal Mercier.

Chapter 3 has been published as: Cochrane, S. A.; Findlay, B.; Bakhtiary, A.; Acedo, J. Z.; Rodriguez-Lopez, E. M.; Mercier, P.; Vederas, J. C. *Proc. Natl. Acad. Sci*. **2016**, 113, 11561–11566. In this work, I assisted with synthesis of lipid II and spot on lawn assays.

Acknowledgments

There are many people to remember, when I am thinking about the five years that passed in going through the different stages to complete my PhD degree requirements. I could not have achieved this without their direct and indirect participation. I would like to thank different staff in our chemistry department, including the cleaning and maintenance staff for the admirable sense of responsibility that they have for their job; NMR facilities, Dr. Ryan McKay, Dr. Pascal Mercier and Mark Miskolzie; Analytical Laboratory, Dr. Wayne Moffat and his colleagues; Biological Services, Gareth Lambkin; Mass Spec Laboratory, Jing Zheng, Bela Reiz, Dr. Angie Morales, and Dr. Randy Whittal, store and general office staff for their remarkable assistance during these years.

I have collaborated and been taught with members from the Vederas group, including Dr. Dave Dietrich, Dr. Chris Lohans, Dr. Brandon Findlay, Dr. Stephen Cochrane. Special thanks go to Dr. Anna Jordan for the invaluable help and support she provided during reading, editing and correcting my thesis. I am thankful to Cherry Ibarra Romero; such a talented and admirable person who supported me a lot emotionally and whom I have benefitted from in consulting with her. Also, I would like to thank Randy Sanichar for reviewing my thesis.

I am especially grateful to my supervisor Dr. John C. Vederas who helped me to develop valuable skills, like critical thinking, to work hard as an independent scientist and to be persistent at times of failures and disappointments. His inspiring passion for science has been a source of motivation and his consultations have helped me in unraveling convolutions in my projects.

I may not be able to fully emphasize how much I feel I owe to my parents and brother. Thanks to my father who was supportive not only during my education but in my life; a strong man who taught me how to be strong. God blesses him, and I hope his soul rests in peace. My kind mother, I never thanked you enough for being there at times of hardship, for being patient at my mood swings. I wish you a healthy and long life.

Last but not least, I would like to thank my undergraduate friends; Hamid Esfahani, Behnam Daneshfar, Ali tolue, Mehdi Lavasani, Mehdi Gholizade, Alireza Iranmanesh, Farzad Zandi, Saber Sadeghi, Mohsen Beige; I wish you the best in your lives.

Thanks to God, who gave me the asset of life and the opportunity to make an effort to explore to see how your wonderful creation works. You are the one who never left me alone, guided me throughout my life and forgave me for my mistakes.

Table of Contents

List of Tables

List of Figures

List of schemes

List of abbreviations

Abu	Aminobutyric acid
ACN	Acetonitrile
AMP	Antimicrobial peptide
ATP	Adenosine triphosphate
AviCys	S-(Aminovinyl)-cysteine
BaCWAN	Bacterial Cell Wall Biosynthesis Network
BCECF	2',7'-Bis(carboxyethyl)-5(6)-carboxyfluorescein
Boc	*tert*-Butyloxycarbonyl
CD	Circular dichroism
CDMT	2-Chloro-4,6-dimethoxy-1,3,5-triazine
CFU	Colony forming unit
CNS	Coagulase-negative *Staphylococci*
Ctr	Ctriporin peptide
CYANA	Combined assignment and dynamics algorithm for NMR applications
DAP	Diaminopimelic acid
DBU	1,8-Diazabicycloundec-7-ene
DdlA	D-Ala–D-Ala ligase
Dha	Dehydroalanine
Dhb	(*Z*)-2,3-didehydrobutyrine
DiBAC$_4$(3)	Bis-(1,3-dibutylbarbituric acid) trimethine oxonol
DIPEA	*N,N*-Diisopropylethylamine

DMAP	4-(Dimethylamino)pyridine
DMF	*N,N*-Dimethylformamide
2D NMR	Two-dimensional NMR spectroscopy
DMSO	Dimethylsulfoxide
DNA	Deoxyribonucleic acid
DPC	Dodecylphosphocholine
EDTA	Ethylenediaminetetraacetic acid
FDA	Food and Drug Administration
Fmoc	Fluorenylmethyloxycarbonyl
G-LII	Gram-negative lipid II
G+LII	Gram-positive lipid II
GlcNAc	*N*-Acetylglucosamine
HATU	1-[Bis(dimethylamino)methylene]-1*H*-1,2,3-triazolo[4,5-*b*]pyridinium 3-oxide hexafluorophosphate
HOAC	Acetic acid
HOBt	1-Hydroxybenzotriazole
HPLC	High performance liquid chromatography
IPA	2-Propanol
IR	Infrared
ITC	Isothermal titration calorimetry
Lan	Lanthionine
LPS	Lipopolysaccharide
LtnA1	Lacticin 3147 A1

LtnA2	Lacticin 3147 A2
LUV	Large unilamellar vesicle
MALDI-TOF	Matrix-assisted laser desorption/ionization
MD	Molecular dynamics
MDR	Multidrug resistant
MeLan	Methyllanthionine
MIC	Minimum inhibitory concentration
MraY	UDP-MurNAc-pentapeptide phosphotransferase
MRSA	Methicillin-resistant *S.aureus*
MS	Mass spectrometry
MurA	UDP-GlcNAc enolpyruvyl transferase
MurB	UDP-MurNAc dehydrogenase
MurC	UDP-MurNAc-L-Ala ligase
MurD	UDP-MurNAc-L-Ala-D-Glu ligase
MurE	UDP-MurNAc-L-Ala-D-Glu-*meso*-Dap ligase
MurF	UDP-MurNAc-tripeptide-D-alanyl-D-Ala ligase
MurG	UDP-GlcNAc-undecaprenyl-pyrophosphoryl-MurNAc-pentapeptide transferase
MurNAc	*N*-acetylmuramic acid
Mw	Molecular weight
NaOAC	Sodium acetate
NMM	*N*-Methylmorpholine
NMR	Nuclear magnetic resonance

NOE	Nuclear Overhauser effect
NOESY	Nuclear Overhauser effect spectroscopy
OBu	2-oxobutyryl
OD	Optical density
OM	Outer membrane
OPr	2-oxopropionyl
PBP	Penicillin-binding protein
PE	Phosphatidylethanolamine
PG	Peptidoglycan
PolyB	Polymyxin B
PuroA	Puroindoline A
PuroB	Puroindoline B
RMSD	Root mean square deviation
RNA	Ribonucleic acid
rRNA	Ribosomal RNA
SAR	Structural activity relationship study
SDS	Sodium dodecyl sulfate
sPLA2	Phospholipase A2
SPPS	Solid-phase peptide synthesis
TES	Triethylsilane
TFA	Trifluoroacetic acid
TIPS	Triisopropylsilane
TLC	Thin layer chromatography

TMS	Trimethylsilyl
TMSOTf	Trimethylsilyl trifluoromethanesulfonate
TOCSY	Total correlation spectroscopy
tRNA	Transfer RNA
Troc	2,2,2-Trichlorethoxycarbonyl
UDP	Uridine diphosphate
UP	Undecaprenyl phosphate
UPP	Undecaprenyl pyrophosphate
UV	Ultraviolet
VST	Valsartan
VRE	Vancomycin-resistant Enterococci
ΔpH	Proton gradient
Δψ	Electric potential

Chapter 1 Antibiotics: types, mechanism of action and resistance

1.1 Introduction

1.1.1 Bacterial infection and importance of antibiotics

Not all bacteria are a threat to human lives. The human body has a symbiotic relationship with the living microorganisms that are involved in important physiological processes, such as digestion or immune response.[1,2] As an example, enzymes produced by the bacterial species *Bacteroides thetaiotaomicron* living in the human intestinal tract help to digest complicated carbohydrates in the portion of our diet made by plants.[3]

However, there are pathogenic microorganisms that account only for 1% of the bacteria population that cause disease in the human body.[4] Antibiotics are the predominant way to treat these bacterial infections. Nowadays, a criterion for the quality of a health care system is an effective control of bacterial infections.[5,6] Different medical fields, including oncology and organ transplantation surgery, depend enormously on modern antibiotics. The large distribution and consumption of antibiotics has caused faster development of antibiotic resistance which has become harder to treat. More importantly, bacteria have developed mechanisms of defense to protect themselves against antimicrobial compounds produced by the human body.[5,7] Consequently, antibiotic resistance has become a serious threat for human health and well-being.[8] Differences in metabolism between human and bacterial cells account for the fact that bacterial survival can be inhibited by antibiotics that do not interfere with human cells. In order to be selective bactericidal or bacteriostatic agents, antibiotics must act on factors that are dissimilar between human and bacterial cells. Interestingly, most of the potent and selective antibiotics, such as

streptomycin and rifampicin, were initially isolated from microorganisms, such as fungi and bacteria.[9] The interaction of antibiotics with their targets and the resultant effects have been studied widely. However, the versatile genetic and biochemical pathways through which bacteria respond and cell death occurs subsequent to antibiotic drug usage is being actively studied by scientists.[10]

1.2 Different classes of antibiotics

The discovery of penicillin can be considered as an initiating point in antibiotic development that spanned 40 years, leading to the production of the main antibiotic classes we use today. However, this bright era ended in the 1970s, and since then only six new classes of antibiotics have received clinical approval.[11] For example, daptomycin, a cyclic lipopeptide antibiotic type, was discovered in the 1980s and approved initially in 2000.[12] Pleuromutilin and its derivates were used widely for about 30 years in veterinary medicine before they were approved in 2007.[17] Fidaxomicin, a macrocyclic antibiotic, was reported for the first time in the 1970s, but it was approved after about 40 years in 2011.[13–15] One approach to study antibiotics is to classify them based on their mechanism of action, for example, as inhibitors of cell wall biosynthesis, inhibitors of nucleic acid synthesis and protein-synthesis inhibitors (Table 1.1).[16]

Targeting Site	Therapeutic classification		Examples
Bacterial cell wall	Penicillins	Natural	Penicillin G
		Aminopenicillins	Ampicillin
		Antistaphylococcal	Nafcillin, oxacillin
		Antipseudomonal	Piperacillin, mezlocillin azlocillin, ticarcillin
	β-lactamase inhibitor & penicillin combinations	Clavulanic acid	+ticarcillin(Timentin)
		Sulbactam	+ampicillin(Unasyn)
		Tazobactam	+piperacillin(Zosyn)
	Cephalosporins	First-generation	Cefazolin
		Second-generation	Cefoxitin, cefotetan Cefuroxime
		Third-generation	Ceftriaxone Ceftazidime Cefotaxime
		Fourth-generation	Cefepime
	Monobactams		Aztreonam
	Carbapenems		Imipenem Meropenem
	Glycopeptides		Vancomycin Teicoplanin
Nucleic acids	Sulfonamide	Antifolates	Cotrimoxazole
	Miscellaneous		Metronidazole
	Quinolones	First-generation	Nalidixic acid
		Second-generation	Ciprofloxacin Ofloxacin Norfloxacin
		Third-generation	Sparfloxacin Levofloxacin
Protein synthesis	Aminoglycosides	First-generation	Streptomycin Kanamycin Neomycin
		Second-generation	Gentamicin Tobramycin Amikacin
	Macrolides	First-generation	Erythromycin
		Second-generation	Azithromycin Dirithromycin
	Lincosamide		Clindamycin

Table 1.1. Different classes of antibiotics based on their targets.

1.2.1 Inhibition of cell-wall biosynthesis

The cell wall plays critical roles for bacterial cells. It defines the general shape of the cell and resists high cytoplasmic osmotic pressure. Furthermore, the cell wall is the anchoring site for membrane components and extracellular protein, including adhesins.[17] Peptidoglycan (PG), which has multiple layers, is an important component of the bacterial cell wall. The PG layer is much thinner in Gram-negative organisms, but they have an extra protecting layer, an outer-membrane (OM). Lipopolysaccharide (LPS) makes up the other leaflet of the outer membrane, but the inner leaflet contains other lipids. Since peptidoglycan does not exist in eukaryotic cells, compounds which target PG biosynthesis are potential therapeutics. The monomeric precursor of peptidoglycan synthesis is called lipid II (Figure 1.1), which is also found to be a target for antibiotics and antimicrobial peptides (AMPs) such as lantibiotics.[18] PG is composed of a polymer of sugar and peptide moieties, with crosslinking bonds between the peptide segments. In Gram-negative bacteria, there is a second barrier that has to be overcome to make them susceptible to antibiotics. Another defense mechanism is the presence of efflux pumps that expel foreign compounds.[19–21]

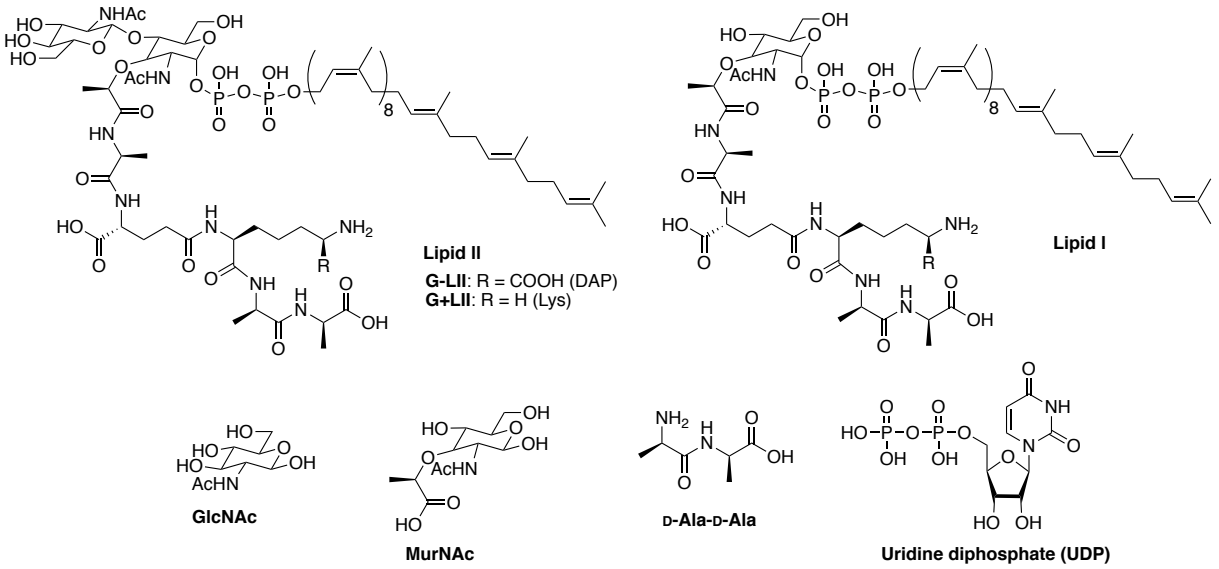

Figure 1.1. Structure of lipid II and some of its precursors in Gram-positive and Gram-negative bacterial strains.

During the peptidoglycan biosynthesis, lipid II is assembled in the cytoplasm.[22] The biosynthesis of lipid II starts with the conversion of uridine diphosphate (UDP) activated *N*-acetyl-D-glucosamine (GlcNAc) into UDP activated *N*-acetyl-D-muramic acid (MurNAc) through enzymatic activity of MurA and MurB (Figure 1.2, Figure 1.1). Coupling of an alanine to MurNAc results from the activity of MurC, which is followed by MurD activity to add D-glutamic acid.[23] Depending o the Gram-positive or Gram-negative bacterial strain, usually either lysine or *meso* diaminopimelic acid (DAP) can be installed on the side chain of glutamic acid by the intermediacy of MurE. To complete the pentapeptide moiety of lipid II, D-Ala-D-Ala dipeptide, which is already biosynthesized by DdlA, is ligated onto the tripeptidyl monosaccharide. The lipid I intermediate is formed by the activity of MraY, which anchors the pentapeptide monosaccharide to the internal face of the inner membrane through a pyrophosphate bond (Figure 1.1).

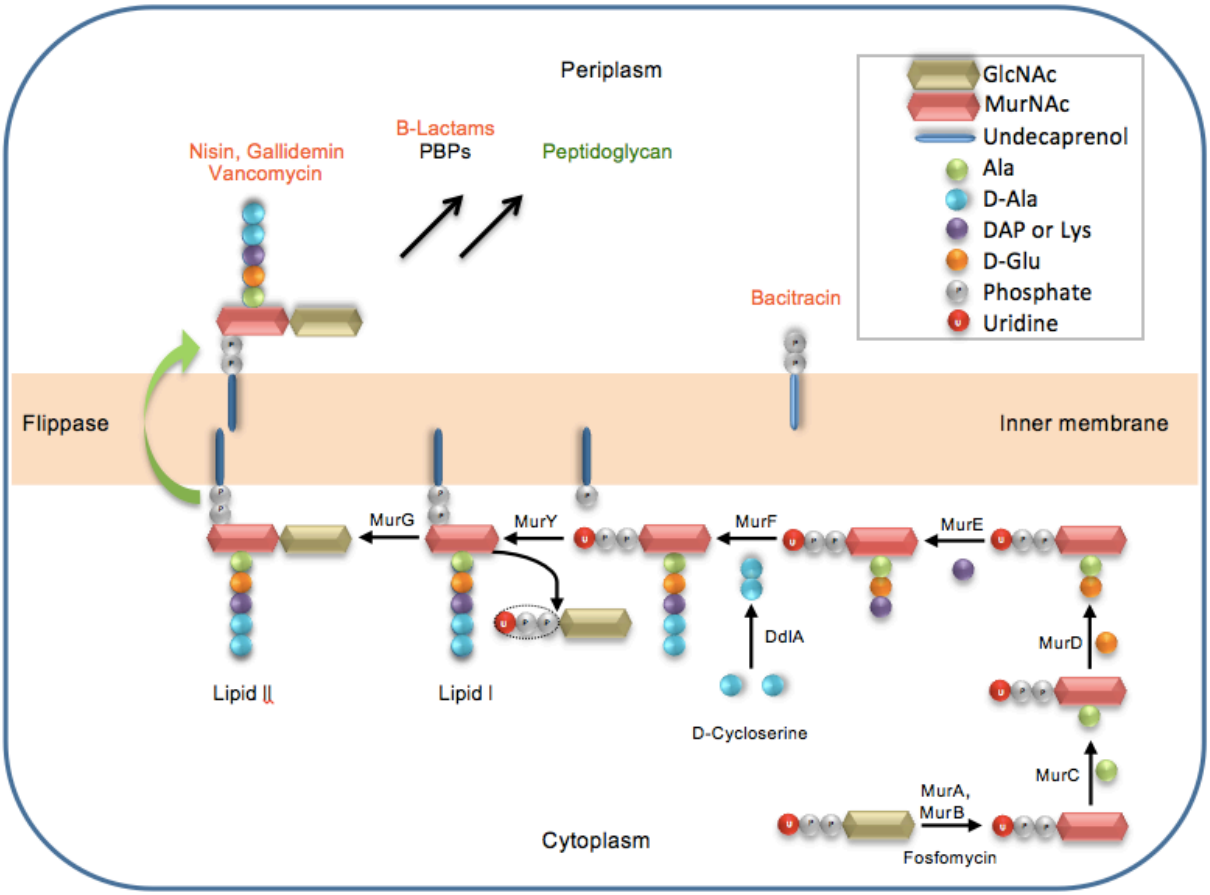

Figure 1.2. Overview of peptidoglycan biosynthesis. Figure is reproduced from the reference.[23]

The formation of lipid II results from the activity of MurG by incorporating the second sugar unit. Lipid II has to be transported by the enzymatic activity of a flippase to the exterior face of the inner- membrane, and can then be incorporated into the peptidoglycan network.[23] These steps are processed by the enzymatic activity of penicillin-binding proteins to produce peptidoglycan. Interruption of the peptidoglycan biosynthesis by an antibiotic results in bacterial cell death. Figure 1.2 and Figure 1.3 provide a summary for peptidoglycan biosynthesis, including essential enzymes and precursors and intermediates. In Figure 1.3, also a summary of different antibiotic targets during peptidoglycan biosynthesis is provided.

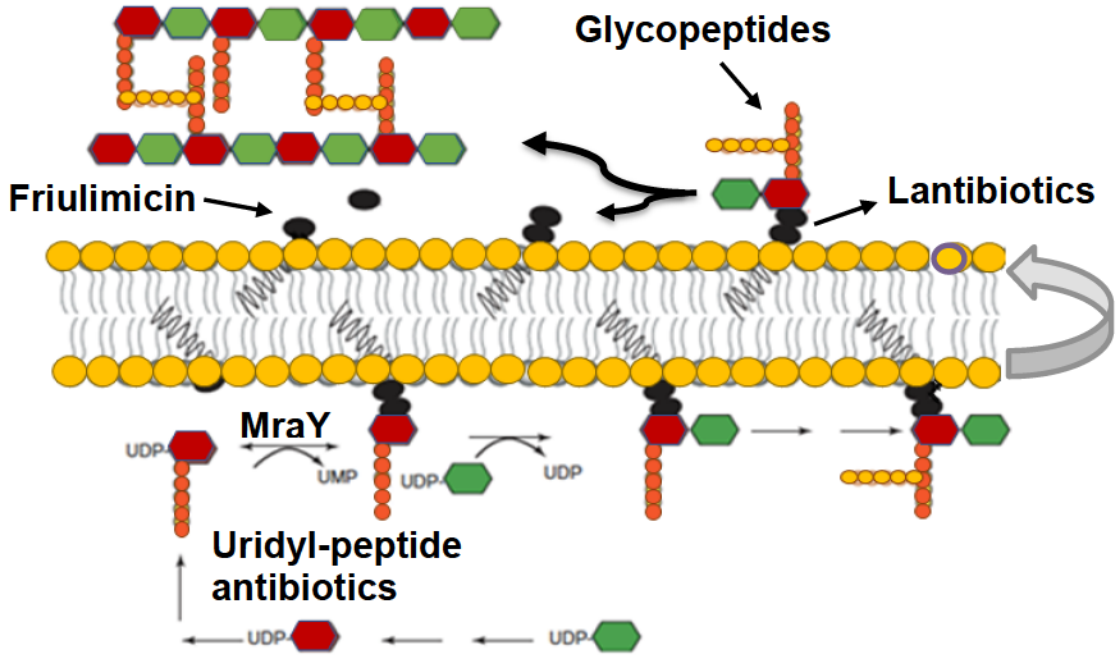

Figure 1.3. The target sites of antibiotics that inhibit peptidoglycan biosynthesis. Figure is reproduced from reference.[249]

1.2.1.1 β-Lactams

β-Lactams antibiotics were first discovered in 1928 in a Penicillium fungus.24 The characteristic structural feature of β-lactams is the presence of an azetidinone nucleus that is indispensable for activity of the compounds. Classification of β-lactams is based on the chemical substitutions on the central β-lactam core (Figure 1.4).25 The azetidinone can be derivatized with a fused saturated or unsaturated pentacycle or hexacycle that may contain heteroatoms like sulfur, oxygen placed in position one of the ring. For example, penams, carbapenams and oxopenams (1), which are from the penicillin family, include a saturated pentacyle (e.g. penicillin (5) and ampicillin (6)). Carbapenems and penems contain a pentacycle which is unsaturated (e.g. imipenem (7)). Cephalosphorins such as cephems, carbacephems, and oxacephems (3) have an unsaturated hexacycle (e.g. cefotaxime (9)). Lastly,

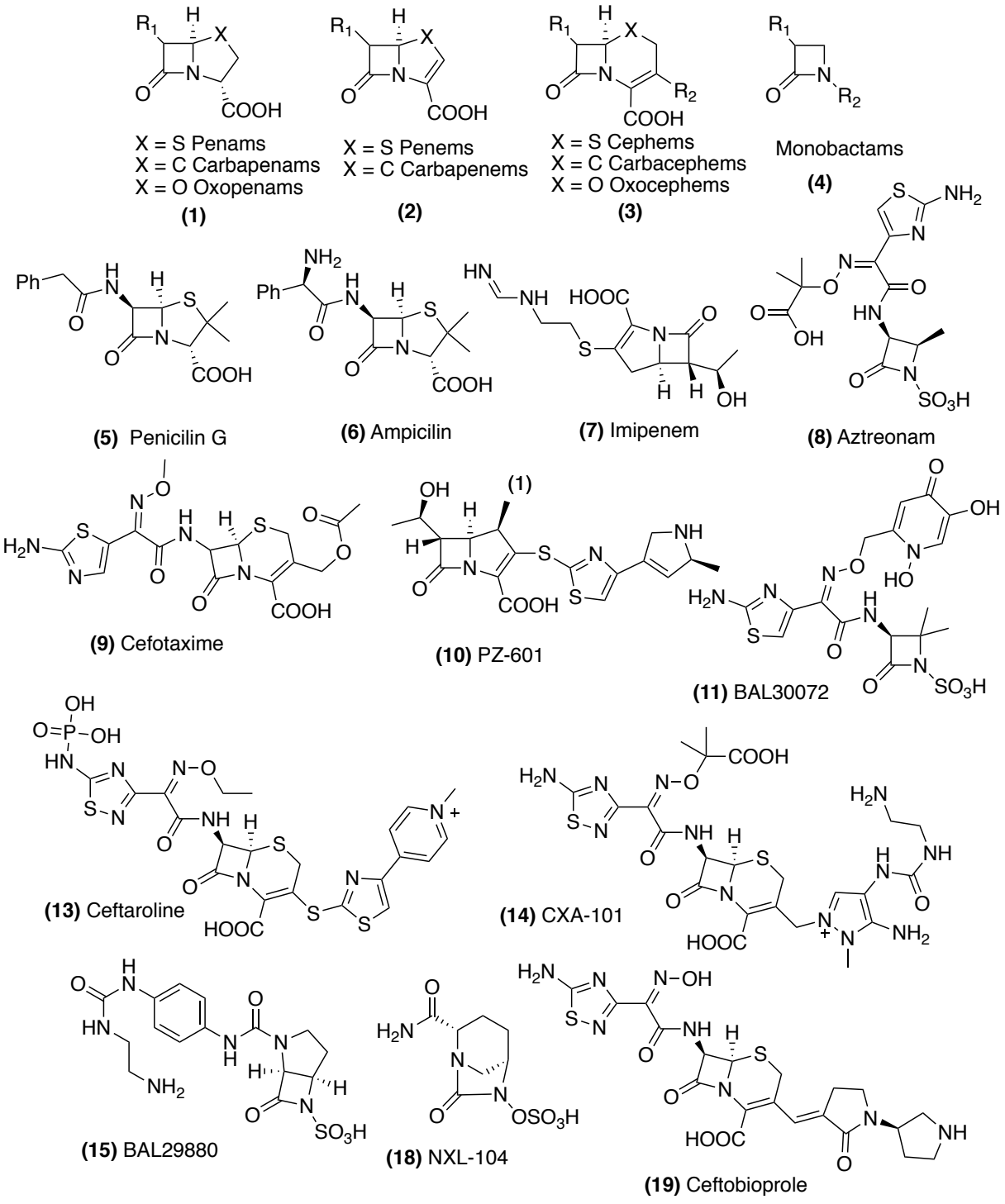

Figure 1.4. β-lactam antibiotics.

azetidinones, such as aztreonam (8), lacking a fused ring with another monobactams. β-Lactams act through targeting penicillin-binding proteins to inhibit cell-wall biosynthesis.[26] These antibiotics can bind in an irreversible manner to the active-site of penicillin-binding proteins. The β-lactam core interacts with DD-transpeptidases by binding to an active-site serine so as to prevent the crosslinking of peptidoglycan, resulting in cell death. The development of penicillins in the 1930s and1940s led to the discovery and production of numerous β-lactams with natural, synthetic and semisynthetic sources.[27–29] As a consequence of structural modifications, compounds such as cephalosporins CXA-101 (14), ceftaroline (9) and ceftobiprole (19) were developed that exert remarkable activity on Gram-positve and some Gram-negative strains including methicillin-resistant staphylococci.[19,30]

In order to retain potency, a β-lactam can be used in combination with a β-lactamase enzyme inhibitor. In this mixed drug formulation (Table 1.1), clavulanic acid was used as the first β-lactamase inhibitor, and was followed by sulbactam, tazobactam and BAL29880 (15). All these compounds possess a β-lactam chemical structure.[29] NXL104 (18), which is a non-β-lactam β-lactamase inhibitor with a novel bicyclic moiety, has been considered for clinical evaluation (Figure 1.4).[29,30]

1.3 Antibiotics with activity on the membrane

The membrane plays an indispensable role for bacterial cells. Probably its most important feature is to provide a selective barrier to maintain cell homeostasis and to regulate metabolism. It also prevents foreign compounds from interrupting biological phenomena inside the cells. A bacterial cell wall is composed of multiple

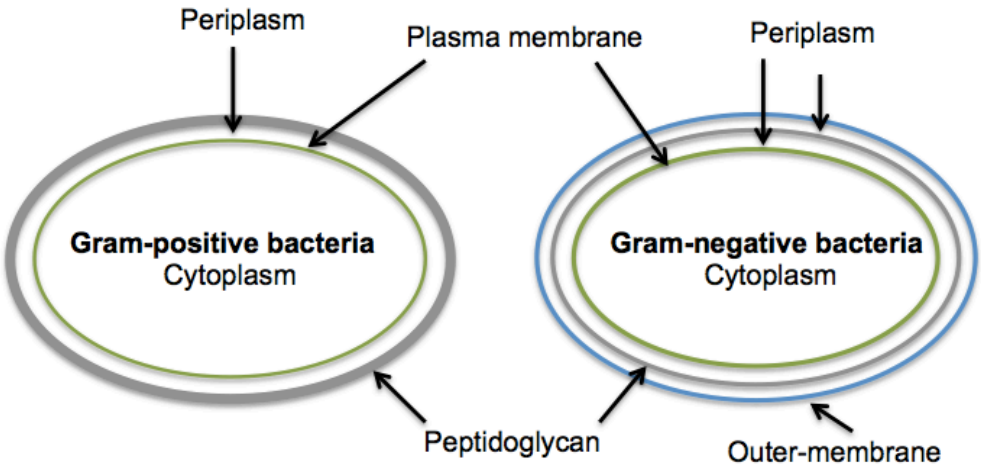

Figure 1.5. Gram-positive and Gram-negative bacterial membranes.

layers, which include one or more membranes, to protect these microorganisms from virulent environmental threats.[31]

Most of the bacterial strains can be classified into two main classes, Gram-negative and Gram-positive. This classification is based on the Gram stain procedure that evaluates the capacity of some bacteria to retain a crystal violet stain under mordanting and subsequent decolorizing conditions. The basis for the different responses to the dying conditions is related to the bacterial cell wall composition.[32] A Gram-negative cell wall contains a thin peptidoglycan; this layer also is surrounded by an outer-membrane, lipopolysaccharide.[17] In contrast to Gram-negative bacteria, Gram-positive bacteria do not contain LPS, but the peptidoglycan layer is much thicker (Figure 1.5). Passing through this peptidoglycan, there are anionic polymers called teichoic acids.[33] The membrane envelopes cytosol, which contains most of the cell's proteins that are responsible for essential physiological functions. These include the transfer of waste produced by biological processes and vital nutrients, production of ATP and regulation of proton motive force powered with the intermediacy of ions.[34]

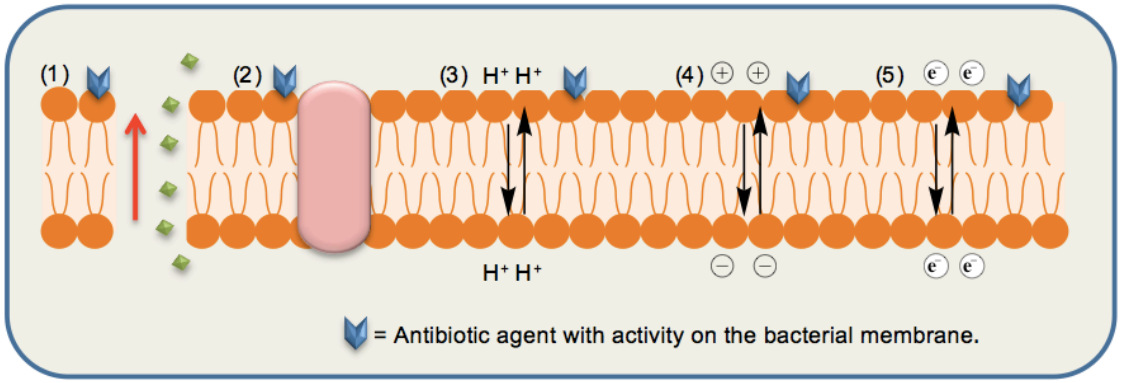

Figure 1.6. Bacterial membrane and examples of the mechanisms of antibiotics activities on it: (1) Lytic activity. (2) Inhibition of the trans-membrane protein. (3) Interruption of the membrane pH gradient. (4) Depolarization of the membrane. (5) Disruption of electron transfer chain.

Membrane-targeting antibiotics provide numerous advantages. For example, they can exert activity against slow growing bacteria since metabolic processes in these bacteria are too slow to be targeted by most antibiotics.[35] The main obstacle to developing an antibiotic with activity against a membrane is related to its selectivity. Agents that attack phospholipid bilayers are prone to be cytotoxic to human cells. The bacterial cytoplasmic membrane is different from the mammalian membrane as it is mostly composed of negatively charged phospholipids. In contrast, the membrane in mammalian cells contains cholesterol and zwitterionic phospholipids resulting in an overall neutral composition.[36] Different mechanisms are suggested for antibiotics exerting activity on the membrane (Figure 1.6).[37] Some agents can rupture this layer, causing leakage of vital components from the cytoplasm and leading to cell death. Moreover, some antibiotics can interact with the membrane components using them as an anchoring point to enhance their activity.[38] This class of antibiotics may cause depolarization of the membrane or perturbation of the pH gradient between its two sides. These modes of action can interrupt vital processes such as ATP generation,

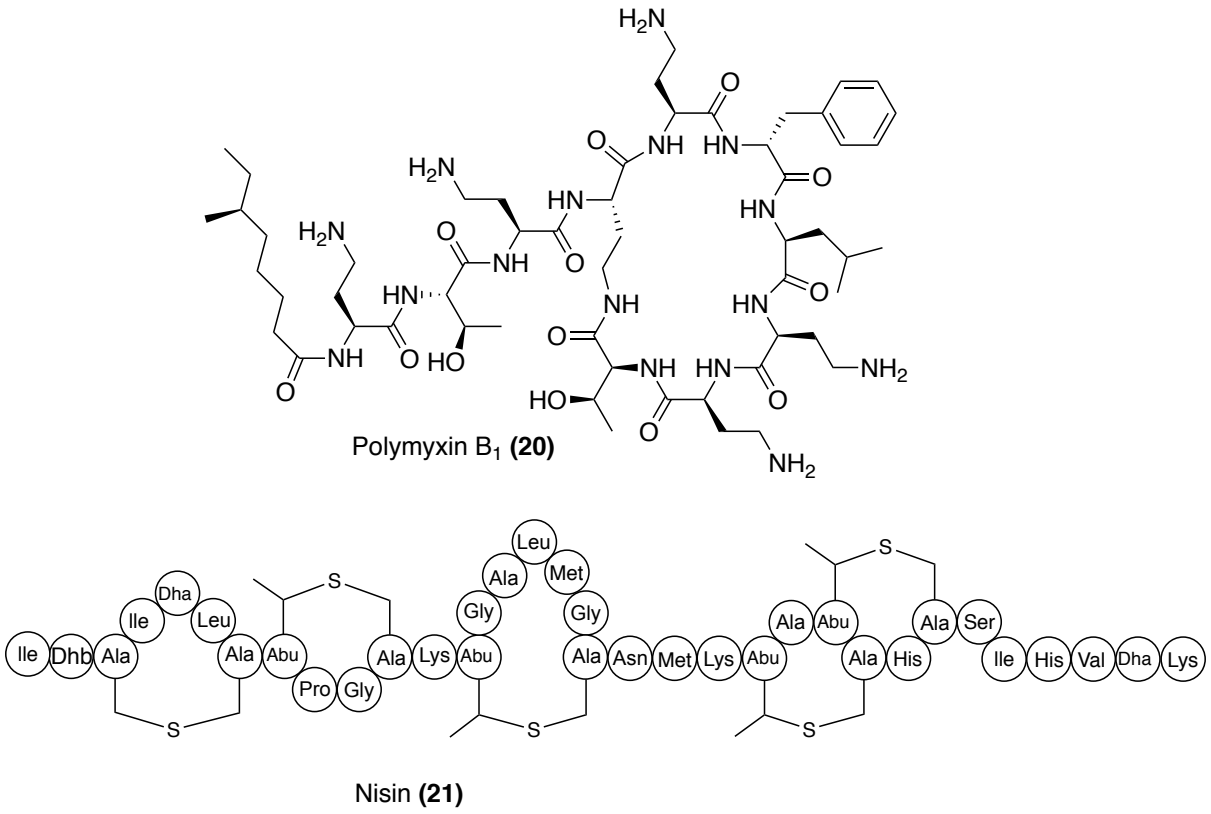

Figure 1.7. Examples of Antibiotics which target cell membrane.

thereby leading to cell to death within a short period of time.

Polymyxin is an old class of nonribosomal cyclic lipopeptide antibiotics originally discovered in 1947 (Figure 1.7).[39] Polymyxin B_1 (20) belongs to a cyclic class of lipopeptides and is produced by *Bacillus* and *Paenibacillus* species. As a membrane-acting peptide, it has potent lytic activity against Gram-negative bacteria. Mechanistically, polymyxins interact with LPS via binding to the phosphate moiety of lipid A, followed by insertion into the inner-membrane to lyse the cell.[40]

Nisin (21) was first discovered in the late 1920s and early 1930s when it was described as a toxic substance present in milk which had an adverse impact on performance of cheese starter cultures.[41] Nisin is an example of a class of antimicrobial peptides called lantibiotics, which are widely studied for their potent

activity against Gram-positive bacterial species. Detailed investigations showed that nisin first binds to lipid II and then can form pores in the membrane, which leads to the loss of essential solutes from the cell.[42] It was also shown that nisin binds to lipid III and IV and disrupts the biosynthesis of teichoic and lipoteichoic acids.[43] In addition, nisin can stimulate the autolysin *N*-acetylmuramoyl-L-alanine amidase in *Staphylococcus simulans.*[44] A consequence of autolysin activity is damage to the cell wall and cell death.

1.4 Mechanism of action of antimicrobial peptides (AMPs)

1.4.1 Membrane related AMPs' mechanism of action

AMPs can cause bacterial cell membrane damage through electrostatic interaction between their positively charged amino acid residues and negatively charged lipids on the cell surfaces. It has been suggested that differences in the physical and chemical properties of the lipids in the cell membrane in eukaryotic and prokaryotic cells define the surface specificity of the AMPs.[45] Negatively charged lipids such as phosphatidylglycerol (PG), cardiolipin and zwitterionic phosphatidylethanolamine (PE) are the main components of bacterial cells.[46] The outer-membrane in Gram-negative bacteria is composed of lipopolysaccharides, whereas the cell surface of the Gram-positive bacteria is formed of acidic polysaccharides (teichoic and teichuronic acids). AMPs, which have positively charged residues within their structures, readily interact with the negatively charged molecules on the surface of the bacterial cells.[47] Therefore, the lipid composition of

the cell membrane and the nature of amino acids within the structure of AMPs may play important roles in membrane and peptide interaction. The secondary structure of such peptides can influence their interaction with membrane.[48] Peptides may orient themselves perpendicularly in order to insert into the lipid bilayer and facilitate the formation of transmembrane pores. Some AMPs can travel across the membrane. AMPs may also induce membrane disturbances, such as pore formation, and disruption of the bilayer such as ‘’barrel stave’’ and “toroidal” model.

One of the primary models to explain membrane disruption is the ‘’barrel stave’’.[47] The AMP binds to the surface of the membrane in a monomeric state, and this triggers peptide oligomerization and pore formation. The size of the pores depends on the degree of peptide recruitment. This can lead to leakage of cytoplasmic contents and cell death. Such peptides may have a hydrophobic α-helix or β-sheet or both to enable pore formation.[49]

The “toroidal” model explains how some peptides insert themselves into the membrane to form a bundle structure. As a consequence, lipid monolayers bend inside the pore and the peptides become interspersed. Examples of AMPs with a toroidal pore formation capacity are magainins, protegrins and melittin.[50] Some AMPs can also cover the surface of the membrane to manipulate its architecture in a detergent like manner; this is called the ‘’carpet model’’.[51] One of the driving force between the interaction of the peptide and the membrane is electrical attraction. As a consequence, when the concentration of AMPs on the membrane surface exceeds a threshold level, the membrane starts to disintegrate and cell lysis happens. However, it is also observed that some peptides have the capacity to form transmembrane

pores at a lower concentration than the threshold. It can be concluded that membrane disruption or permeation capacities of AMPs can be modulated by their concentrations.[46]

By comparison, in barrel stave model bundles of amphipatic helices oligomerize and form transmembrane pores with hydrophilic residues facing toward the pore. The minimal inhibitory concentration required to dissipate the transmembrane potential should be below the μM concentration.[52] However, in toroidal pore model, antimicrobial peptide helices insert into the membrane and induce the lipid monolayers to bend continuously through the pore so that water core is lined by both the inserted peptides and the lipid head groups.[53]

In addition to the AMPs, which act directly on membrane lipids, some peptides need a receptor on the surface to exert their optimal activity. The fact that antimicrobial activities of all-L and all-D enantiomers of some peptides are distinct from each other strengthens this idea.[54,55]

Cell lysis resulting from membrane disruption has been reported as a mechanism of action by the majority of AMPs. However, there are other mechanisms which involve intracellular targets such as inhibition of the cell wall biosynthesis, DNA, RNA and protein synthesis. [47] Moreover, an AMP may have the capacity to act with a combination of mechanisms; in other words, it may have more than one cellular target.[56] The conditions under which AMPs' mechanism of action are studied, such as the media pH, presence of salts and temperature, may affect their observed mechanisms of action.[57]

1.4.2 Lantibiotics: AMPs with activity on the membrane

Bacteriocins are antimicrobial peptides produced by some bacteria. Most of the time they are small peptides which are produced ribosomally.[58] An important class of bacteriocins are the lantibiotics. Lantibiotics are ribosomally synthesized and contain interesting post-translational modifications that include thioether bridges. In addition, the presence of other modified amino acids within their structures is also common.[42] Certain lantibiotics inhibit peptidoglycan biosynthesis by targeting lipid II, and some are also capable of forming transmembrane pore.[59,60] The latter can lead to efflux of essential molecules (e.g. amino acids, ATP) and ions (e.g. K^+, PO_4^{-3}) from the cytoplasm.[61] Mersacidin (49) is a widely studied lantibiotic. It is effective against methicillin-resistant S.*aureus* (MRSA) in a murine infection model (Figure 1.8).[62] Mersacidin and nisin have different binding regions on lipid II. Nisin binds to the phosphate segment of lipid II, whereas mersacidine probably interacts with the sugar segment.[63,64] Both peptides inhibit peptidoglycan biosynthesis.[65]

A sub-class of lantibiotics includes two-peptide family that show their optimal antimicrobial activity in a synergistic manner, even though these peptides are transcribed independently.[66,67] Lacticin 3147, staphylococcin C55, plantaricin W and haloduracin are examples of the two-peptide lantibiotic family.[66,68–70] It is important to emphasize that lantibiotics can act via the lipid II mediated mechanism of action; however, other bacteriocins can also target lipid II. For example, lcn972 is a class II bacteriocin suggested to exert a mechanism of action by interacting with lipid II.[71]

Non-ribosomally synthesized peptides, such as vancomycin (23), daptomycin (24), have also suggested to act by cell-wall inhibition mechanism through targeting

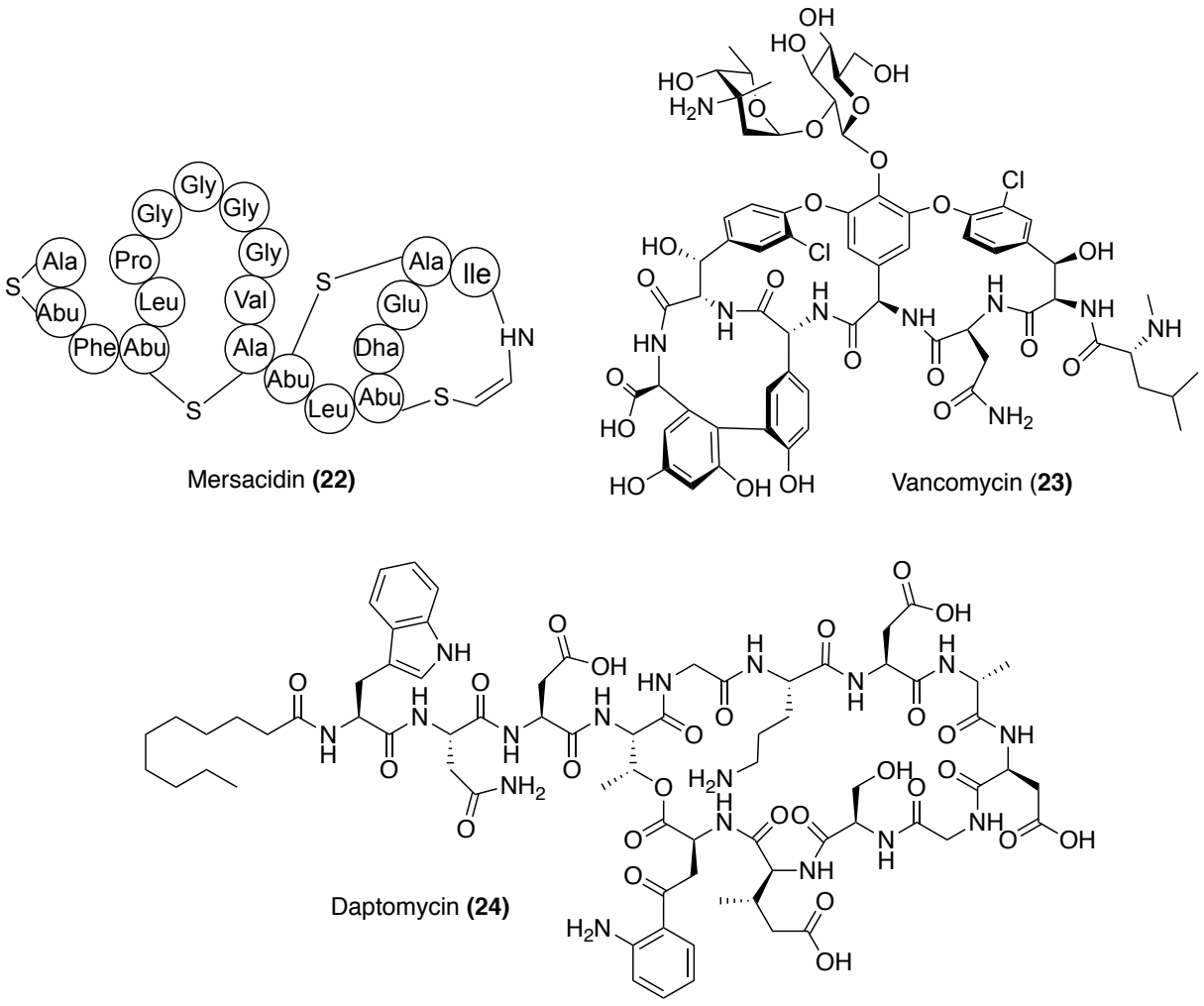

Figure 1.8. Examples of antimicrobial peptides that inhibit cell wall biosynthesis.

targeting lipid II biosynthesis pathway (Figure 1.8).[42]

Antibiotics targeting the bacterial cell wall are valuable agents because this barrier provides cell integrity and mammalian cells do not have a similar structure. A combination of cell wall biosynthesis inhibition and cell membrane disruption shown by some AMPs provide a potential to hinder the emergence of resistant bacterial strains. For example, no persistence resistance develops against tridecaptin A1 in *Escherichia coli* cells exposed to subinhibitory concentrations of this peptide during one month period.[72]

1.4.3 Glycopeptides

Dalbaheptides are sugar-containing linear peptides with seven amino acids cross-linked to form a rigid structure, with a specific stereochemical configuration to exert a particular antibiotic activity by complexation with the D-alanyl-D-alanine terminus of the bacterial cell-wall component. The term dalbaheptides is underlining their mechanism of action; D-al(anyl-D-alanine)b(inding)a(ntibiotics) having hept(apept)ide structure.[73,74]

Vancomycin, which was discovered in 1954, was the first dalbaheptide to be used clinically.[75] Interestingly, vancomycin was introduced into clinical application 25 years before its structure was elucidated (Figure 1.8).[76] The bacterial strain from which vancomycin was isolated was *Streptomyces orientalis* (now known as *Amycolatopsis orientalis*).[27] Teicoplanin (52), another glycopeptide, was introduced in 1988 (Figure 1.9).[77] Since glycopeptide antibiotics do not have the capacity to pass through the outer-membrane of Gram-negative bacteria, they only show efficacy against Gram-positive infections.[77] In fact, vancomycin and teicoplanin were chosen for clinical application owing to their high activity against Gram-positive pathogens, such as many coagulase-negative *Staphylococci* (CNS), corynebacteria, *Clostridium difficile*, multiresistant staphylococcus *aureus* and highly gentamicin-resistant enterococci.[74]

A second generation of glycopeptides with improved activity was developed later due to the resistance observed for vancomycin that resulted from its wide usage at the time. Total synthesis of these complex structures provided an alternative way

to access these compounds.[78] Some of the reported structural modifications of the native glycopeptides structure include the selective removal of sugar moieties, glycosylation, deacylation, deamination, dechlorination, introduction of halogen atoms, esterification or amidation of the terminal carboxyl and acylation or alkylation of the terminal (or sugar) amino groups.[78–82] Structural-activity relationship studies (SAR) showed that an important feature is the type of sugars within the structure, since aglycones showed a weak activity against selected Gram-negative bacterial strains.[83–85] Some modifications on the native structure resulted in novel dalbaheptides with activity against resistant species.[86,87]

For example, some structural features that promote dimerization lead to a tighter binding interaction with the biological target. [88,89] Furthermore, more lipophilic the side chains of the dalbaheptides often give more anchoring capability. Teicoplanin-related glycopeptide A40926, which is derivatized to dalbavancin (28), oritavancin (26), which is derived from vancomycin-related glycopeptide, chloroeremomycin, and telavancin (27) obtained approval by the Food and Drug Administration (FDA) in the United States in 2009.[88,89] For example, telavancin was approved to be used to treat pneumonia as well as SSTIs caused by Gram-positive organisms.[90]

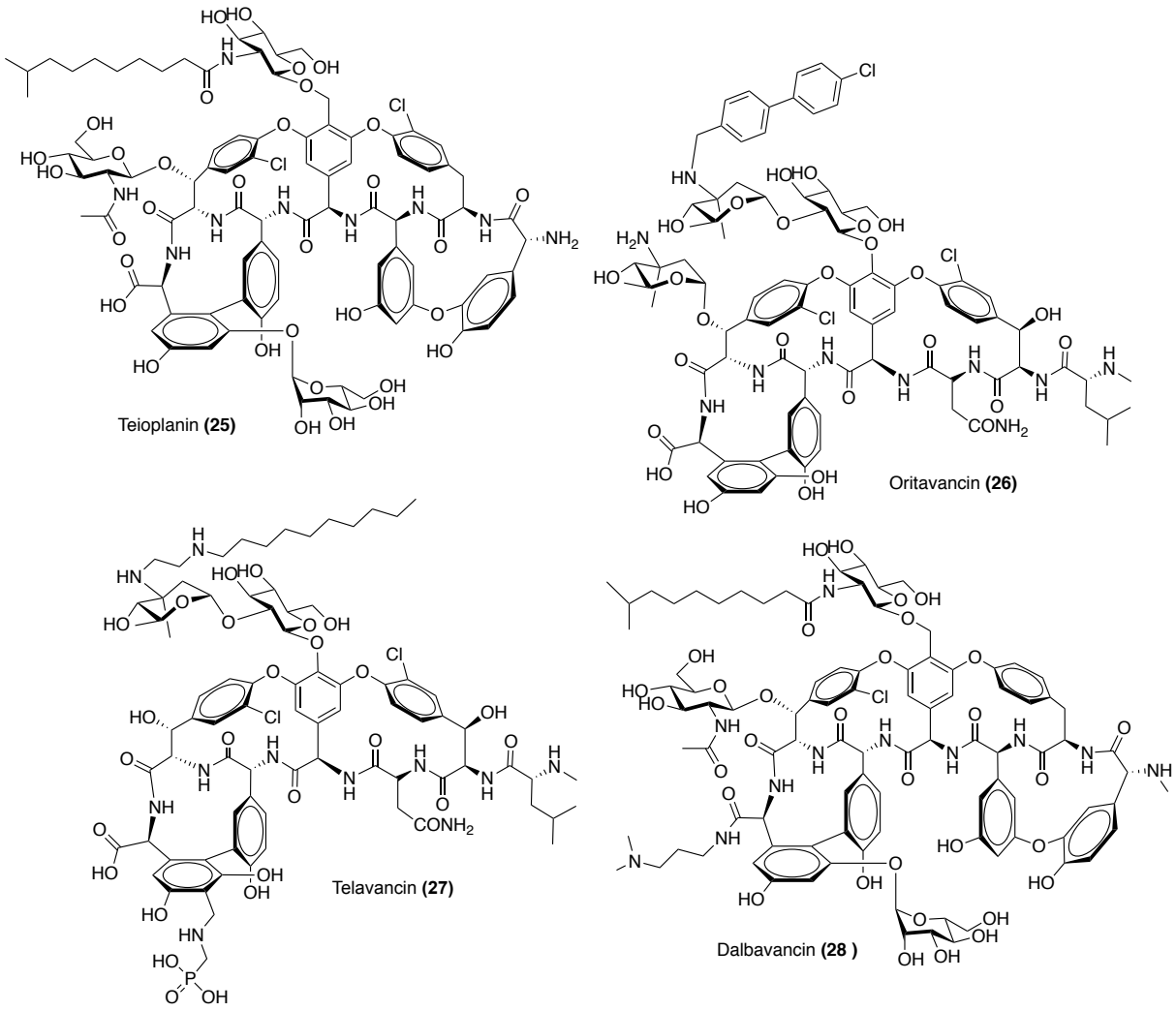

Figure 1.9. Examples of glycopeptide family.

1.4.4 AMPs and inhibition of nucleic acid synthesis

Some AMPs can traverse outer and inner membrane of bacterial cells to target intracellular molecules, such as nucleic acids and proteins. Some linear and cationic peptides, like buforin II with 21 amino acids, have the capacity to cross the cell membrane and enter the cytoplasm without permeabilization. Buforin II binds to DNA and RNA of *Echerichia coli* and causes inhibition of macromolecule synthesis inside

the cell. [91]

Indolicidin is a small antimicrobial peptide with a unique amino acid composition, containing 39% tryptophan and 23% proline and a total of 13 amino acids. It has cationic charge and can depolarize membrane and inhibit DNA synthesis. As a result, it causes induction of filamentation of *E. coli* cells.[92] Structure-function studies on indolicidin resulted in a peptide called CP10A, which is a derivative with three proline residues replaced by alanine.[93] This peptide inhibits nucleic acid and protein synthesis in Gram-positive bacteria.[94]

Puroindoline (PIN) is a peptide similar to indolicidin, and there is large number of tryptophan residues within its structure (positions 39-45). Puroindoline A (PuroA) has been shown to exert a strong antimicrobial effect against Gram-positive and Gram-negative bacteria, which is mediated by membrane disruption. Puroindoline B (PuroB) does not show as strong antimicrobial activity as puroindoline A, despite sequence similarity between them. Different PuroB analogues were synthesized that have higher potency compared to the natural parent. Interestingly, PuroB peptides cannot destabilize the integrity of lipid bilayers. The primary mode of action was found to involve binding to DNA.[95] Using radioactive precursors for DNA and RNA, it was observed that puroindoline peptides are generally capable of inhibiting transcription and translation, and it was suggested that positively charged residues of these peptides interact with phosphate groups of the nucleic acids.[91]

Human neutrophils have evolved to produce AMPs such as defensins. Human HPN-1 not only can permeabilize cell membranes but also can inhibit nucleic acid and protein synthesis in *E. coli.* It was also suggested that this AMP can inhibit the

cell wall biosynthesis through binding to lipid II.[96] These studies further support the idea that some AMPs have evolved in a way that can cause bacterial death through multiple mechanisms of action.

Microcidin B17 is a bacterial peptide that can target DNA gyrase, the enzyme that relieves strain on the double-stranded DNA while it is unwound for DNA replication.[97] Hence, it is an inhibitor of DNA replication. Mutation in DNA gyrase can lead to bacterial resistance.[98] Many microcins interact with bacterial components to take advantage of active transport into the cell. After release from their transporter, they can exert their mechanism of action. For example, microcidin B17 and microcidin J25 enter into the bacterial cell with aid of the inner-membrane protein sbmA. Inside the cell, RNA polymerase is the target, and bacterial transcription is inhibited.[99]

1.5 Antibiotic resistance and its mechanisms

Bacterial infections have claimed a significant number of lives throughout history. The problem was alleviated to some degree after the discovery of penicillin and other types of antibiotics that could effectively work against the infectious diseases. However, soon after the clinical application of antibacterial drugs started, a new issue in this regard emerged: antibacterial resistance.[100,101]

When antibiotics MICs (minimal inhibitory concentration) for certain microorganisms are above a predefined threshold, these microorganisms are classified as resistant. Antimicrobial resistance places a financial burden on the health care system of a society not only because of treatment failure but also because of the possibility of its spread to become an infection-control problem

later.[102] An antibiotic causes selective pressure, such that adapted organisms evolve and spread the resistance among other strains.

Bacterial cells have a short generation time. Although DNA replication in bacteria is a process with high accuracy, it is still a source of random mutation. In the laboratory, replication and mutation may take only minutes. As a result, the number of mutations can increase exponentially as the population of the cells increases.[103] Genes responsible for resistance can be integrated into the genome when the bacteria are exposed to natural compounds with antibiotic properties. Enzymes involved in resistance mechanisms may exert their activity through a range of chemical reactions, such as hydrolysis, group transfer and redox mechanisms (Table 1.2). It is suggested that antibiotic resistance will turn into a major health issue claiming 10 million lives per year and may cost up to $100 trillion. Therefore, we need novel antibiotics in order to overcome this threat.[104]

1.5.1 Antibiotic resistance caused by enzymes

Some enzymes evolve to attack the chemical structure of antibiotics in order to make them inactive. One of the earliest reports on antibiotic resistance was about the β-lactmase penicillinase by pathogenic *E.coli*.[101] For example, the β-lactam ring of penicillins and cephalosporins can be opened as a result of the enzymatic activity of amidases. Another example is macrolide resistance caused by esterases or fosfomycin resistance resulting from ring-opening epoxidases in the presence of water (Figure 1.11). These enzymes are produced and released by the bacterial cell and can intercept antibiotics.

Mechanism	Type	Example of enzyme	Target antibiotic
Hydrolysis		BlaZ	β-Lactams
		EreA, EreB	Macrolides
		FosA, FosX	Epoxides
Group transfer	Phosphoryl	APH (3′)	Aminoglycoside
		MPH	Macrolide
	Acyl	CAT	Chloramphenicol
		AAC(6′)	Aminoglycoside
	Nucleotidyl	ANT(2′)	Aminoglycoside
		LinA, LinB	Lincosamide
	ADP-ribosyl	ARR	Rifamycin
	Glycosyl	Mtg	Macrolide
		Not characterized	Rifamycin
Redox	Oxidation	TetX	Tetracycline
		Iri	Rifamycin

Table 1.2. Enzymatic modifications leading to antibiotics resistance.

These β-lactamases can be classified into two main groups: 1) Ser-β-lactmases that have a serine as a nucleophile in their active site, such as BlaZ, and 2) metallolactamases, which have a Zn^{+2} ion bound to water to mediate their enzymatic activity (Figure 1.10).

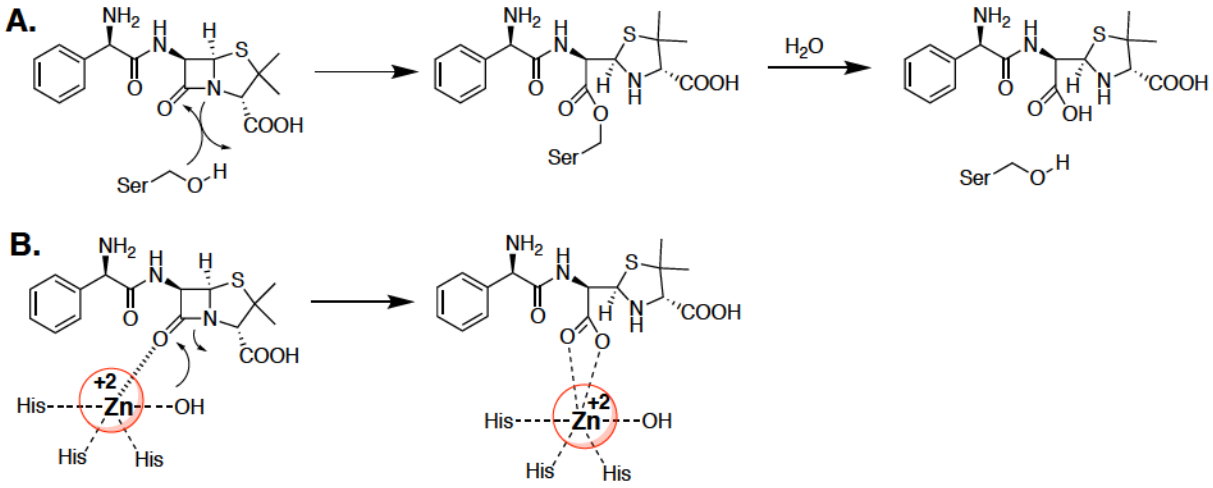

Figure 1.10. Basic enzymatic mechanism for (A) Ser-β-lactamases (B) metallo-β-lactamases.

In the biosynthesis of peptidoglycan (Figure 1.2), transpeptidase is the enzyme responsible for crosslinking the peptide moiety of lipid II. The β-lactams target trans-peptidases such as penicillin binding proteins (PBPs) to prevent the crosslinking of lipid II on its peptide moiety, which is important for the cell-wall integrity. There are similarities between peptidoglycan transpeptidases and Ser-β-lactmases both mechanistically and structurally. It is likely that these two enzymes have a similar evolutionary history. Metallo-β-lactamases are classified as Zn-dependent hydrolases and considered the major cause for resistance to carbapenems in Gram-negative bacteria (Figure 1.10).[105–107]

One strategy by which macrolides interfere with bacterial protein synthesis is by obstructing the peptide exit tunnel at the large subunit of the ribosome. A thioesterase catalyzes the ring-closing step to form 6-deoxyerythronolide B (for the 15-membered ring of erythromycin).[108,109] Macrolide-resistance enzymes act through reverse ring opening by attacking this key bond. High levels of resistance in *E. coli*

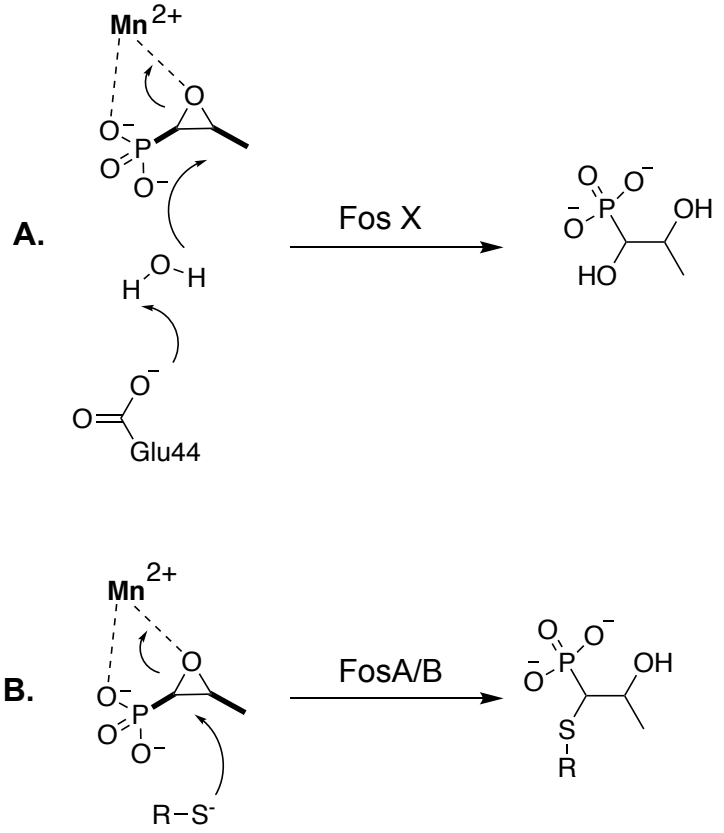

Figure 1.11. Mechanism of chemical ring opening catalyzed by fosfomycin resistance enzymes (A) Fos X and (B) FosA (R = Glutathione) and FosB (R = Cys).

strains result from two erythromycin esterases that are encoded by ereA and ereB genes.[110,111] These proteins have about 43 % similarity and were isolated from two different strains of *E. coli.* These genes, which are on mobile genetic elements,[112] have the capacity to spread in a microbial community as was detected by the presence of esterases in environmental isolates of *Pseudomonas sp*.[113]

Fosfomycin is classified as an epoxide antibiotic that covalently binds MurA, which is a major enzyme for the synthesis of the *N*-acetylmuramic acid moiety of lipid II.[114] Resistance to this antibiotic takes place by enzymatic ring opening of its reactive

epoxide moiety. FosA, which is a metalloenzyme found in Gram-negative bacteria, and enzyme FosX catalyze the epoxide ring opening via glutathione and water- aided reactions, respectively. In the catalytic site of these enzymes there is an important divalent metal cation: Mn^{+2} (Figure 1.11).[106]

Lantibiotics belong to a class of antimicrobial peptides produced by Gram-positive bacteria. Many lantibiotics exert their antibiotic activity by the inhibition of bacterial cell-wall biosynthesis (Figure 1.3).[115] As an example, nisin is a lantibiotic with 34 residues produced by certain *Lactococcus lactis* strains. In nisin producers, a mechanism has evolved to protect the producer against the toxic effect of nisin. This system contains the lipoprotein NisI and the ABC transporter system NisEFG. In strains of *L. lactis* that do not produce nisin, there is a gene (nsr) that can encode a 35 KDa protein (NSR). The latter induces nisin resistance by digesting the antimicrobial peptide.[116]

1.6 Objectives of the projects explained in chapters 2 and 3

In chapter two, mechanistic studies to unravel the mechanism of action of lacticin 3147 peptides are described. The ultimate goal of this project was to obtain a three-dimensional structure of lacticin 3147 peptides bound to a synthetic analogue of lipid II. In chapter three, a collaborative project to study the mechanism of action of tridecaptin A1 peptide and the synthesis of its analogues are presented. The results from both chapters are published.[72,117]

Chapter 2 Mechanistic studies on the lantibiotic lacticin 3147

2.1 Introduction

2.1.1 Lantibiotics: peptides with antibiotic activity

Lantibiotics are a class of peptides of 19-38 amino acids with antimicrobial activity that are ribosomally synthesized. They are produced by a variety of bacterial species, including *Firmicutes* and *Actinobacteria*. A prominent structural feature of this class of AMPs is their post-translational modification by the presence of thioether bridges that provide the structure of lantibiotics with some rigidity. For the formation of these thioether bonds, residues serine and threonine are dehydrated enzymatically to yield 2,3-didehydroalanine (Dha) and (*Z*)-2,3-didehydrobutyrine (Dhb), respectively. Consequently, if nearby there are cysteine residues within the structure, they may undergo a 1,4-Michael addition onto Dha and Dhb to form a lanthionine (Lan) or methyllanthionine (MeLan) bridge, respectively (Figure 2.1). The term *lantibiotic* refers to Lan-containing antibiotics. As further structural modifications, it is possible that C-terminal Cys residues may form S-aminovinyl-cysteine (AviCys) or an *N*-terminal may have 2-oxopropionyl (OPr) and 2-oxobutyryl (OBu) groups.[115]

It has been reported that the formation of Dha and Dhb frequently occur in the *N*-terminal part of the peptide structure. Another example of such post-translational modification is the formation of D-Ala from L-Ser after it is converted to Dha.[118] Within the lantibiotic structures, there may be non-proteinogenic amino acids, and the extent of the post-translational modification may be different between them. For example, one of the peptides with the least modification is lactocin S (24%). However, compound 107891 contains a large level of modification (58%).[119] The presence of these modifications provides this class of peptides with considerable structural

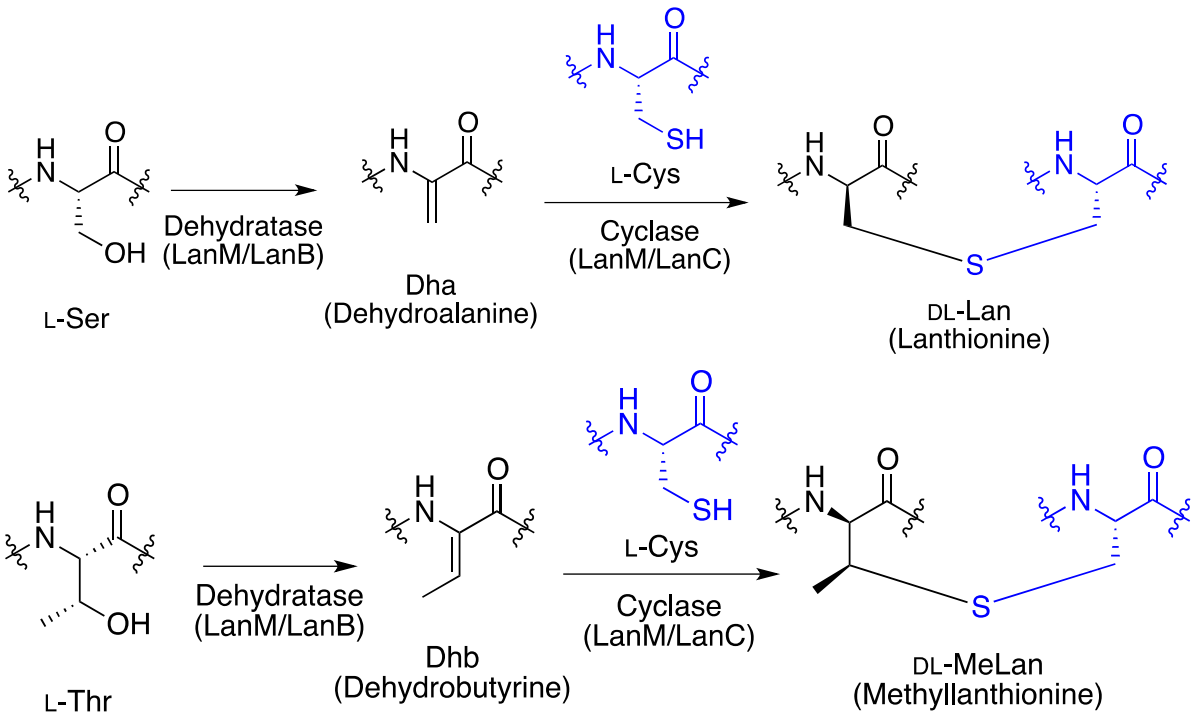

Figure 2.1. Thioether bridge formation, the most common lantibiotics post-translational modification.

diversity. These peptides posses leader peptides during biosynthesis, which is important for the secretion of lantibiotics and to complete their maturation by post translational modification.[120,121] Furthermore, the leader peptide may hinder lantibiotic activity prior to its export out of the cell.[122] Most lantibiotics are active against Gram-positive bacteria. The prototype compound in this family of AMPs is nisin (Figure 2.2), which was discovered in the 1920s and has been used industrially for food preservation purposes for more than 50 years.[123] It is produced by *Lactococcus lactis* and is among the extensively studied members of the lantibiotic class of AMPs. There is growing interest and potential for lantibiotics to be applied in human and animal health.[124,125]

Lantibiotics can be classified by their biogenesis: class I where the formation of

Lan requires two separate enzymes, a dehydratase and a cyclase; and class II where there is only a single enzyme capable of performing both transformations.[126]

Mechanistically, lantibiotics from either class may exert their antimicrobial activity through binding to lipid II and sequestering it from incorporation into the cell wall.[38] Moreover, lantibiotics may target different segments of lipid II compared to other classes of AMPs, such as glycopeptides (e.g. vancomycin).[74] Some lantibiotics show activity against multidrug-resistant (MDR) Gram-positive pathogens, and their potential is promising as drugs. An example that was considered as a developmental candidate is compound NVB-302 (aminoheptylamido-deoxyactagardine B) (30). It is a semisynthetic derivative of deoxyactagardine B which was isolated from *Actinoplanes liguriare* (Figure 2.2).[127, 128] In such an approach, specific software has been designed that allows effective screening among lantibiotics with cell-wall inhibiting capacity.[129]

Another example of a lantibiotic with strong potency is NAI107 (32). Interestingly, some novel modifications within the structure of this compound were identified that included chlorinated tryptophan and mono or dihydroxylated proline. This compound was considered as a developmental candidate to treat nosocomial infections caused by Gram-positive pathogens.[130] Similar application of the screening program resulted in the identification of lantibiotics belonging to class I, with compound 97518 (31) as an example. This compound has structural features similar to that of NAI-107, however, it contains two carboxylic acid functionalities.[131] Derivatization of the acidic residues provided analogues with enhanced activities.[132]

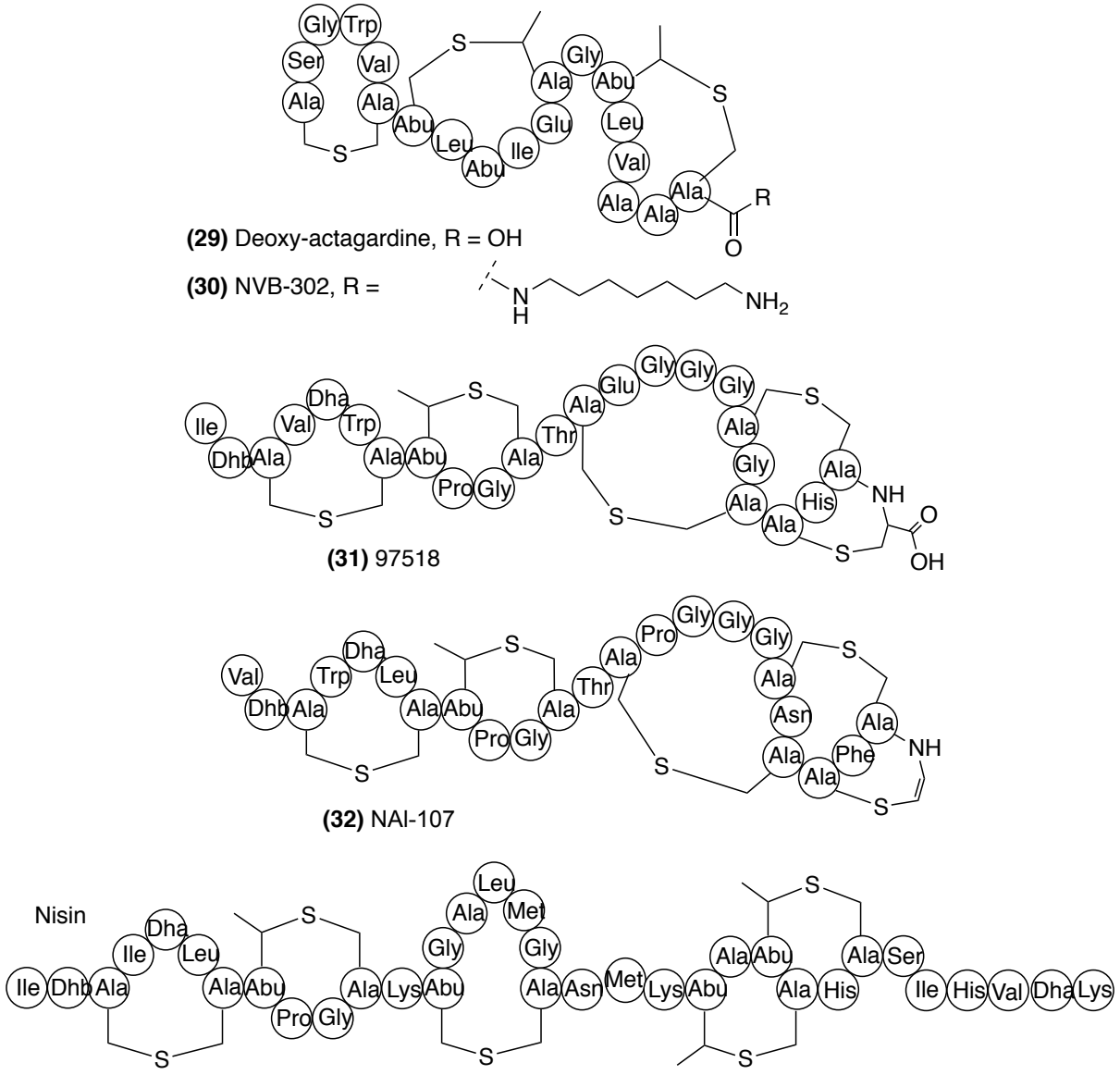

Figure 2.2. Structures of selected lantibiotics**.**

2.2 Biological properties and applications of lantibiotics

The majority of lantibiotics exert their bactericidal activity against various strains of Gram-positive bacteria in nanomolar ranges. They show promising potential against methicillin-resistant *Staphylococcus aureus* (MRSA), vancomycin-resistant

enterococci (VRE) and oxacillin-resistant Gram-positives. The lantibiotic mutacin 1140 is produced by *Streptococcus mutans*, which can cause dental decay. Mutacin 1140 was found to show broad activity against many strains of the same species, and this has potential as a dentistry agent.[133,91] In a different approach, the usage of lozenges with a salivaricin A -producing strain, *S. salivarius,* has been introduced as a probiotic to be effective against *S. pyogenes* in the oral cavity and for the prevention of halitosis.[134,135]

Cinnamycin and the related duramycins act as strong inhibitors of phospholipase A2. During body's inflammatory response, phospholipase A2 (sPLA2) enzymatically hydrolyzes phospholipids and releases arachidonic acid. Arachidonic acid is transformed to eicosanoids, which are classified as inflammatory mediators.[136]

Duramycin was investigated in clinical trials for its capacity to remove mucus secretions from the lungs affected by cysts.[137] The enterococcal lantibiotic cytolysin has lytic activity against polymorphonuclear leukocytes.[138]Lantibiotics are usually not active against Gram-negative bacteria as they cannot permeate the outer-membrane. Compared to other conventional non-peptidic antibiotics, there has been very limited resistance development observed in Gram-positive species against the lantibiotics.[139]

2.3 Different classes of lantibiotics

Here three classed of lantibiotics are discussed. The lantibiotic peptides that are included in class I are modified by two dissimilar enzymes: LanB enzyme is responsible for dehydration of Thr and Ser, while LanC is involved in cyclization. LanT (ABC transporter) is responsible for exporting the peptide. In class I lantibiotics,

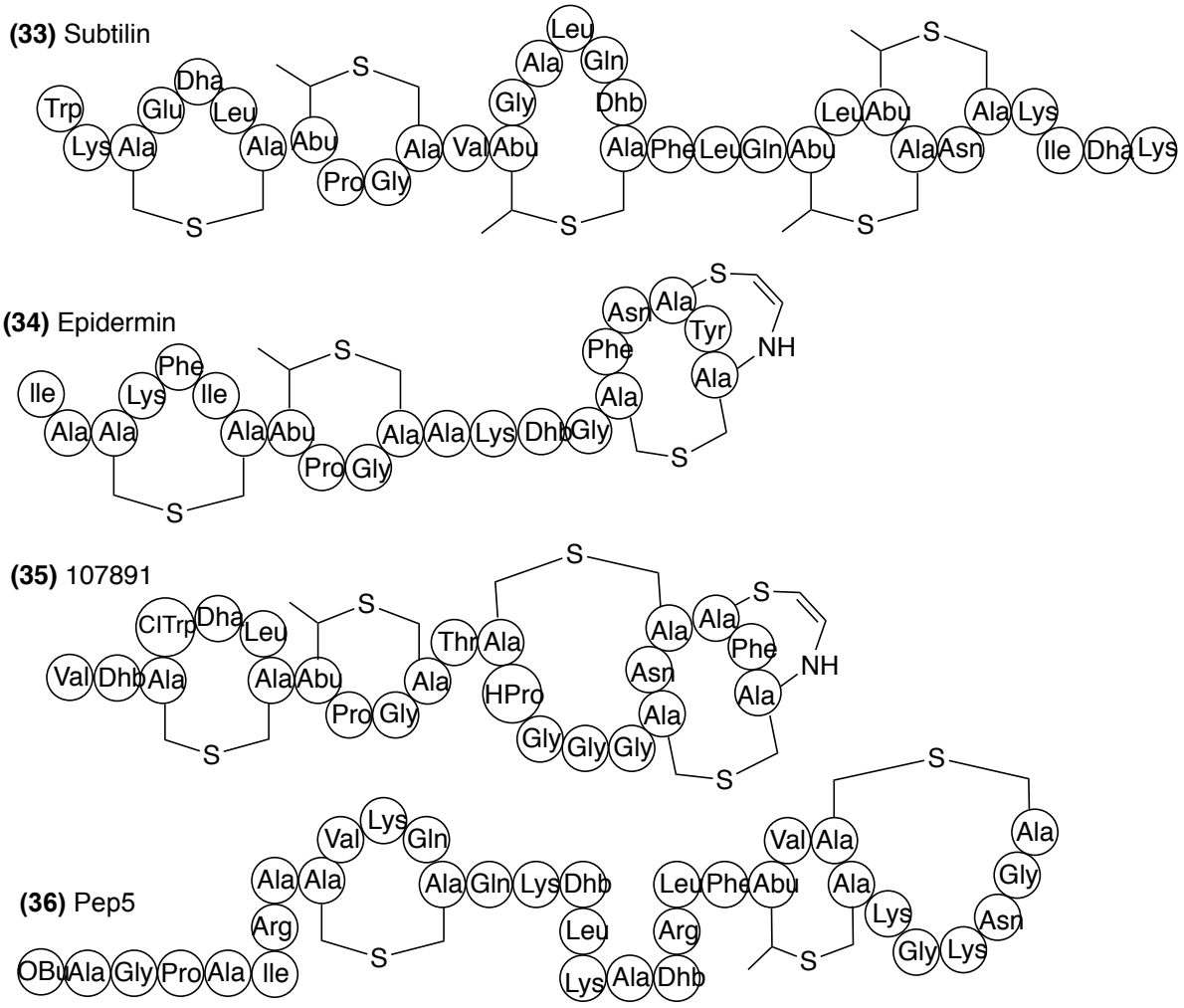

Class I

Figure 2.3. Representative examples of class I lantibiotics.

the leader peptide is removed as a result of the activity of an enzyme called LanP, which is a subtilisin-like serine protease. Structurally, lantibiotics for this class are more extended and flexible than those of class II (Figure 2.3).[140]

In class II lantibiotics, large enzymes (LanM) with up to 1000 amino acids are responsible for both dehydratase and cyclase catalytic activities. They have no homology to LanB proteins, but they have a sequence similarity to LanC enzymes.[141]

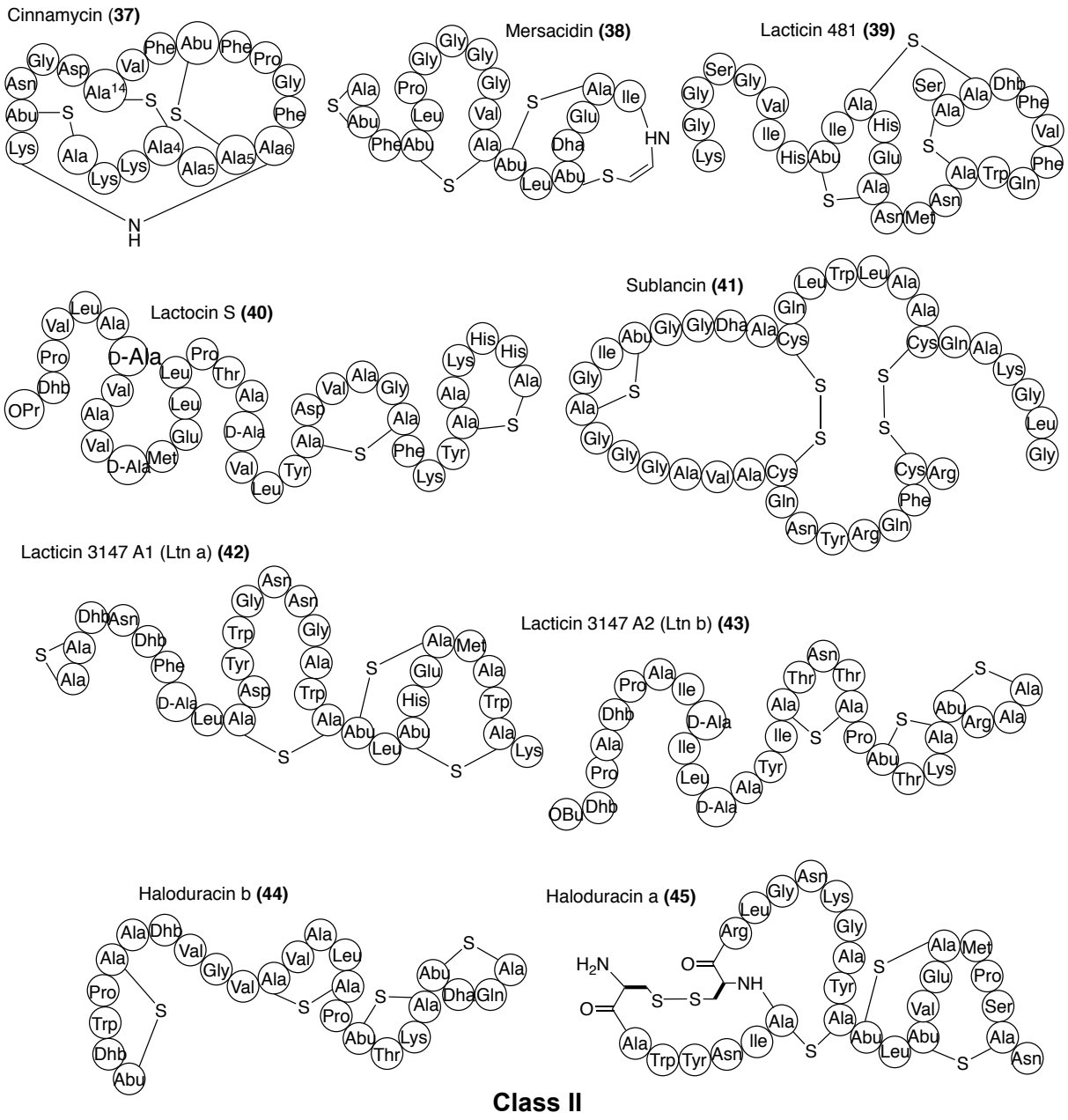

Figure 2.4. Representative examples of class II lantibiotics.

A second multifunctional enzyme with a protease domain is responsible for both lantibiotic secretion and processing of the leader segment in class II lantibiotics (Figure 2.4). [140]

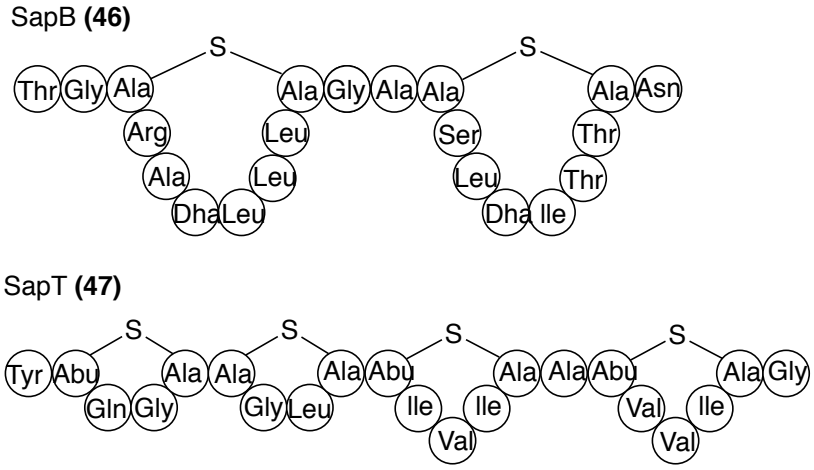

Figure 2.5. Representative examples of class lll lantibiotics.

Although there are differences between the exporters in class l and class ll, they share the same designation (LanT). Within class ll, there are some two-component lantibiotics. In this class, each peptide has its structural gene, and its modification is performed by distinctive LanM enzymes.[69,142] However, to form the mature antibiotic, two peptides work together. Furthermore, only a single enzyme (LanT) can cut the leader peptide and secrete both products.

In earlier studies, a third class of lantibiotics, with little antibiotic activity and unknown cellular functions, was proposed.[123] Some examples include SapB (46) secreted by *S. coelicolor*,[143–145] AmfS is produced by *S. griseus*[146] and SapT (47) produced by *S. tendae* (Figure 2.5).[144,145] Different methodologies have been applied to determine their structure. For example, the structure for SapT was elucidated using NMR spectroscopy, whereas the structure for SapB was deduced using mass spectroscopy for amino acid sequencing.[143]

2.4 Antibiotic production and the mystery of self-immunity

It may be expected that the sustainable production of antibiotics by bacteria necessitates a mechanism to confer resistance against these compounds upon the producer strain. In the case of lantibiotics, the immunity protein LanI and/or ABC transporter enzymes can provide immunity. The responsible genes for encoding these proteins are *lanFEG*. For example, Pep5 (36) is a lantibiotic with cationic charges that exerts its mechanism of action through pore formation.[123] The producer obtains immunity against its antibiotic by the action of PepI. Pep I is a immunity protein that is suggested to work based on a mechanism of target shielding.[147] In other words, PepI is produced and transported out of the cell and to accumulate and to act at the membrane-cell wall interface. Higher extent of protection may be obtained through cooperation between LanI and ABC transporters. Nisin activity against its producer is intercepted by NisI, an immunity protein that is composed of a lipoprotein that attaches itself to the exterior face of the membrane. As a result of the activity of this immunity protein and the transporter, free nisin levels are reduced.[147] NuKH is a variant of LanI/LanFEG that provides immunity against nukacin ISK-1.[123] NuKH is smaller than the NisI and is composed of three transmembrane domains. NuKH works cooperatively with the NuKFEG transporter, resulting in self-protection and also conferring immunity to lacticin 481 (39), a lantibiotic with a similar structure. For lantibiotics such as mersacidin and epidermin, there are only immunity transporters and no lipoproteins were found in their gene clusters.[148,149]

2.5 Mechanism of action for lantibiotics and their structures

Developments in peptide engineering have improved the study of peptide structure-activity relationships, and enhanced understanding of the different modes of action of lantibiotics.[150] Different variants of nisin are produced by *L.lactis*, that have have 34 residues within their structure. Considering nisin A as the protoype, nisin Z deviates by one amino acid whereas there are four positions in which nisin Q is distinct.[151,152] Another homologue of nisin A, nisin U with 78% sequence similarity, is produced by *Streptococcus uberis*. However, nisin U is missing three residues from the C-terminal compared to nisin A.[152] Structurally, nisin is somewhat flexible and contains two amphiphilic domains with three N-terminal rings (labeled A, B, C). In its C-terminal there are two rings, D and E, joined with a flexible hinge area.[153]

A unique mode of action known for lantibiotics related to nisin is membrane pore formation assisted by docking to lipid II.[154,155] The pyrophosphate moiety of lipid II is believed to interact with amides in rings A and B of the N-terminal segment of nisin.[38,156–158] Binding to the pyrophosphate segment of lipid II is also known in other lantibiotics, such as subtilin, epidermin, gallidermin and mutacin 1140.[159,160] However, epidermin and gallidermin do not have the C-terminal tail of nisin, and that makes them shorter (30 Å) compared to nisin (50 Å). Such a difference can account for the observation that epidermin and gallidermin are inactive against some species on which nisin shows pore formation type of activity.[159]

Further studies on nisin indicate that the C-terminus portion is inserted in the membrane through a perpendicular alignment with respect to the membrane surface.[38,161] As a consequence of this insertion, pores with a size of 2–2.5 nm in

diameter are formed.[162] It is suggested that each pore is stabilized with the incorporation of eight nisin and four lipid II molecules.[157] However, in the reported NMR structure for nisin and lipid II, this stoichiometry is 1:1 nisin-lipid II.[63] The nisin–nisin interactions may account for the difference in the reported stoichiometries for interaction between nisin and lipid II. Further studies on nisin Z showed that the flexible hinge area is an essential structural feature that facilitates obtaining the proper transmembrane conformation for the pore formation, however, the binding affinity to lipid II can still be retained even if a mutated peptide does not have such a flexible hinge region.[163,164]

Nisin and mutacin 1140 can interfere with the functional localization of lipids during cell wall biosynthesis.[165,166] In other words, if bacterial cells are treated with nisin, lipid II will be sequestered from the biosynthesis of peptidoglycan. Moreover, the relative rarity of nisin resistance emphasizes the importance of the dual mechanism of action; that is, the combination of pore formation activity and the inhibition of cell wall biosynthesis through sequestration of lipid II.[157,160]

Subtilin (33) (Figure 2.3) and ericin S are produced by *B. subtilis* ATCC6633 and *B. subtilis A1/3*, respectively. Structurally, these bacteriocins contain MeLan and Lan bridging similar to that of nisin. Ericin A, produced by *B. subtilis* A1/3, has a conserved N-terminal bridging pattern that is distinct from subtilin by 13 amino acids and by the position of the C-terminal MeLan residues. There are astonishing similarities between the encoding gene clusters for subtilin and ericin A and S.[167]

Lacticin 481 (39) belongs to a family of lantibiotics that share some degrees of structural similarity.[123] At pH 7, they do not have any net charge, and they are all

hydrophobic. All other members have a linear N-terminus and a globular C-terminus resulting from three thioether bridges (Figure 2.4) that are interlocked. Site-directed mutagenesis studies on mutacin II, another member of this family, indicated that the presence of its hinge is essential for the activity.[168] The three thioether bridges are not mandatory for the peptide to show activity.[169] Furthermore, replacing either Lan or MeLan residues with each other has no significant impact on the activity of lacticin 481 and mutacin II.[168–170] Pore formation is suggested as a mechanism of action for lacticin 481 and its close relatives.[168] In this family, ring A resembles ring C within the structure of mersacidin, which is known to be involved in its activity.[171] In the producer strains, immunity proteins interfere with peptides coming into close proximity of the membrane, which suggests that the membrane is a possible target.[168]

Mersacidin (38) (Figure 2.4) is a lantibiotic with activity against methicillin-resistant *S. aureus*.[62] In contrast to lantibiotics with a positive charge, such as nisin, mersacidin does not exert antimicrobial activity by pore formation. In fact, mersacidin is known to disrupt peptidoglycan biosynthesis in the transglycosylation step.[65] More studies are needed to clarify the molecular details of this mechanism. Nuclear magnetic resonance spectroscopy aided in indicating the conformational change that mersacidin undergoes in the presence of lipid II.[64] These studies further suggested that the glutamate residue within ring C of mersacidin is important for the recognition. Interestingly, ring C is a common motif among lacticin 481 and related members, the two-component lantibiotics,[68] and also plantaricin C.[67]

Duramycin variants and cinnamycin are produced by streptomycetes and have a lysinoalanine ring.[172] They show binding interaction with phosphatidylethanolamine

(PE) with 1:1 stoichiometry.[173]

2.6 Two-component lantibiotics

The two-component lantibiotics consist of two peptides, each of which exerts weaker or no antimicrobial activity by itself, but gives stronger synergistic activity in combination with its partner.[123] Examples of such lantibiotics include plantaricin W, staphylococcin C55, cytolysin L, Smb, BHT-A, haloduracin (44, 45) and lacticin 3147 (42, 43) (Figure 2.4). The peptides may be designated as LanA1/LanA2 when they are not yet mature, but after modification they are designated as Lanα/Lanβ. One of these two-component lantibiotics whose structure has been elucidated by NMR spectroscopy is lacticin 3147.[69] The structure of haloduracin has also been proposed based on tandem mass spectroscopy.[174] Interestingly, a combination of structural data plus sequence homology suggests that the topology of the three C-terminal rings within the structure of all α-peptides is similar. By comparison with mersacidin, it is suggested that these rings are important for lipid II binding capability.[69] Within the structure of β-peptides, except for lacticin 3147 and staphylococcin C55, the N-terminal MeLan ring is conserved, with Halβ as an example.[69] Furthermore, this ring is followed by a sequence of hydrophobic amino acids. Within the structure of LtnA2 of lacticin 3147, Ser is converted to D-Ala although it is absent in BHT and Smb. The ring B also is conserved to some extent among the known two-component lantibiotics. With the exception of cytolysin, the two Lan/MeLan rings located in the C-terminal part of the β-peptides are also conserved.

An interesting mechanism of action, similar to nisin, has also been proposed

for lacticin 3147.[156,175] It has been predicted that Ltnα interacts with lipid II and then recruits Ltnβ to form pores in the cytoplasmic membrane. Alanine scanning of lacticin 3147 shows that 36 amino acids (out of 59 residues within the sequences of both peptides) can be replaced without complete loss of bioactivity.[176]

Enterococcal cytolysin is known for a number of distinctive features. While it has antimicrobial activity (functioning as a bacteriocin), it induces cytolytic activity toward erythrocytes and other eukaryotic cells.[138] Comparing the enterococcal cytolysin sequence with that of lacticin 3147 and haloduracin, it is found that in the N-terminal part of both peptides there is a MeLan residue and an extra Lan ring.

The structure of the propeptides $CylL_L$ and $CylL_S$ is modified by the intermediacy of the enzyme CylM, and the exporting process is mediated by a dual-function transporter/protease to form the $CylL_L'$ and $CylL_S'$ peptides.[177] To finish the maturation of peptides, a serine protease CylA outside the cell is responsible for a second proteolysis stage, and as a result of this activity a sequence of six residues is cut from the N terminal segment of each peptide to yield $CylL_L''$ and $CylL_S''$.[138] Related system is found with carnolysin, produced by *Camobacterium maltaromaticum C2.*[178]

The hydrophobic peptides SapB and SapT have 21 residues within their structure, and they show high surface activity (Figure 2.5). Furthermore, at the interface between water and air, these peptides have self-assembly capacity.[179] Based on a modeling study, hydrogen bonding within polar side chains is discouraged in macrocyclic structures.[145] This forces the nonpolar side chains toward the surface of the molecule to trigger the formation of patches with hydrophilic and

hydrophobic properties. Among the identified structural genes, some residues are conserved. This suggests their importance for the activity of the peptide. These residues include the Cys and Ser, which are responsible for the formation of Lan bridges, and Ser that remain as Dha in mature SapB. Another preserved feature is the hydrophobicity of the two rings.[145] More studies are needed to uncover the details of the mechanism by which these peptides interact with the cell wall. However, it is predicted that amphiphilicity and hydrophobicity play important roles.

2.7 Lacticin 3147

This two-component lantibiotic is produced by *Lactococcus lactis.* subsp*. lactis.* DPC32147.[66] LtnA1 and LtnA2 (Figure 2.6) show strong antimicrobial activity in the nanomolar range. Such a potent activity is achieved only when both peptides are present to interact synergistically, whereas individual peptides show only marginal activity. The mechanism of action suggested for lacticin 3147 is that LtnA1 first interacts with lipid II in the bacterial cytoplasmic membrane. Subsequently, the lipid II-LtnA1 complex can recruit LtnA2, leading to the inhibition of the peptidoglycan biosynthesis and pore formation.[156] The structure of the lacticin 3147 peptides was determined, and shows that there are similarities between LtnA1 and other lipid II binder lantibiotics, such as mersacidin. [66]

Some studies of different classes of two-component antimicrobial peptides suggest that the two peptides are interacting with a 1:1 ratio.[70,180–183] Based on previous studies, LtnA1 is capable of showing inhibitory activity with a MIC_{50} of 200 nM that is enhanced by about 30 fold (to 7 nM) in the presence of LtnA2. It was

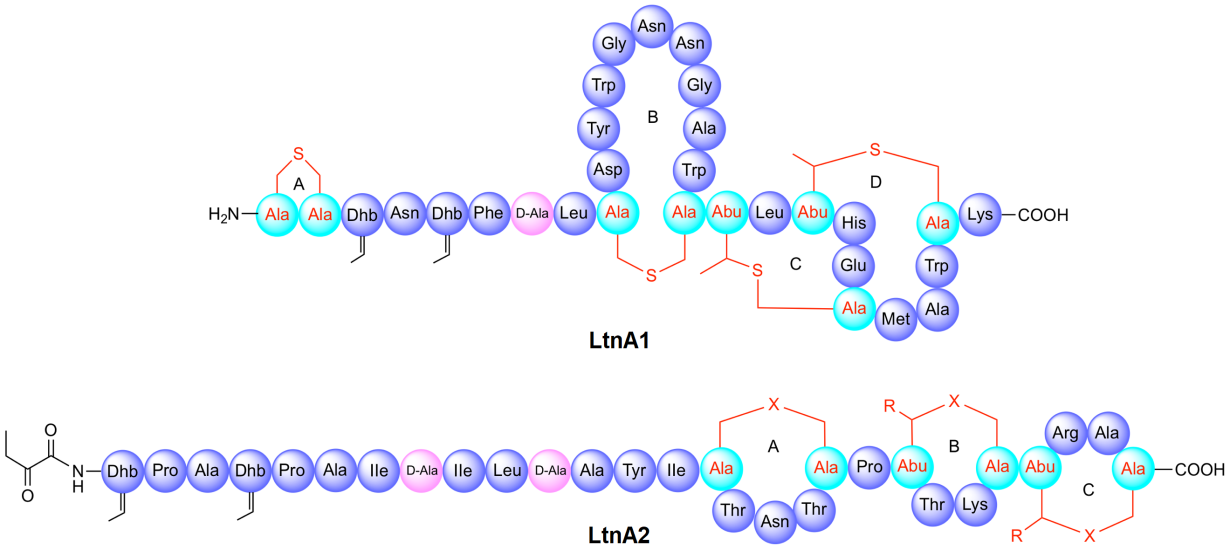

Figure 2.6. Lacticin 3147 A1 and A2. LtnA2: X = S, R = Me; oxa-LtnA2: X = O, R = Me; desMe-LtnA2: X = S, R = H.

suggested that lipid II is a receptor or docking molecule for LtnA1.[181] The participation of docking molecules, or receptor, in bacterial systems provides the possibility for AMPs to exert their effects in the nanomolar range, whereas eukaryotic AMPs that directly disrupt membranes usually are active in micromolar concentrations.[175] There are notable similarities between the structures of LtnA1, mersacidin, actagardine and Plwα, a peptide from two-component lantibiotic plantaricin W.[182,184] These include the lanthionine-bridging pattern, specifically concerning the C-terminal rings. Lacticin 3147 peptides may potentially participate in stopping the transglycosylation step of the peptidoglycan biosynthesis via a binding interaction with lipid II.[65,154,185–187]

The conserved CTLT-EC motif among the LtnA1 peptide, mersacidin and actagardine which suggests that it may have crucial roles for the mechanism of action of these peptides.[188]

Potassium ion release experiments showed that at low nanomolar concentration, LtnA1 is not capable of K^+ efflux induction in *Lactococcus lactis* subsp. *cremoris* HP target cells. Therefore, it was suggested that pore formation may not be the primary mode of action for the peptide without its partner and its activity may be due to inhibition of peptidoglycan biosynthesis from its precursor, lipid II.[175] Although LtnA1 alone shows activity in the micromolar concentration range, the optimal activity of lacticin 3147 is observed with both components in the nanomolar range.

In nisin both pore formation activity and inhibition of peptidoglycan biosynthesis can be performed by a single peptide. In lacticin 3147 these activities are proposed to require two peptides. The shorter peptide, mersacidin, has only one of these mechanisms of action; the inhibition of peptidoglycan biosynthesis at the transglycosylation step.

Furthermore, lacticin 3147 peptides show potent activity against a broad range of Gram-positive bacterial strains. Indeed, clinically significant human pathogens are inhibited by the antimicrobial activity of lacticin 3147.[189] In addition, lacticin 3147 is a potent killer of all mastitic staphylococcal and streptococcal isolates that were tested.[190,191]

2.7.1 Objective of our studies on lacticin 3147

Lacticin 3147 project started with the aim to study the presence of interaction between lacticin 3147 peptides and lipid II using isothermal calorimetry (ITC). If such an interaction could be detected, the next step would be to obtain the three-dimensional structure for the complex with the aid of nuclear magnetic resonance spectroscopy (NMR). Toward this goal, an analogue of lipid II with a shorter lipid tail

(e.g. farnesyl) than the natural variant, containing an undecaprenyl lipid tail, was targeted for synthesis. Such a synthetic compound makes NMR experiments feasible as the natural lipid II has poor solubility, can form micelles, and generates many overlapping signals. Portions of the following have been published.[117]

2.7.2 ITC and in vitro assays to assess pore formation characteristics of lacticin 3147

Isothermal titration calorimetry (ITC) commonly is used to assess the lipid II binding properties of antimicrobial peptides.[72,192,193] We used ITC to study the interactions between natural and synthetic analogues of lacticin 3147 peptides as well as synergistic mixtures and Gram-positive lipid II. Gram-positive lipid II often contains lysine in its pentapeptide chain whereas Gram-negative lipid II usually contains diaminopimelic acid. To better mimic a bacterial membrane, 1 mol% lipid II was incorporated into large unilamellar vesicles (LUVs) for the ITC experiments. In these LUVs, lipid II is symmetrically distributed between the inner and outer leaflets and cannot translocate the artificial membrane without a flippase. Therefore, the actual concentration of lipid II present on the outer leaflet is 0.5 mol%.[194] LtnA1 binds to membrane-embedded lipid II in a 2:1 ratio with a binding affinity (kd) of 0.9 μM, which is consistent with its minimum inhibitory concentration (1 μM) (A). However, none of the LtnA2 analogues bind to lipid II (Figure 2.9). Given the synergistic relationship between LtnA1 and LtnA2, the binding interaction between these peptides was also assessed by ITC. LtnA1 binds strongly to LtnA2 in a 1:1 ratio

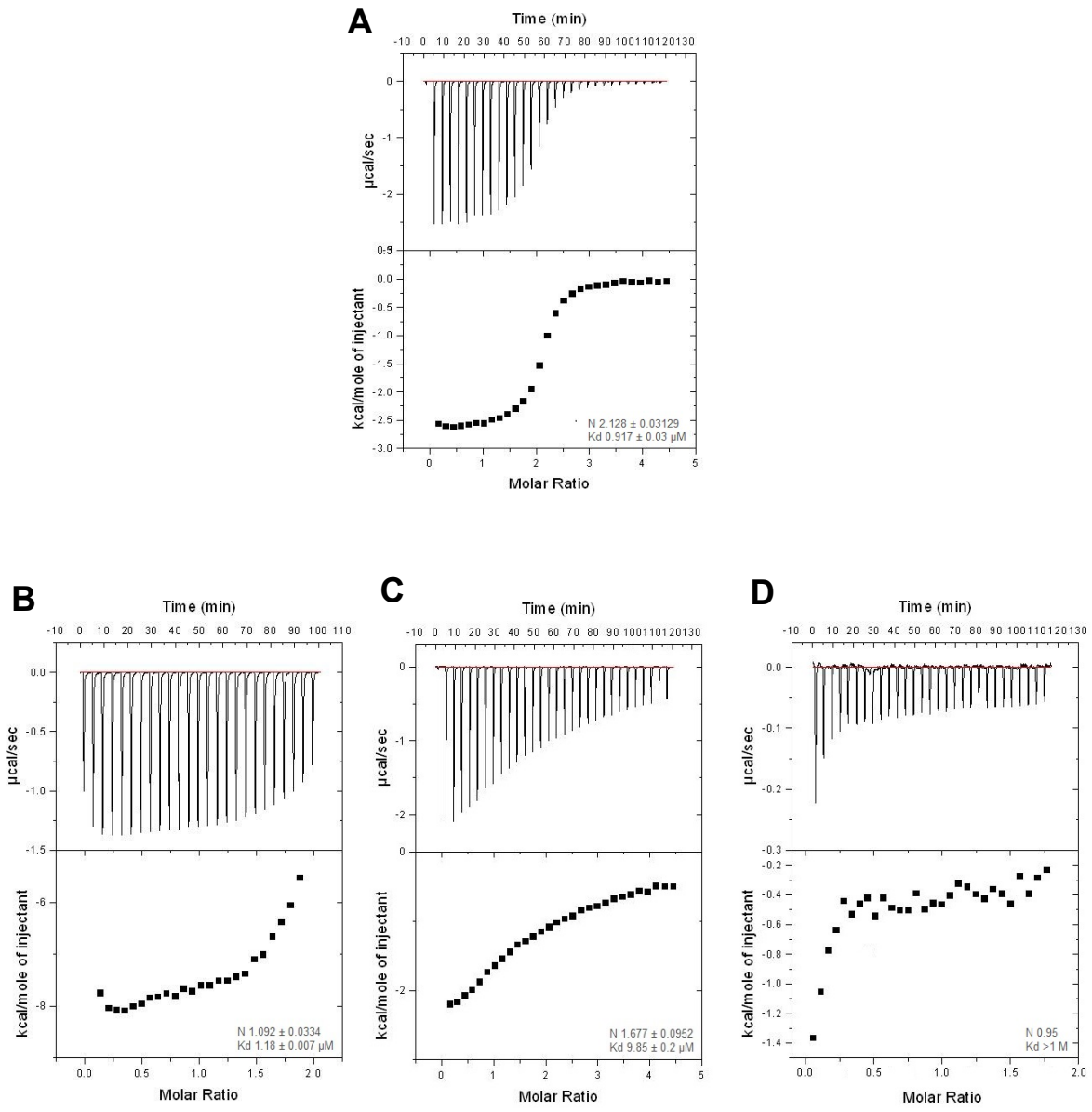

Figure 2.7. ITC binding experiments with natural and synthetic lacticin 3147 analogues and phospholipid LUVs containing 1 mol% Gram-positive lipid II. (A) Lipid II added to LtnA1. (B) LtnA1 added to LtnA2. (C) Lipid II added to 1:1 LtnA1: LtnA2. (D) LtnA1 added to desMe-LtnA2

with a Kd of 1.2 μM . When lipid II LUVs were added to a 1:1 mixture of LtnA1: LtnA2, the binding isotherm changed (C). The resulting isotherm is characteristic of a heterotropic interaction, in which cooperative binding occurs between a

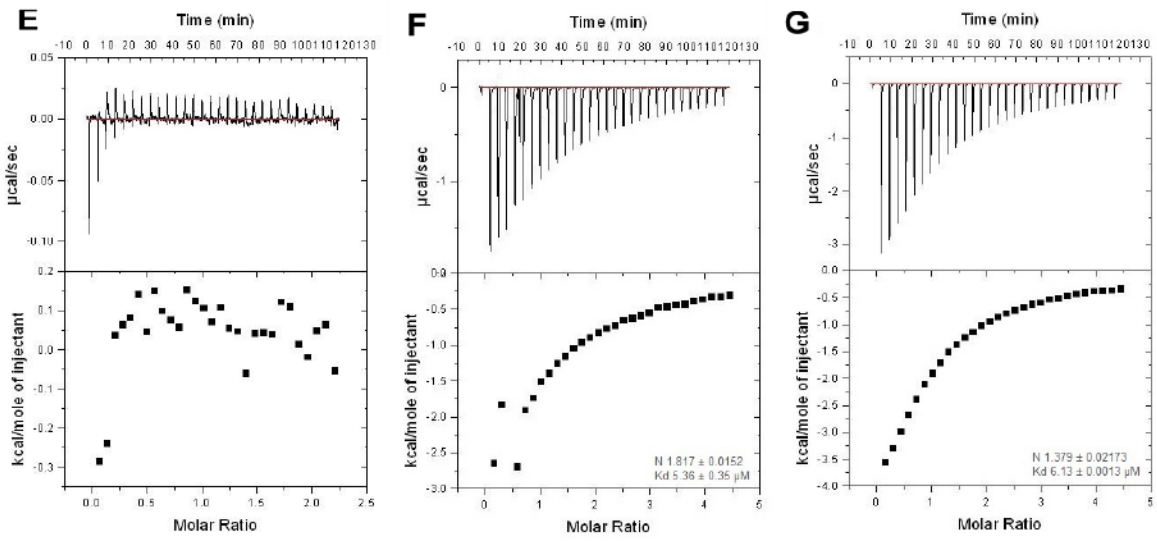

Figure 2.8. ITC binding experiments with natural and synthetic lacticin 3147 analogues and phospholipid LUVs containing 1 mol% Gram-positive lipid II. (E) LtnA1 added to oxa-LtnA2. (F) Lipid II added to 1:1 LtnA1: desMe-LtnA2. (G) Lipid II added to 1:1 LtnA1: oxa-LtnA2.

macromolecule (LtnA1) and two different ligands (LtnA2 and lipid II).[195] Therefore, it is not accurate to measure the number of binding sites or binding affinity by this method as it only gives an average of the various possible binding states between LtnA1, LtnA2 and lipid II embedded in the LUVs. The binding of LtnA1 to synthetic LtnA2 analogues was also tested, and it was found that LtnA1 binds weakly to desMe-LtnA2 (Figure 2.8 D) and does not bind to oxa-LtnA2 at all (Figure 2.8 E). These measurements are consistent with our previous observations that desMe-LtnA2 has reduced synergistic activity with LtnA1, but oxa-LtnA2 is not synergistic with LtnA1.[196,197] Then, the binding of LtnA1 + des-LtnA2 to lipid II (Figure 2.8 F) and LtnA1 + oxa-LtnA2 to lipid II (Figure 2.8 G) were analyzed. The resulting curves are very similar to LtnA1 + LtnA2 + lipid II. In the case of oxa-LtnA2, this is surprising,

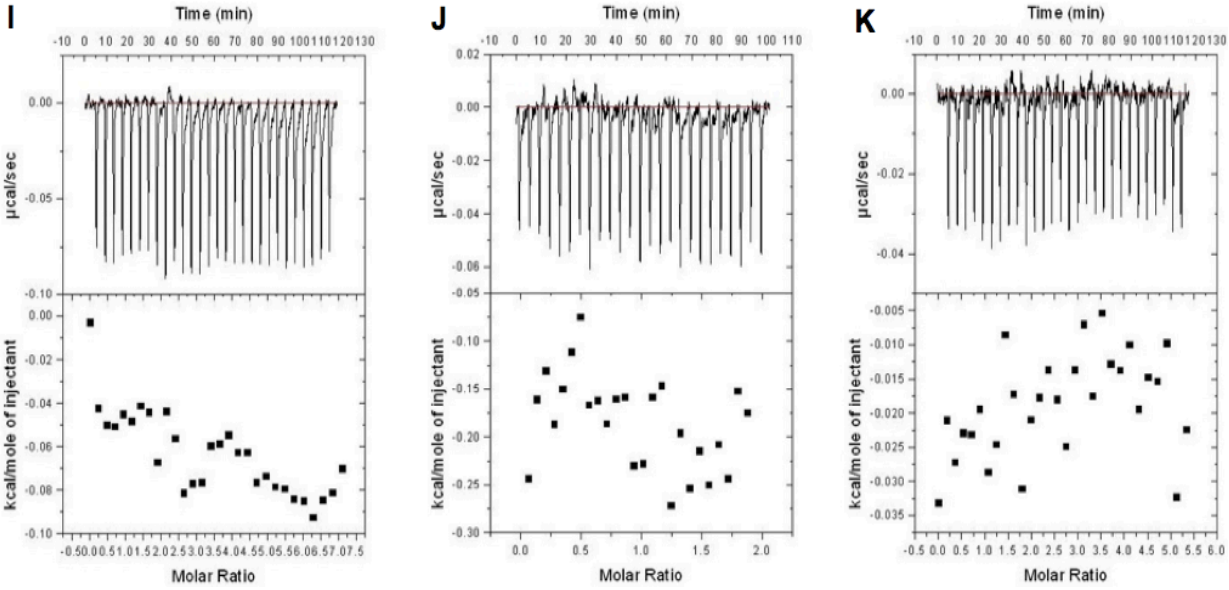

Figure 2.9. Isothermal calorimetry (ITC) experiments to determine if lacticin 3147 A2 and its analogues bind specifically to lipid II in large unilamelar vesicles (LUVs). The lipid II was from Gram-positive bacteria (contains L-lysine in the stem peptide) and was purchased from BaCWAN at University of Warwick. (I) LtnA2 + lipid II. (J) desMe-LtnA2 + lipid II. (K) Oxa-LtnA2 + lipid II. Results show that lacticin 3147 A2 and its analogues do not specifically bind to lipid II.

given that it does not bind to LtnA1. It is possible that upon formation of the LtnA1: lipid II complex, oxa-LtnA2 is then able to bind to this structure. However, at this stage, further experiments were required to determine how these binding studies relate to antimicrobial activity.

2.7.3 In vitro membrane lysis assays

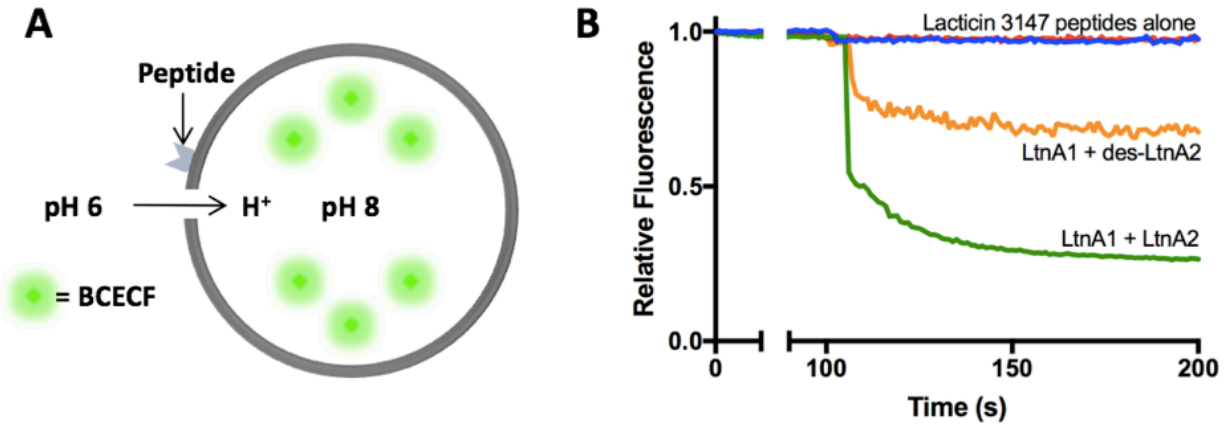

Figure 2.10. (A) Cartoon schematic of the assay used to assess membrane lysis of the lacticin 3147 analogues. (B) Relative fluorescence vs. time graph showing the effects of adding lacticin 3147 analogues to LUVs containing BCECF. Peptide concentrations are 5 μM.

To link the ITC results to the effect on cell membranes, a series of pore-formation assays were performed using LUVs containing the pH sensitive dye 2′,7′-bis-(2-carboxyethyl)-5-carboxy-fluorescein (BCECF).[198] In this assay, LUVS are constructed with an internal pH of 8 and then placed in a buffer at pH 6. If pore formation occurs, there is a decrease in intra-vesicle pH, which is observed as a decrease in BCECF fluorescence (Figure 2.10 A).[72,198] To assess the effect of membrane bound lipid II on membrane lysis, LUVs with and without lipid II were constructed. In LUVs lacking lipid II, no membrane lysis was observed for any of the lacticin 3147 analogues at concentrations up to 5 μM (Figure 2.10 B). However, a 1:1 mixture of LtnA1: LtnA2 (5 μM) caused rapid membrane lysis. The synergistic mixture of LtnA1: desMe-LtnA2 caused a smaller degree of membrane lysis in vesicles

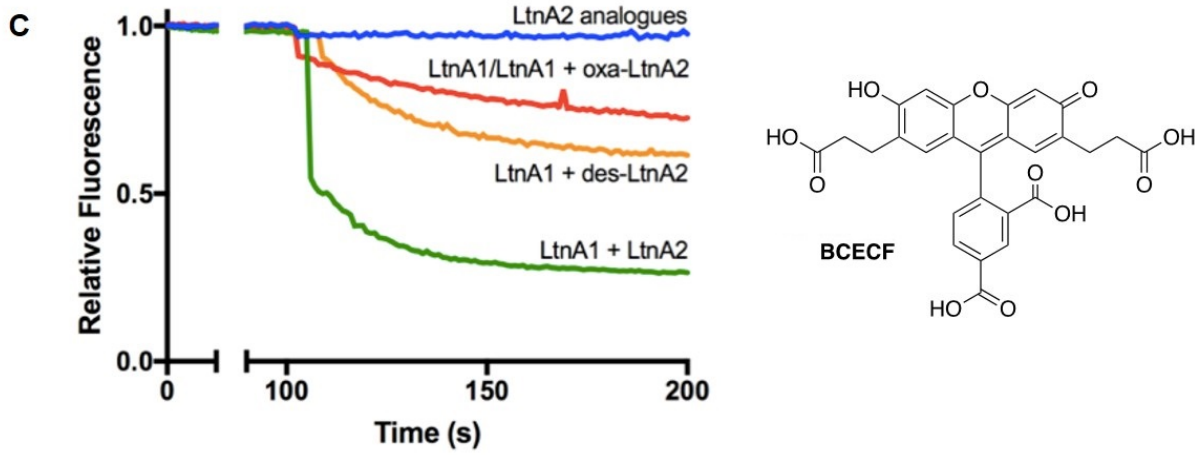

Figure 2.11. *In vitro* membrane lysis assays. (C) Relative fluorescence vs. time graph showing the effects of adding lacticin 3147 analogues to LUVs doped with 1 mol% lipid II and containing BCECF. Peptide concentrations are 100 nM.

lacking lipid II, however, no effect was observed for LtnA1:oxa-LtnA2.

These results are consistent with the ITC studies that showed that oxa-LtnA2 does not bind to LtnA1. When lipid II was incorporated into the LUVs, the concentration of 1:1 LtnA1: LtnA2 or 1:1 LtnA1: desMe-LtnA2 required for membrane lysis dropped significantly to 100 nM. Consistent with the absence of lipid II binding found during the ITC studies, none of the LtnA2 analogues caused membrane lysis. In contrast, LtnA1, which was shown by ITC to bind to lipid II, caused moderate membrane lysis at 100 nM (Figure 2.11). These results show that although lacticin 3147 can cause membrane lysis without lipid II, the presence of lipid II significantly enhances activity. An anomaly observed during the ITC studies was the binding curve for 1:1 LtnA1:oxa-LtnA2 + lipid II. Even though oxa-LtnA2 does not bind to LtnA1, the binding curve was nearly identical to the synergistic mixture of the natural peptides + lipid II, suggesting a similar interaction. However, the degree of membrane lysis observed for 1:1 LtnA1:oxa-LtnA2 is identical to LtnA1 alone, suggesting that the

major interaction resulting in the ITC binding curve is LtnA1 binding to lipid II. Having linked lipid II binding to membrane lysis, we next sought to relate this to antimicrobial activity.

2.7.4 Time-kill assays

Time-kill assays often are used to determine if an antibiotic is bacteriostatic or bactericidal.[72] In these experiments, *Lactococcus lactis* subsp*. cremoris* HP cells were incubated in the presence of set concentrations of lacticin 3147 peptides (1 μM or 250 nM) for 8 hours. At certain time points, aliquot of the bacterial suspension were removed, spread on an agar plate and grown overnight. Then, the colony forming units (CFUs) per mL were counted and plotted over the course of the 8-hour experiment (Figure 2.12 A and B). In a time-kill assay, bacteriostatic agents (e.g. chloramphenicol) are easily identified as the number of CFUs will remain constant over the time-course of the experiment. Bactericidal agents kill cells, therefore, the number of CFUs will decrease over time if cells are exposed to a bactericidal compound.

Furthermore, membrane-lysing agents cause rapid cell death, with the number of CFUs typically being reduced to 0 within 30 min. At both 250 nM and 1 μM, LtnA1 halted cell-growth but did not significantly reduce the number of CFUs over an 8-hour period. This shows that LtnA1 binding to lipid II exerts a bacteriostatic effect. In contrast, LtnA2 is bactericidal. At 250 nM all cells are killed over the 8-hour time-course, however, at 1 μM the time taken to kill all cells is reduced to 30 min. This

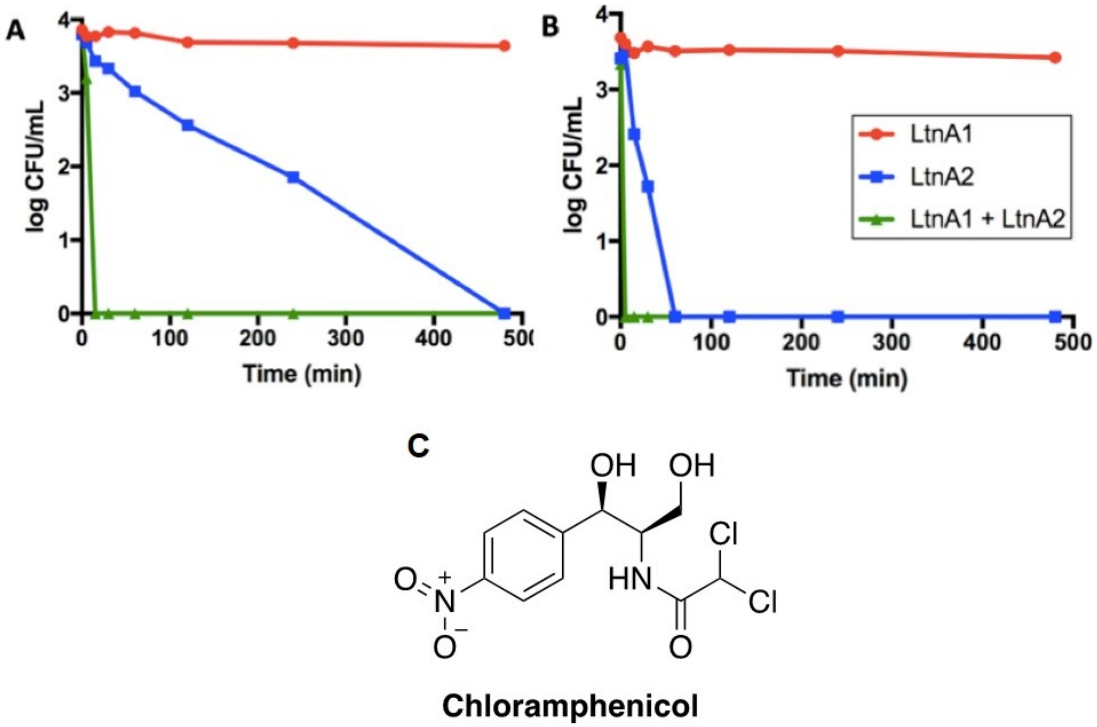

Figure 2.12. Time-kill assays. *Lactococcus lactis* subsp. *cremoris* HP cells treated with 250 nM (A) or 1 μM (B) of peptide, and the number of viable cells determined at different time points.

suggests that at higher concentrations, LtnA2 alone can kill Gram-positive bacteria by lysis of the cell membrane. In the *in vitro* membrane lysis assay, LtnA2 showed no lytic activity against LUVs with or without lipid II. Therefore, these artificial membranes either lack the lipid composition required for LtnA2 induced membrane lysis or LtnA2 binds to a membrane embedded biomolecule that is not present in the LUVs. To confirm this, an in vivo membrane lysis assay was required. The synergistic mixture of LtnA1 and LtnA2 kills all cells within 10 min at 250 nM and 5 min at 1 μM, which is highly suggestive of rapid membrane lysis (Figure 2.12, Figure 2.13). These results corroborate that the synergistic mixture of LtnA1 and LtnA2 kills Gram-positive bacteria by rapid membrane lysis. To confirm these findings in vivo, SYTOX Green membrane lysis assays were performed.[72]

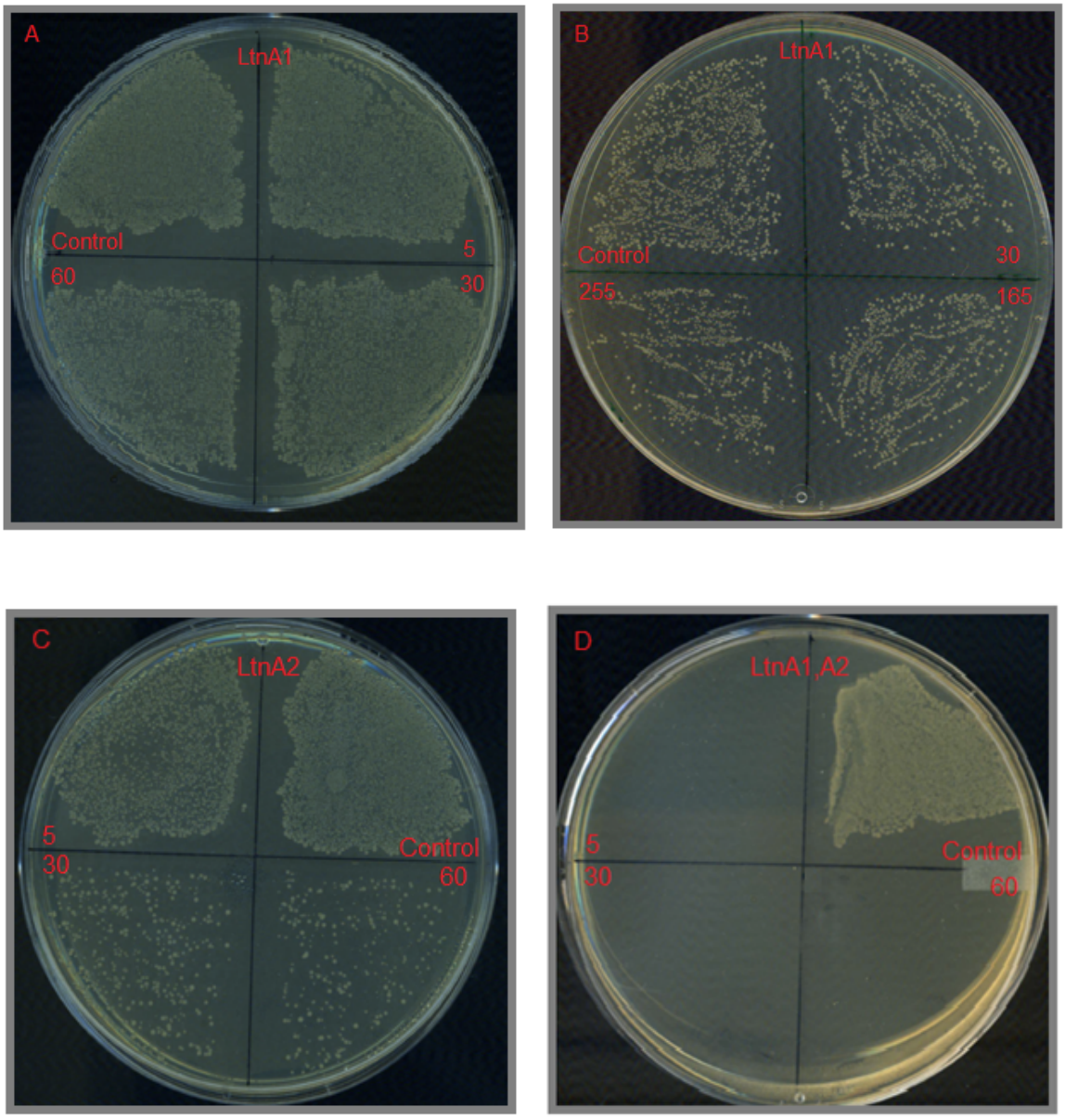

Figure 2.13. Time-kill assays using lacticin 3147 A1, A2 or A1+A2 (Plate representation). The number of viable *Lactococcus lactis* subsp. *cremoris* HP cells were assessed at various time points (values given in minutes). (A) LtnA1 (250 nM) had no observable effect on cell viability over 1 hour (5 min, 30 min, 60 min). (B) Higher concentrations of LtnA1 (1 μM) appeared to halt cell growth, suggesting it is bacteriostatic. (C) LtnA2 (250 nM) killed most cells by 1 hour, showing it is bactericidal. (D) LtnA1 + LtnA2 (250 nM) killed all cells within 5 minutes, suggesting rapid membrane lysis.

2.7.5 *In vivo* membrane lysis assays

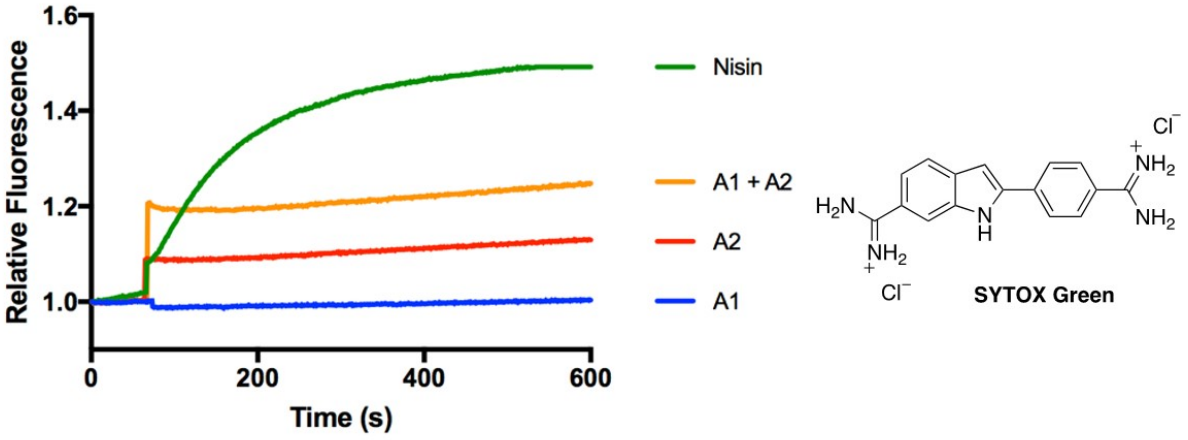

Figure 2.14. *Lactococcus lactis* subsp. *cremoris* HP cells pre-treated with SYTOX Green were exposed to antimicrobial peptides (100 nM) and the extent of membrane lysis visualized as an increase in fluorescence.[72]

To assess the effect of lacticin 3147 peptides on whole-cell membranes, in vivo membrane lysis assays were performed using SYTOX Green (Figure 2.14). SYTOX Green is a membrane-impermeable reagent that penetrates cells with compromised cell membranes, binding to nucleic acids and emitting a fluorescent signal.[199] *Lactococcus lactis* subsp. *cremoris* HP cells were incubated with SYTOX Green, and then peptides were added to a final concentration of 100 nM. Nisin is known to cause rapid pore-formation at this concentration and indeed showed rapid membrane lysis in the SYTOX Green assay.[72] LtnA1 did not cause membrane lysis, which is consistent with the previous experiments in this study. The synergistic mixture of LtnA1 and LtnA2 caused immediate membrane lysis although not to the same extent as nisin. Gratifyingly, LtnA2, which did not cause membrane lysis in the in vitro assay

but showed bactericidal kinetics consistent with a lytic peptide, caused membrane lysis in this whole-cell experiment. This provides further evidence that either the artificial membranes lack the lipid content required for LtnA2 lysis or they lack a membrane embedded biomolecule that LtnA2 binds to induce membrane lysis.

2.7.6 CD spectroscopy and membrane-depolarization assay using $DiBAC_4(3)$

As shown above, the two peptides that constitute lacticin 3147 act synergistically. Circular dichroism (CD) spectroscopy, as an analytical tool, allows us to study if the peptide can obtain different secondary structure, such as α helix, parallel or antiparallel β sheets and under different conditions they are studied. The resulting CD data shows that LtnA1 may not be able to attain detectable structure in the presence and absence of LtnA2. However, LtnA2 can attain α-helicity, and this helical structure becomes even more stable, as can be seen from the CD graph, in the presence of LtnA1; this is depicted in the graph with one positive band at 190 nm and two negative bands in 208 and 222 nm. This higher degree of α-helicity could be resulted from synergistic activity between the two peptides (Figure 2.15, see section 4.3).

The synergistic activity of lacticin 3147 peptides was studied further by using a membrane depolarization assay. This is a common experiment to assess the interaction of antimicrobial compounds with the membrane. $DiBAC_4(3)$ is one of the biosoxonal dyes that provides the possibility to visualize the membrane potential on the inner membrane of bacterial cells.[200] As a member of the oxonol family of slow-response probes, it is a small negatively charged fluorophore that shows

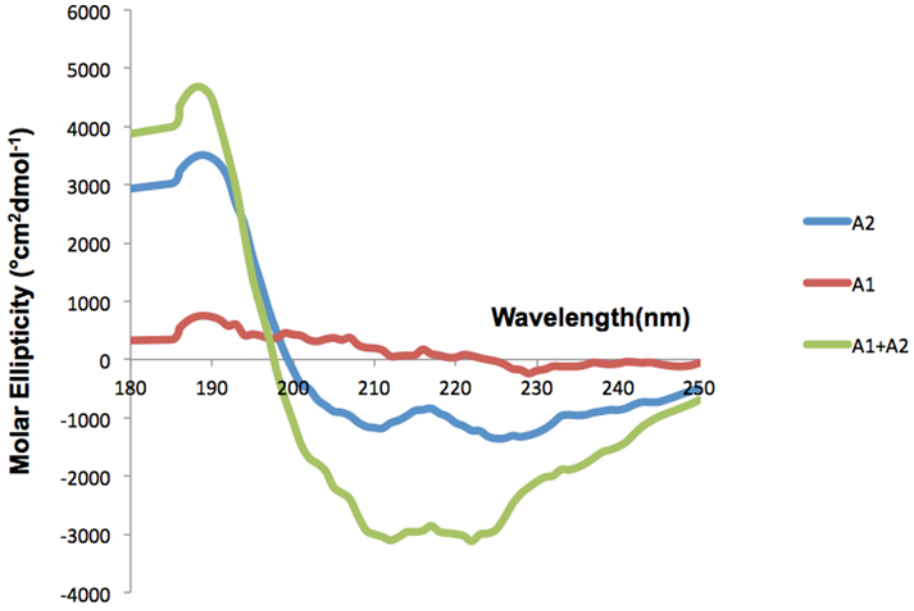

Figure 2.15. CD spectroscopy of lacticin 3147 A1, A2 peptides and the mixture of them in water.

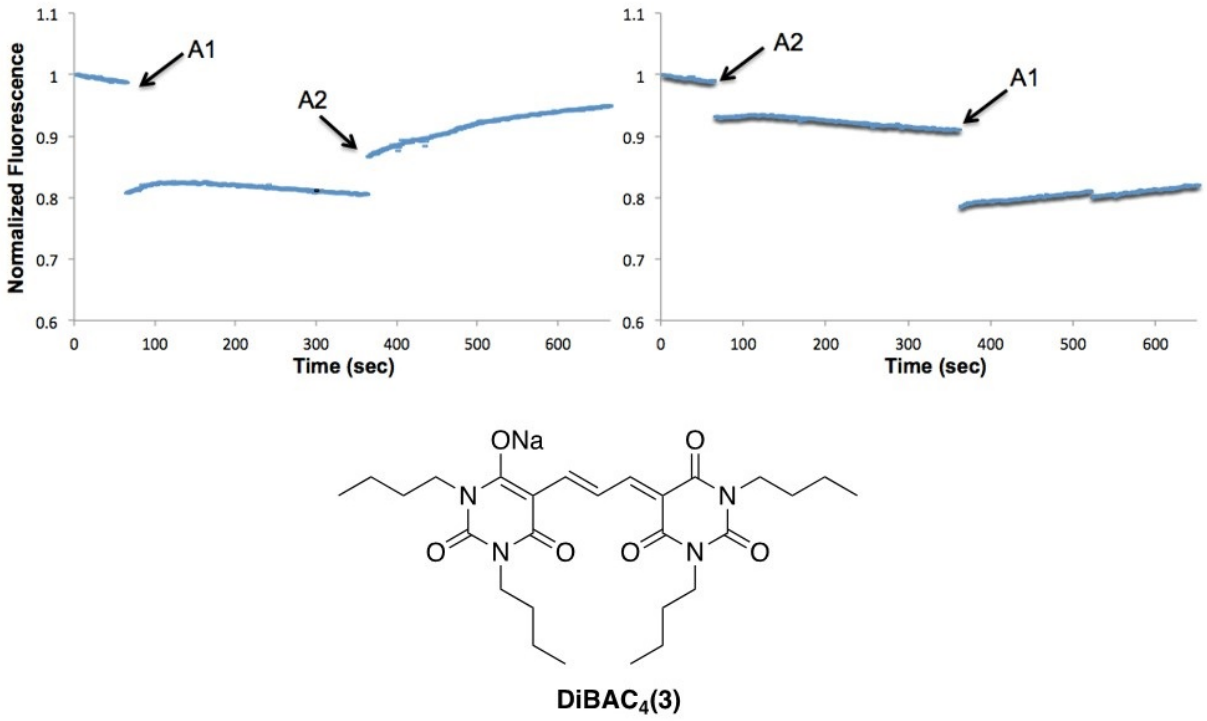

Figure 2.16. Lacticin 3147 peptides and membrane-depolarization assay.

fluorescence enhancement when it binds to hydrophobic proteins in the cytoplasm. The dye accumulates on the exterior of the inner-membrane due to the high concentration of potassium ions in there. If the membrane is depolarized, the potassium gradient will be disrupted, and the fluorescence signal increases as a result. This study suggests if ltnA1 is added first, it may dock to the membrane, and upon addition of ltnA2 depolarization of the membrane could be observed. However, if ltnA2 is added first, it attacks the membrane and lyses it, so no depolarization could be observed (Figure 2.16, see experimental 4.2.10).

2.7.7 Total synthesis of (*E,E*)-farnesyl lipid II for NMR studies

Having identified LtnA1 as a lipid II binding peptide, we sought to identify exactly how it binds to lipid II by calculating the NMR solution structure of the complex. Natural lipid II has a long undecaprenyl chain (C55) that is not very amenable to NMR studies as it has poor solubility and its multiple methylene units can mask important signals from the peptide. Therefore, a shorter chain version, (*E,E*)-farnesyl lipid II (Scheme 2.1), was synthesized by adapting a previously published methodology.[201,202] Breukink and co-workers prepared biosynthetically a Gram-postive lipid II analog with an (*E,E*)-farnesyl terpene chain that was used to elucidate the NMR solution of nisin in the presence of lipid II.[38] To obtain a final model for the nisin and lipid II interaction, lipid II was docked into the structure, providing a model for the nisin-lipid II complex. It was found that the properties of the terpene chain, length and geometry, do not affect the binding interaction between nisin and lipid probably because it is embedded in the cell membrane.[63]

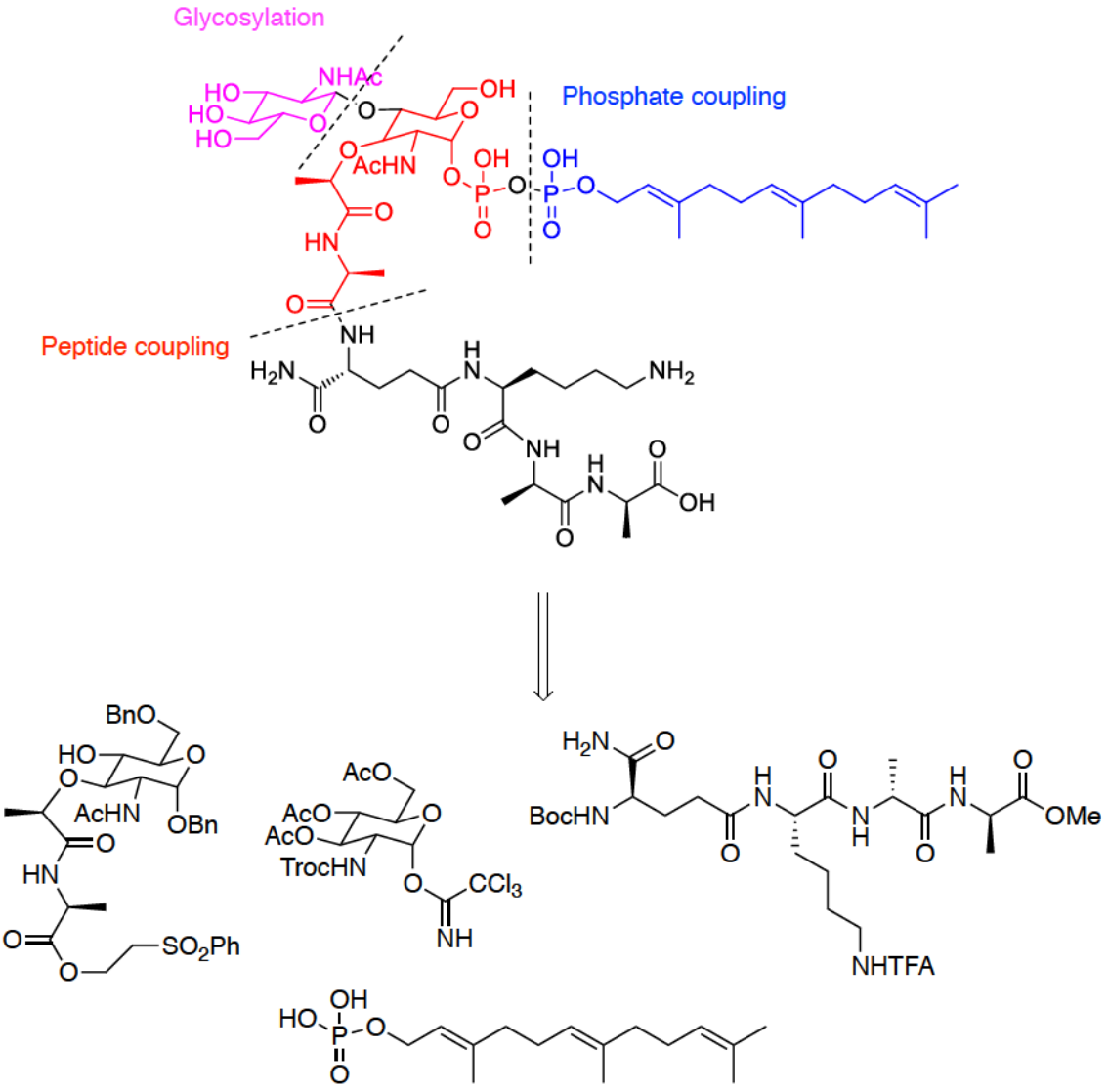

Scheme 2.1. Retrosynthetic approach to prepare (*E,E*)-farnesyl lipid II.

VanNieuwenhze and coworkers reported the first total synthesis of the peptidoglycan precursors.[201,202] To synthesize (*E,E*)-farnesyl Gram-positive lipid II, the previously reported procedures by VanNieuwenhze and coworkers were applied with some modifications.

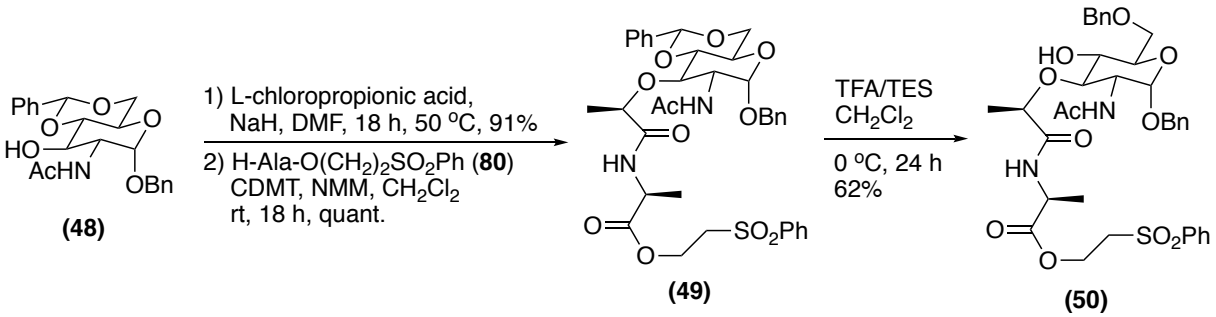

Scheme 2.2. Synthesis of glycosyl donor (50).

In the retrosynthetic plan, the lipid II structure was broken into four linear synthetic targets (Scheme 2.1). The main disaccharide segment of the structure was prepared by combining the glycosyl donor with glycosyl acceptor. This was followed by coupling to the tetrapeptide after intermediate protecting group manipulations. The last main segment of the structure to be attached was the lipid tail (62). Glycosyl donor (50) was initially prepared from N-acetyl-D-glucosamine (79).

However, compound (50) also was prepared from glycol (48), available commercially (Carbosynth, UK) in large quantities, to scale up the synthesis of primary intermediates (Scheme 2.2). Compound (48) was treated with L-chloropropionic acid, and this was followed by coupling with derivatized alanine (80) with the aid of the coupling reagent CDMT/NMM to result in benzylidene (49). In Compound (49), the 4-hydroxyl group was deprotected selectively using TFA/TES to yield (50).

The glycosyl acceptor (53) segment of the lipid II structure was synthesized from D-glucosamine (51) in four steps (Scheme 2.3). First, the amine functionality was protected as Troc-carbamate, and this was followed by acetylation of all the

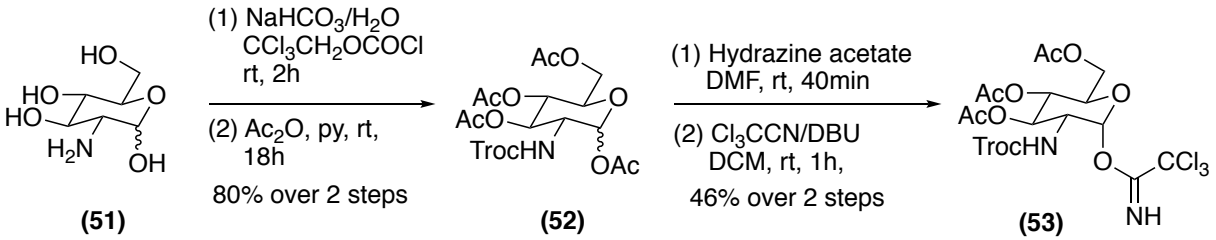

Scheme 2.3. Synthesis of glycosyl acceptor (53).

other hydroxyl groups to yield carbohydrate intermediate (52). The anomeric position of sugar (89) was deprotected selectively using hydrazine acetate, and the resulting free hydroxyl group was treated with Cl_3CCN and DBU to yield glycosyl acceptor (53).

Solution phase Boc chemistry synthesis was used to prepare the tetrapeptide in five steps (Scheme 2.4). The first coupling was between H-D-Ala-OMe and Boc-D-Ala-OH using EDCI.HCl coupling reagent to yield Boc-dipeptide (54).

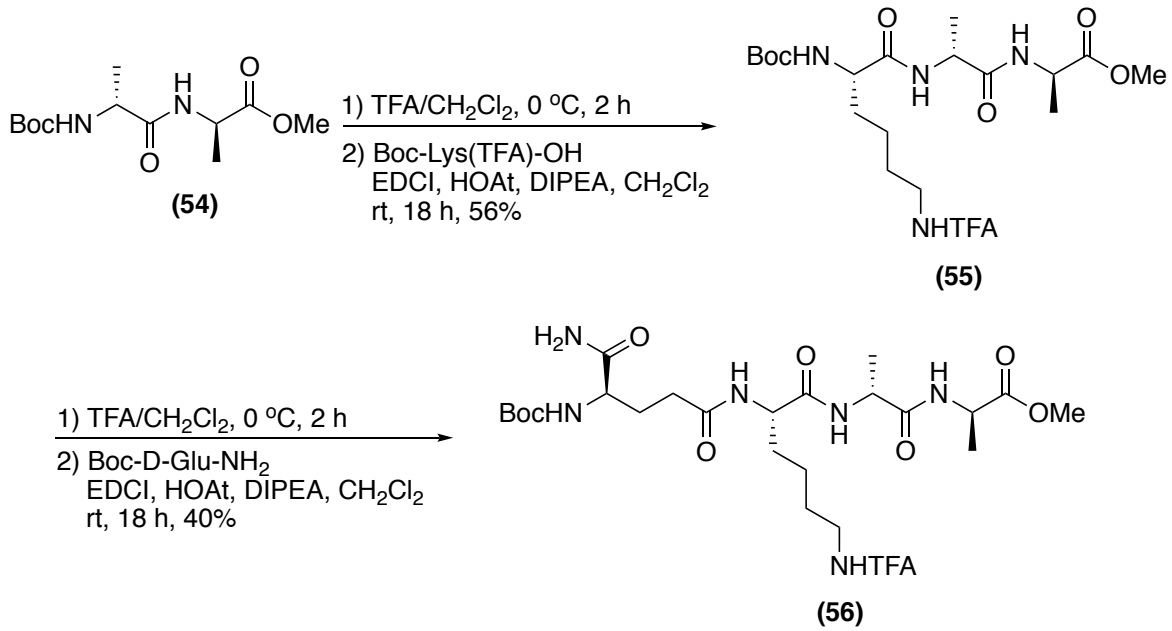

Scheme 2.4. Synthesis of Boc-tetrapeptide (56).

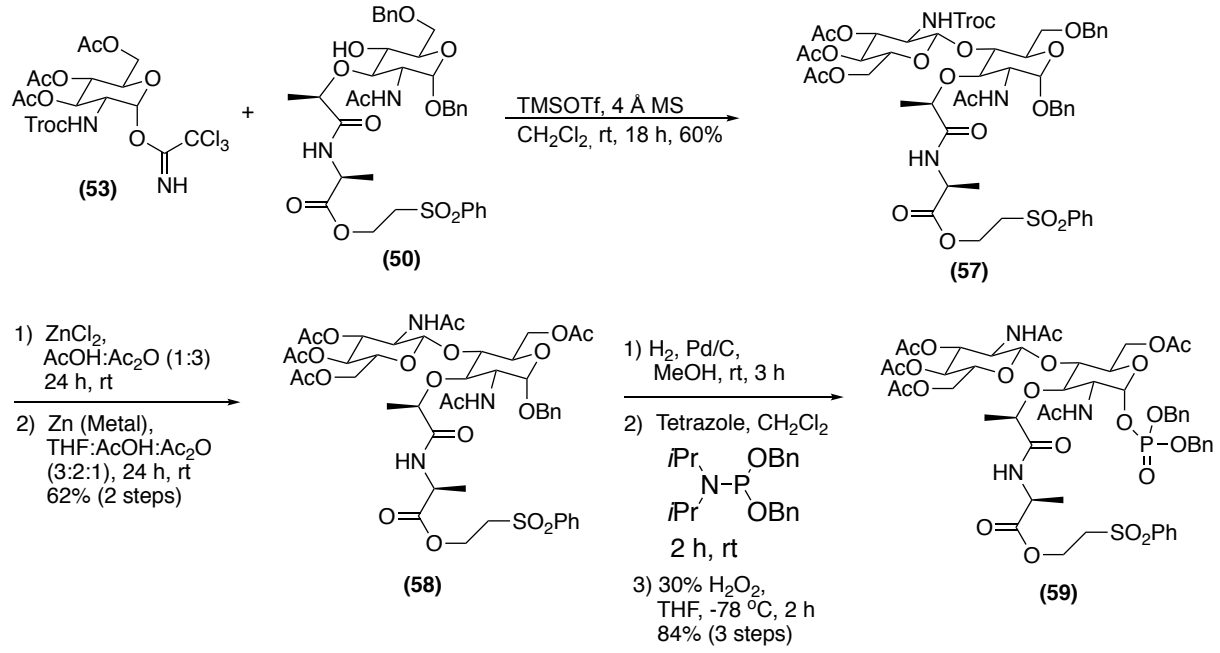

Scheme 2.5. Total synthesis of (*E,E*)-farnesyl lipid II (part 1).

After deprotecting the Boc-dipeptide, it was coupled with Boc-Lys(TFA)-OH to form the Boc-tripeptide (55). Lastly, Boc-tripeptide was deprotected to couple to the last amino acid, Boc-D-γ-Glu-NH2, to prepare the tetrapeptide (56).

By preparing the main lipid II segments separately, the synthesis of lipid II could be finalized (Scheme 2.5). TMSOTf catalyzed glycosylation was carried out between glycosyl donor (50) and glycosyl acceptor (53) sugar units to yield disaccharide (57).

Next, the benzyl ether functionality at 6-position on (57) was deprotected using $ZnCl_2$, and this was followed by reprotection in the form of acetate ester. The next step was deprotection of Troc-carbamate using a Zn insertion mechanism and reprotection as an acetamide to produce disaccharide (58). In the following step, benzyl ether was deprotected through hydrogenolysis in the presence of a Pd catalyst

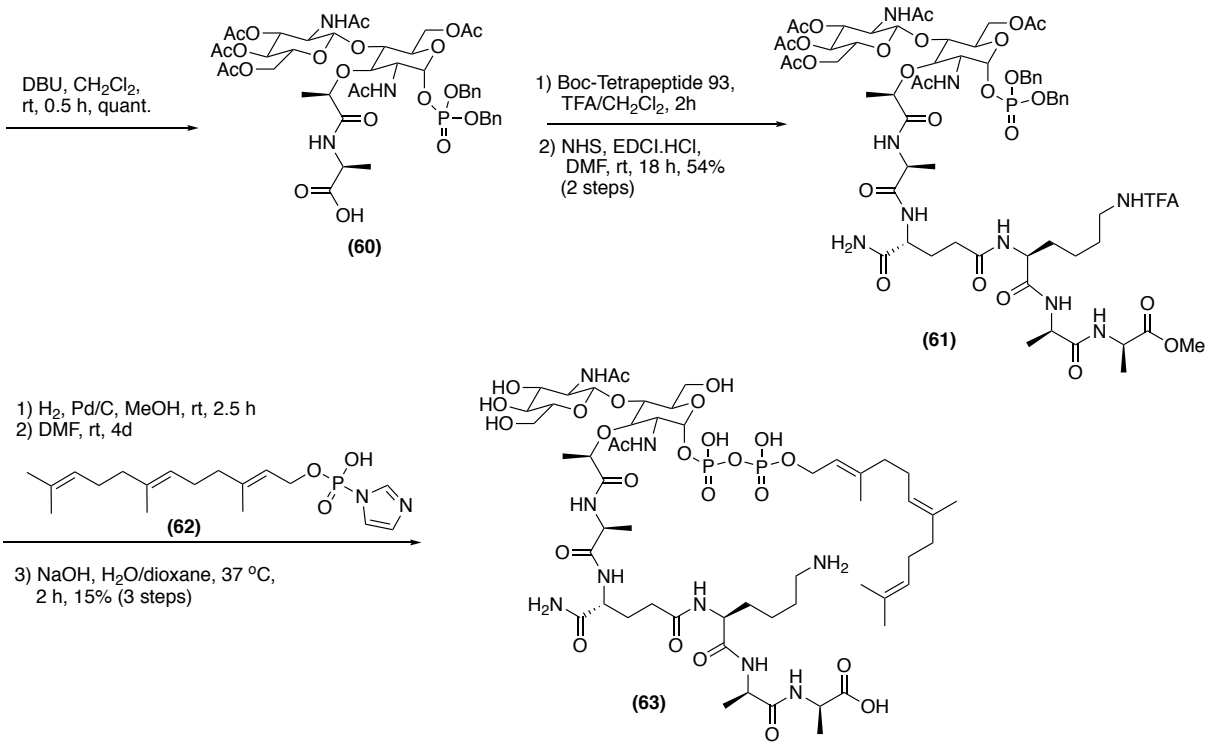

Scheme 2.6. Total synthesis of (*E,E*)-farnesyl lipid II (part 2).

which was followed by phosphorylation of the MurNAc anomeric position with dibenzyl *N,N*-diisopropylphosphoramidite and oxidation of the resulting phosphite with H2O2 to yield phosphate (59). Deprotection of the 2-(phenylsulfonyl) ethyl ester with DBU gave acid (60), which then was coupled to the Boc-deprotected tetrapetide moiety, and as a consequence, pentapeptidyl disaccharide (61) was produced. In the final stage, the benzyl ether on compound (61) was removed using a Pd catalyst and hydrogen. In the following step, the final phosphate was coupled to CDI activated (*E,E*)-farnesyl phosphate (62). Lastly, to obtain the lipid II derivative, a global deprotection was performed using aqueous NaOH reagent under shown conditions (Scheme 2.6).

2.7.8 Efforts toward the NMR study of isotopically labeled lacticin 3147 peptides

Experimental data from CD spectroscopy and isothermal calorimetry support the idea that LtnA1 and LtnA2 are interacting together to exert their synergistic activity. Therefore, obtaining the structure resulting from these peptides while they are together was set as a research goal. X-ray crystallography and nuclear magnetic resonance are among the strongest available tools for this purpose. The probability of obtaining a crystal structure for proteins and peptides is inversely related to the size and structural flexibility of the biomolecules. So far, as part of a collaboration, obtaining the crystal structure of the lacticin 3147 peptides has been an ongoing research project. Meanwhile, we started to apply an NMR approach to elucidate the structures of LtnA1 and LtnA2 and their binding to target molecules. Different NMR techniques have been developed to expand the application of solution NMR to larger biomolecules such as proteins.[203] One the of main limitations of using basic proton-proton two-dimensional NMR spectroscopy (2D NMR) to study a large protein system is related to the challenging analysis of the resulting spectra that have many correlations with overlapping peaks. In the 1990s, labeling of proteins with stable ^{15}N and ^{13}C isotopes was applied as an effective approach to overcome this limitation.[204,205] Protein isotope labeling plus the development of powerful heteronuclear multidimensional NMR spectroscopy, especially development of triple-resonance and $^{13}C/^{15}N$-resolved three and four-dimensional NMR experiments, enabled the structural study of large proteins, either as individual biomolecules or involved in interactions with a ligand.[206,207]

2.7.8.1 Effort to optimize available media to grow *Lactococcus lactis* subsp. *lactis* DPC3147

Isotope labeling by ^{13}C and ^{15}N isotopes is a useful technique to determine the overall function and structure of biological macromolecules like proteins. In order to produce labeled proteins, cells should be grown in media containing the desired isotopes. Isotopes are usually included as amino acid precursors, such as ^{15}N ammonium salts as a source for ^{15}N and ^{13}C-labeled glucose or acetate as a ^{13}C source. Rich media, such as Celtone® and Bioexpress®, which contain labeled amino acids and nutrients, also can be used for high-yielding protein expression.[208–210] To obtain labeled peptides, different media, either directly or as mixtures with the conventional media were used to grow the lacticin 3147 producer. The results are summarized in Table 2.1.

Media Tested	Results
Bioexpress® 1000	Slow growth; impractical rate of bacteriocin production
Celtone® complete	Slow growth; impractical rate of bacteriocin production
50:50 (customized media: Bioexpress 1000)	Slow growth; impractical rate of bacteriocin production
Bioexpress®1000 + Multi vitamin	Growth; low rate production with oxidation of the bacteriocin
Bioexpress®1000 enzymatic treatment (chymopapain+pepsin)	Growth; impractical bacteriocin production

Table 2.1. Media optimization results.

2.7.8.2 Processing of Bioexpress media

Bioexpress® was a media that was tried for growth of *Lactococcus lactis* subsp. *lactis* DPC3147 in order to obtain labeled LtnA1 and LtnA2 for NMR experiments. However, it was found that the strain grew sluggishly in this media as well as supplemented variants. Addition of a multi-vitamin solution (1 mL/L) enhanced the growth rate. Unfortunately, addition of the multi vitamin caused extensive oxidation of the isolated peptides.

Next, it was decided to enzymatically process the Bioexpress® media to make it more digestible for the bacterial strain and to remove unknown hydrophobic components. A 25 mL portion of the media was lyophilized to produce about 2 g of solid. A literature procedure previously published by our group was followed for further processing.[211] The solid media was extracted in a Soxhlet extractor using ethyl acetate as the solvent. After 24 h, the solvent was removed on a rotary evaporator, and about 0.2 g of a foamy material was left in the flask. After extraction, the solid media was suspended in water (1.5 g/100 mL). This was followed by two steps of enzymatic digestion, first with pepsin (Sigma; 3300 units/mg, 70 units/mL), pH 2.0, and 37 °C for 12 h. Subsequently, using concentrated HCl, the pH was adjusted to about 6.7, and as a second step of enzymatic digestion, chymopapain (Sigma; 4.5 units/mg, 1 unit/mL) was used for 36 h at 37 °C. The solution was filter-sterilized (Millipore Stericup) and inoculated with the bacterial strain. Unfortunately, the bacteria were still growing at a diminished rate and no improvement was achieved.

2.7.9 NMR binding study between LtnA1 and lipid II

LtnA1 and (*E,E)*-farnesyl lipid II were both characterized separately by ^{1}H-NMR, ^{1}H-^{1}H COSY, ^{1}H-^{1}H TOCSY, ^{1}H-^{1}H NOESY and ^{31}P-NMR (Table 4.6).[212] The chemical shifts were then assigned in a 1:1 mixture of LtnA1 and (*E,E*)-farnesyl lipid II (Table 4.1, Table 4.2, Table 4.3, Table 4.4). A significant chemical shift perturbation (~1.0 ppm) was observed in the pyrophosphate signals in the presence LtnA1 (Figure 2.17) while no similar chemical shifts changes were observed in the pyrophosphate segment of lipid II when mixed with LtnA2 (Figure 2.18). Spectra for LtnA1 in the presence and absence of lipid II were processed and overlaid, and similar processing was done for TOCSY spectra of lipid II. The largest ^{1}H-chemical shift changes in LtnA1 were observed in the amide N-H signals of the C-terminal residues (Figure 2.19) while in lipid II similar chemical shift perturbations were observed mostly on the peptide moiety (Figure 2.20).

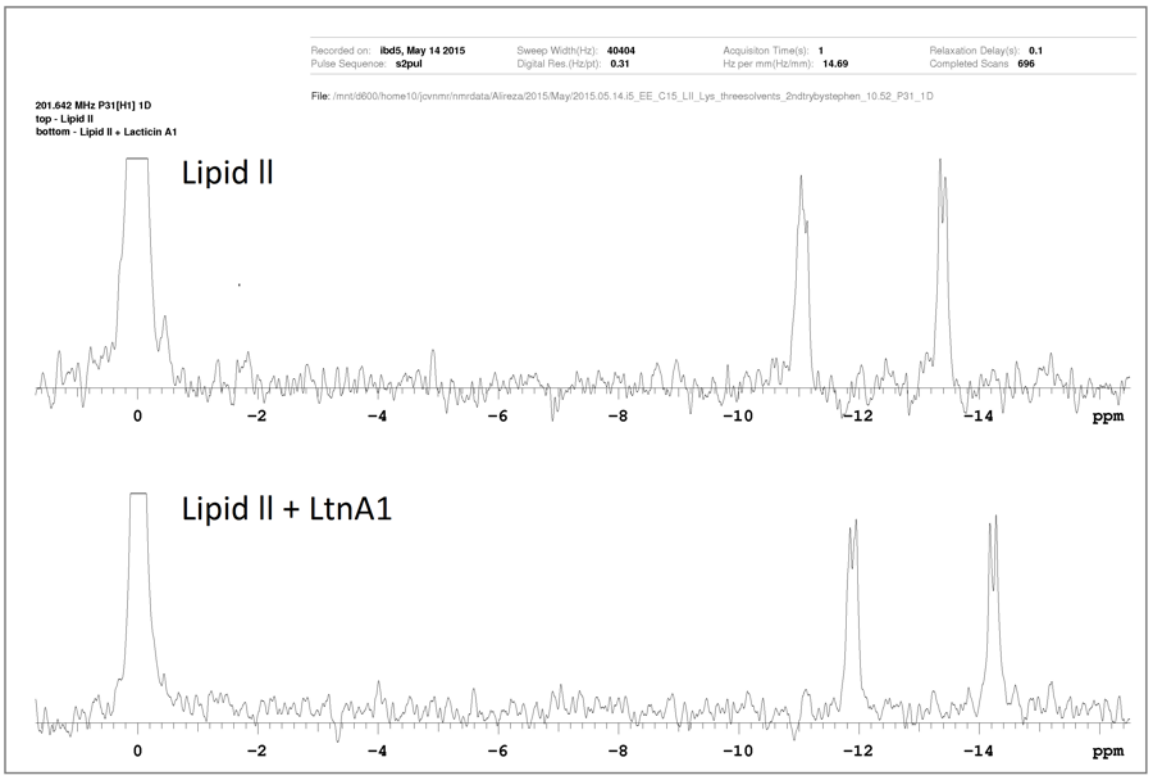

Figure 2.17. ^{31}P-NMR chemical shift perturbation when lacticin 3147 A1 binds to (*E,E*)-farnesyl lipid II, the analog of lipid II from Gram-positive bacteria. Solvent 1:1:1; CD_3OH: ACN: H_2O (phosphate buffer, 25 mM, pH 6.7).

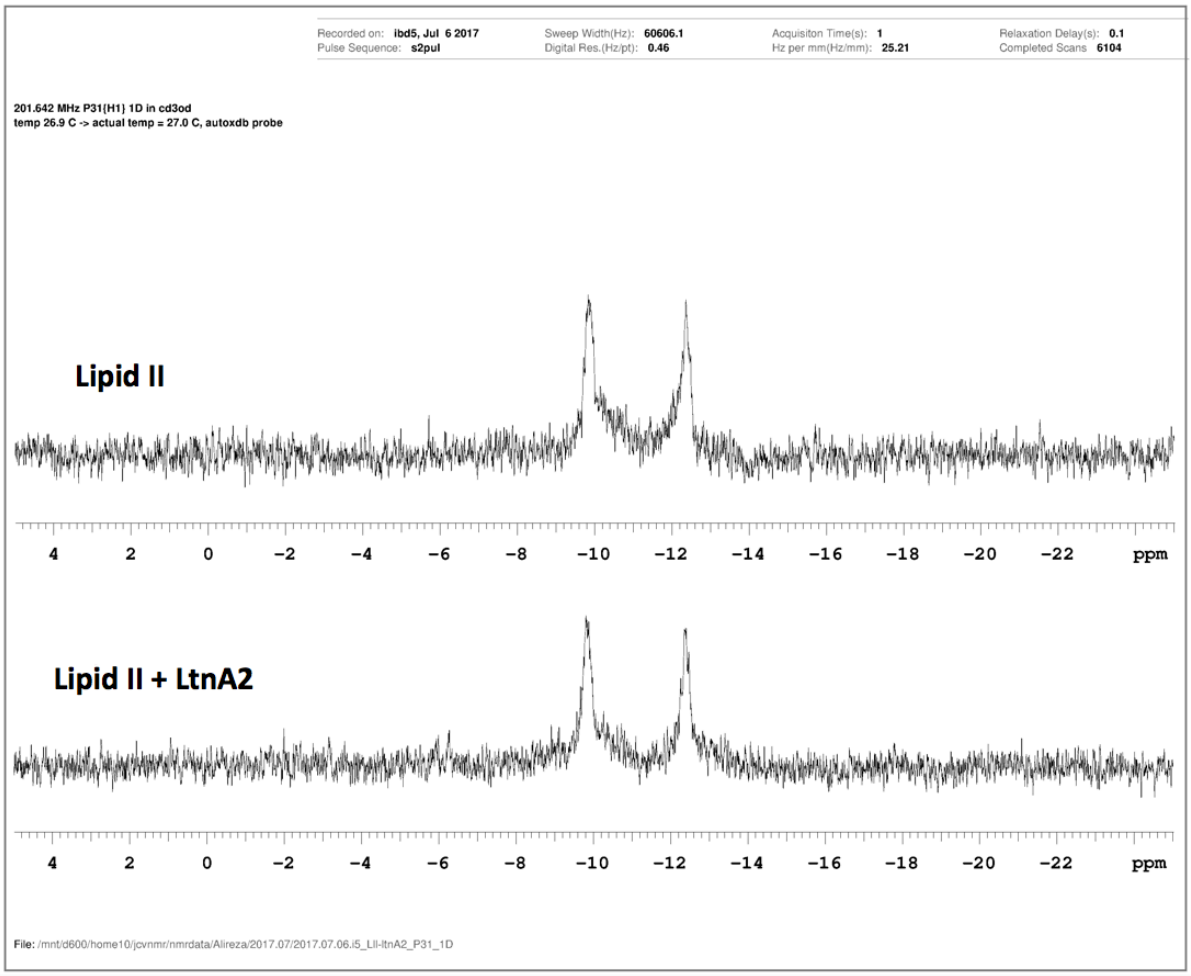

Figure 2.18. ^{31}P-NMR chemical shifts when lacticin 3147 A2 is in the presence of (*E,E*)-farnesyl lipid II, the analog of lipid II from Gram-positive bacteria: solvent CD_3OD.

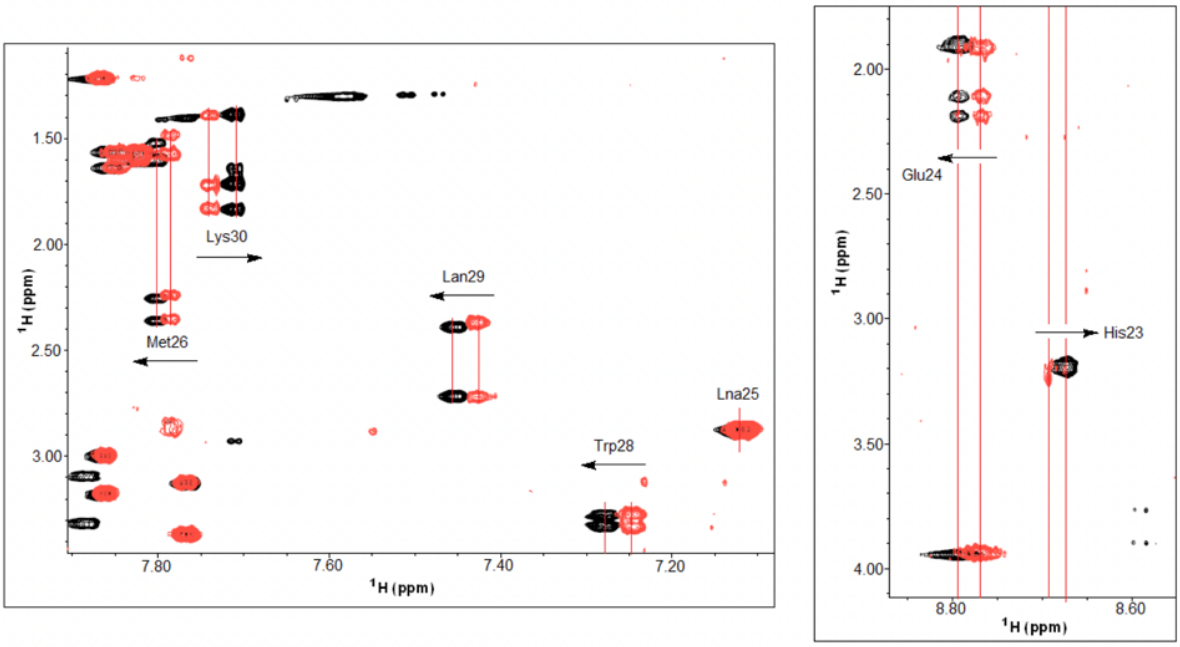

Figure 2.19. Overlay of the amide cross peak regions from the TOCSY spectra of lacticin 3147 A1 (red) and lacticin 3147 A1 + lipid II (black). Residues that underwent significant chemical shift changes upon addition of lipid II are shown.

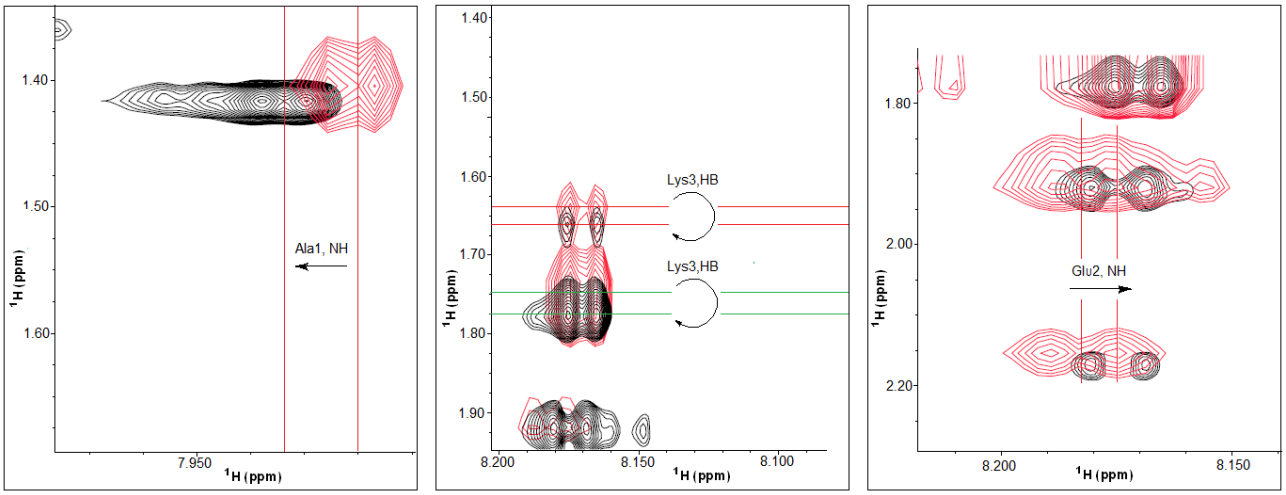

Figure 2.20. Overlay of the amide cross peak regions from the TOCSY spectra of lipid II (red) and lipid II + lacticin 3147 A1 (black). Residues that underwent significant chemical shift changes upon addition of lacticin 3147 A1 are shown.

2.7.10 CYANA structural calculations

The NMR solution structure of the LtnA1: lipid II complex was calculated using CYANA from the NMR data (experimental section, Table 4.5). Overlay of the 20 calculated lacticin 3147 A1 structures by CYANA illustrated a high degree of structure in the C-terminus, where the interactions with lipid II happen, while the N-terminus is less structured (Figure 2.21, Figure 2.22). [213] As the largest chemical shift deviations occurred in the pyrophosphate of lipid II and C-terminus of LtnA1, a distance constraint was placed between these portions to aid structural determination. The resulting model was supported experimentally by 8 intermolecular NOEs found during NMR characterization of the complex.

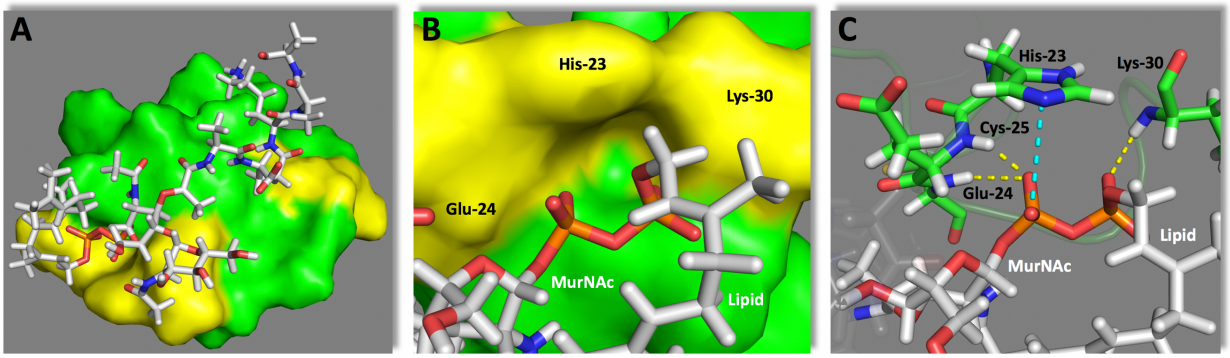

Figure 2.21. (A) NMR solution structure of LtnA1 and (*E, E*)-farnesyl lipid II calculated using CYANA. LtnA1 is shown as a surface representation with hydrophobic residues green and hydrophilic residues yellow. Lipid II is represented as a stick model. LtnA1 binds mainly to the pyrophosphate and pentapeptide regions of lipid II. (B) The pyrophosphate binding pocket of LtnA1 as a surface representation. (C) Key binding interactions between the C-terminal residues of LtnA1 and pyrophosphate of lipid. Suggested potential interactions: H-bonds between the lipid II pyrophosphate and the amide protons of Glu24, Cys25 and Lys30, as well as a pi-anion interaction between the lipid II pyrophoshate and the imidazole ring of His23.

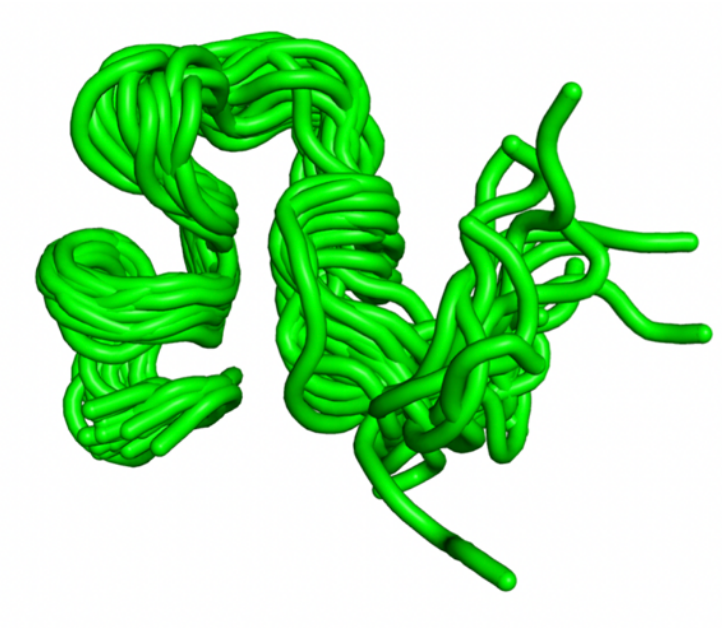

Figure 2.22. Overlay of the 20 calculated lacticin 3147 A1 structures by CYANA. There is a high degree of structure in the C-terminal residues (left), where the most significant chemical shift deviations occur upon addition of lipid II. The N-terminus (right) is less ordered.

LtnA1 binds predominantly to the pyrophosphate and pentapeptide moieties of lipid II (Figure 2.21 A). Closer analysis of the structure indicated that the C-terminal portion of LtnA1 forms a hydrophilic groove that binds to the pyrophosphate on lipid II (Figure 2.21 B). Looking into the generated structure, we suggested that the amide protons of Glu24, Cys25 and Lys30 form hydrogen bonds with the P=O oxygen atoms in lipid II (Figure 2.21 C). Furthermore, the electron-deficient imidazole ring on His23 may form a pi-anion with a P-O oxygen anion in lipid II. Medium chemical shift deviations were found in all of the amide chemical shifts of these LtnA1 residues, further supporting the CYANA generated LtnA1: lipid II model. Unfortunately, ltnA1 and ltnA2 have different solubility; therefore, we could not try to run NMR for the mixture of peptides and lipid ll.

2.8 Comparison to other lipid II binding lantibiotics

Having identified that LtnA1 binds to the pyrophosphate of lipid II, we next sought to compare this binding mechanism to other lipid II-binding lantibiotics (Figure 2.23). The NMR solution structure of the nisin:lipid II complex was previously determined in DMSO.[63] This Type-A(I) lantibiotic adopts an elongated structure in which the N-terminal residues bind to lipid II (Figure 2.237 A). In contrast, as a Type-B-like lantibiotic, LtnA1 adopts a globular structure, with lipid II binding occurring at the C-terminus (Figure 2.23 B). The pyrophosphate cage adopted by nisin (Figure 2.23 D) is shallower than that adopted by LtnA1 (Figure 2.23 E), with binding occurring exclusively through amide intermolecular hydrogen bonds. As well as intermolecular hydrogen bonding, LtnA1 also uses an interesting pi-clamp interaction to bind to the lipid II pyrophosphate. For both nisin and LtnA1, the major interaction is with the lipid II pyrophosphate. The NMR solution structure of mersacidin was previously determined in DPC micelles containing Gram-positive lipid II.[64] However, the NMR solution structure adopted by lipid II in this complex was not determined. Mersacidin has significantly higher affinity for lipid II than lipid I (which lacks GlcNAc)[214] and has increased activity in calcium enriched media.[215] These findings suggest that mersacidin may bind to both the pyrophosphate and GlcNAc moieties in lipid II. In the absence of a structure of the mersacidin:lipid II complex, lipid II analogue 63 was ocked into the NMR solution structure of mersacidin using AutoDock Vina (C and F). [216] This Type-B lantibiotic adopts a globular structure similar to LtnA1. In the resulting model, the C-terminal residues of mersacidin that have previously been shown to interact with lipid II are involved in lipid II binding.

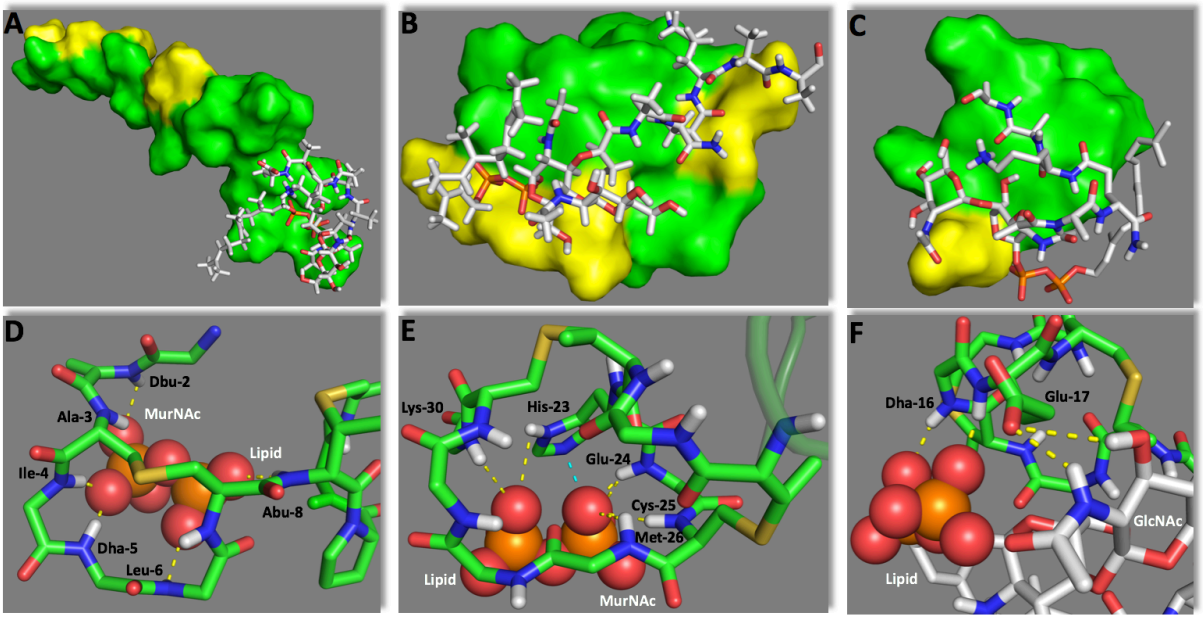

Figure 2.23. (A) NMR solution structure of the nisin-lipid II complex (1WCO), (B) Model of the LtnA1-lipid II complex and (C) Lipid II docked into the NMR solution structure of mersacidin bound to lipid II in DPC micelles (1MQZ). In (A) – (C) peptides are shown as a surface representation with hydrophobic residues green and hydrophilic residues yellow, and lipid II is represented as a stick model. Nisin adopts an elongated structure and binds to lipid II with its N-terminal residues, whereas both LtnA1 and mersacidin adopt a globular structure and bind to lipid II through their C-terminal residues. (D) The nisin-lipid II pyrophosphate cage, (E) the LtnA1-lipid II cage and (F) a model of the proposed mersacidin-lipid II intermolecular bonds. In (D) – (F) the peptide backbone is shown a stick model wherein carbon = green, oxygen = red, nitrogen = blue and sulfur = yellow, and some side-chain residues have been included. The pyrophosphate moiety within lipid II is represented by spheres with the rest of lipid II omitted for clarity, unless needed to show key intermolecular bonds. Nisin forms a tight pyrophosphate cage with several intermolecular hydrogen bonds, whereas the LtnA1 pyrophosphate cage is looser, with less intermolecular hydrogen-bonds but with a pi-clamping interaction. The mersacidin-lipid II model suggests hydrogen-bonding between Glu-17 and both the pyrophosphate and GlcNAc moieties of lipid II and is supported by all experimental evidence of mersacidin-lipid II binding to date.

There are predicted intermolecular H-bonds between the amides of Dha16 and Glu17 and the pyrophosphate, as well as the carboxylate group of Glu17 and GlcNAc. Glu17 was previously shown be very important in the antimicrobial activity of

mersacidin, with mutation of this residue to alanine abolishing activity.[176] Care must be taken when comparing the structures of nisin, LtnA1 and mersacidin bound to lipid II, as they were calculated in different solvents. Ideally these would be calculated in the same solvent system for comparison, however this is not possible due to the differing solubility's of the respective peptide:lipid II complexes.

2.9 Conclusions

These studies suggest that the two-component lantibiotic lacticin 3147 A1 has several mechanisms of action. LtnA1 binds to peptidoglycan precursor lipid II by the formation of a "pyrophosphate cage" using its C-terminal residues. In model systems, LtnA1 alone does not form pores or cause membrane lysis to a significant extent. It may attack Gram-positive bacteria by inhibition of peptidoglycan formation although this is uncertain.[156] Co-administration of LtnA1 and LtnA2 causes rapid lysis at 5 μM concentrations in model membranes without lipid II, indicating direct pore forming activity by these peptides. However, the presence of lipid II greatly enhances this activity at nanomolar concentrations. This supports an earlier proposal[156] that a ternary complex of LtnA1, LtnA2 and lipid II is critical for the most potent antimicrobial action. The current work also reveals three dimensional aspects of the LtnA1 interaction with lipid II. Synthetic LtnA2 analogues show that the precise geometries of the lanthionine and methyl-lanthionine rings are also critical for this synergistic activity.

Chapter 3 The lipopeptide tridecaptin A1: synthesis and mechanism of action

3.1 Introduction

3.2 Background: antibiotic development for Gram-negative bacteria

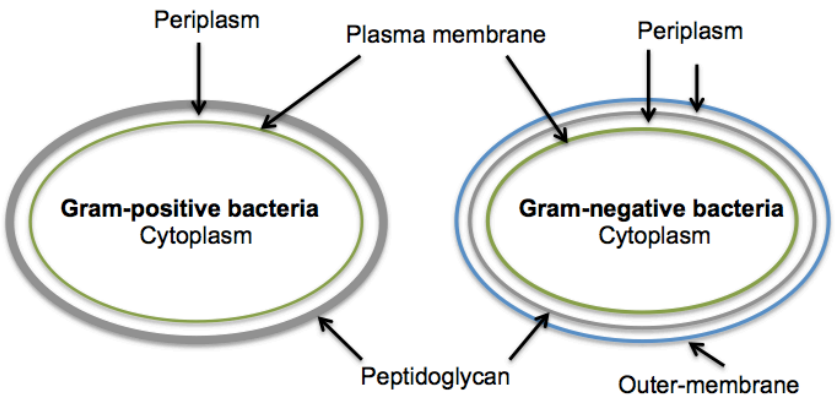

Figure 3.1. Differences between Gram-positive and Gram-negative bacterial cell wall.

One of the main features by which Gram-negative and Gram-positive bacteria are different from each other is the composition of their cell wall (Figure 3.1). Although both Gram-negative and Gram-positive bacteria have peptidoglycan as a constituent of their membrane, the thickness of this layer in Gram-positive bacteria is higher than that in Gram-negative bacteria. However, Gram-negative bacteria have an outer membrane as an extra barrier. The outer membrane in Gram-negative bacteria provides some protection against antibiotics with negative charges or those that are hydrophobic. As part of their mechanism of defense, Gram-negative bacteria take advantage of multiple efflux pumps that are capable of removing foreign compounds and/or enzymes. Furthermore, some chemically modify the structure of antibiotics and/or their targets.[19–21] Developing a new antibiotic compound to be active against Gram-negative bacterial strains is often more challenging than for Gram-positive bacterial strains.

3.3 Lipopeptides: structure, antibiotic activity and preparation

Lipopeptides are a class of AMPs with interesting properties. Lipopeptides can be either linear or cyclic and are acylated with a short fatty acid chain, usually on their *N*-terminus. Owing to lack their potential applicability as antibiotics was ignored for a long time because they were thought to cause systemic toxicity. Eventually, the emergence of antimicrobial resistance brought lipopeptides to attention, and several of them obtained FDA approval to treat multidrug resistantant infections. Examples include daptomycin and polymyxin B (Figure 3.2).[217] *Bacillus* and *Paenibacillus* strains may produce numerous lipopeptides with potent activity, including polymyxins.[218] Lipopeptides often show enhanced stability to proteases in blood plasma. This may be due to the presence of both D and L amino acids.[219] The lipid tails are commonly branched and may contain a β-hydroxyl group.[220] Formation of lipopeptides with a cyclic structure usually results from amide or ester bond formation that gives the lipopeptides more structural rigidity. These linkages are normally formed between the amino acid side chains, or the lipid tail and/or the C-terminus. Lipopeptides normally target cell membranes, and the development of resistance against them is slow in comparison to other antibiotics.[218]

Synthetically, linear lipopeptides are much easier to prepare than cyclic lipopeptides, such as polymyxin B. Solid-phase synthesis is a convenient method to prepare linear peptides. However, preparation of cyclic peptides by chemical synthesis is more demanding since it requires orthogonal side chain protection followed by a cyclization at the final steps of the synthesis. In other words, among the different classes of AMPs, linear lipopeptides are synthetically more approachable.[218]

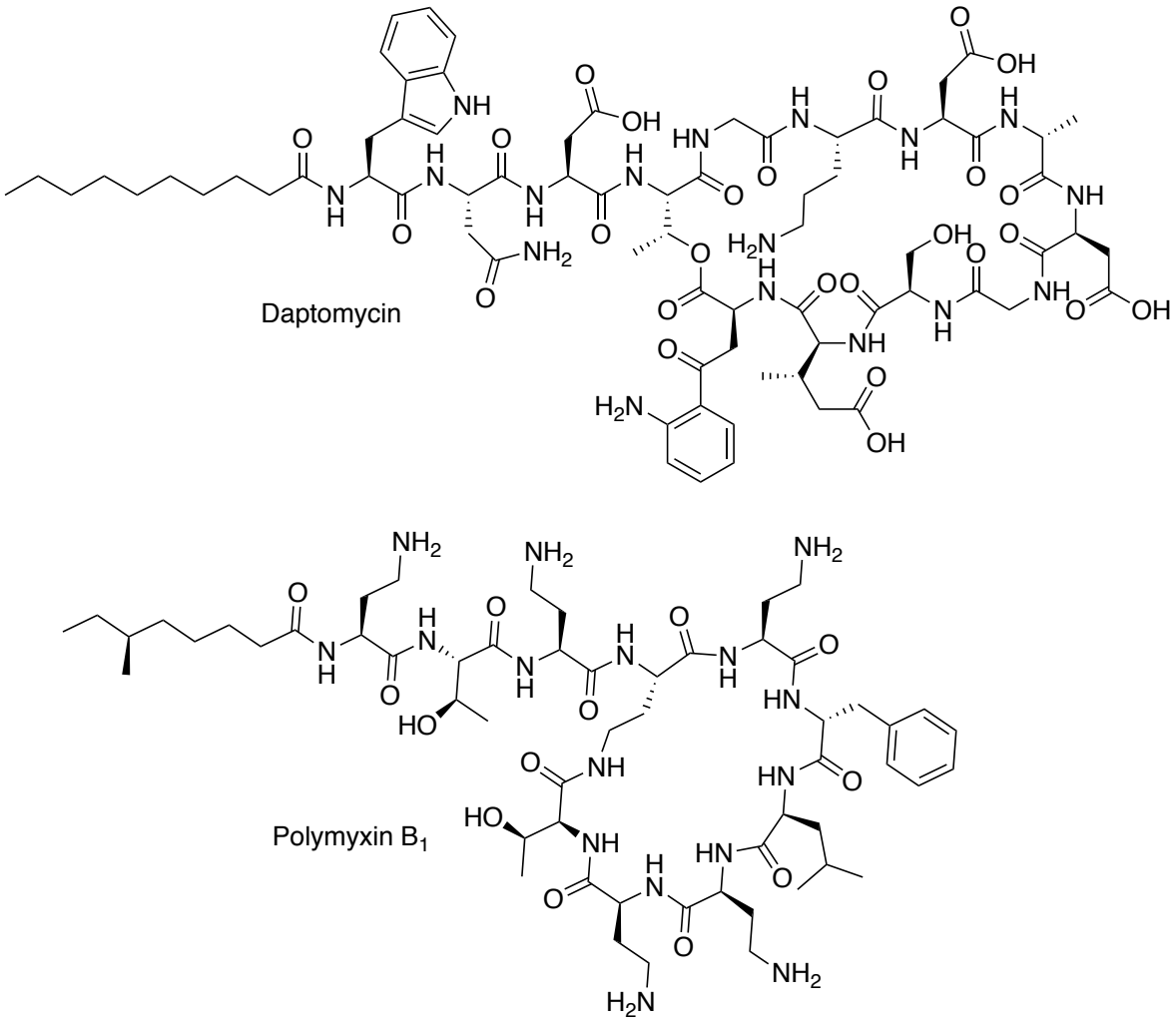

Figure 3.2. Examples of lipopeptide antibiotics with clinical application.

3.4 Tridecaptins

Tridecaptins belong to the linear class of lipopeptides. They were isolated from *P. polymyxa* species in the1970s.[221,222] Within their structure, they contain both L- and D-amino acids and a *N*-terminal lipid tail with a β-hydroxyl group (Figure 3.3). Tridecaptins show potent antimicrobial activity against Gram-negative bacteria.

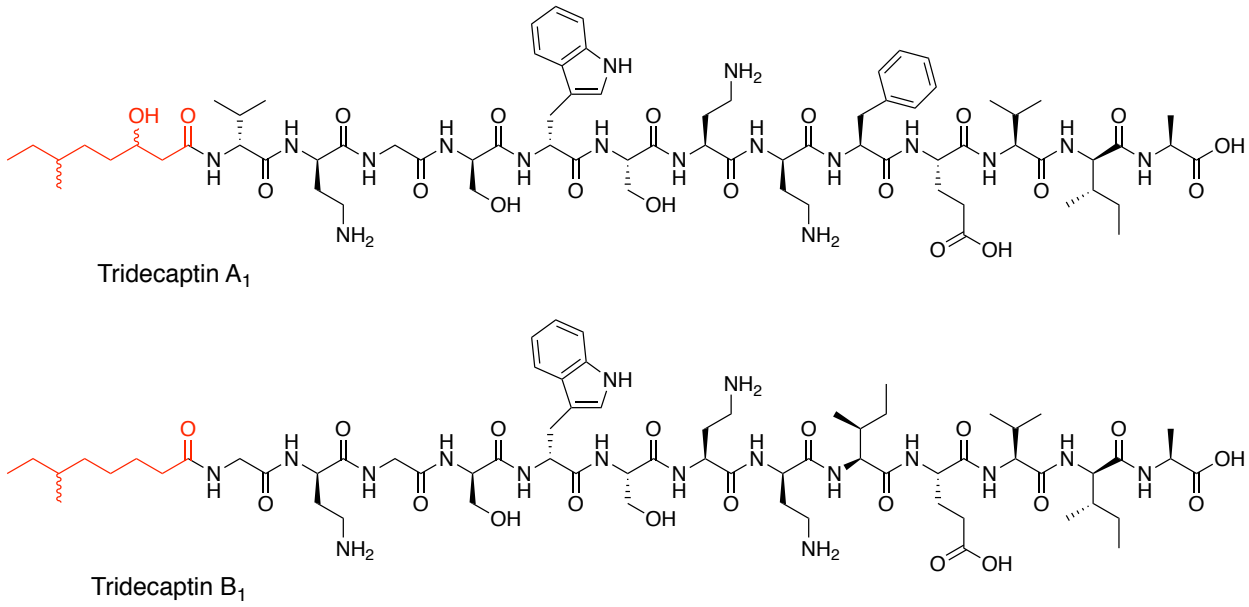

Figure 3.3. Structure of Tridecaptin A1 and Tridecaptin B1.

Chemical synthesis was applied to enhance the potency of tridecaptin A1 by modifying its lipid tail. As a result, analogues with simpler structure were prepared, and it was found that the stereochemical aspects of the tridecaptin A1 lipid tail are not crucial for its antimicrobial activity.[223]

3.4.1 Synthesis of tridecaptin A1 analogs using solid phase peptide synthesis

Tridecaptin A1 and its analogs were prepared by solid phase peptide synthesis (SPPS) chemistry.[224] This well-established synthetic method was invented by Robert Bruce Merrifield who was awarded the Nobel Prize for his revolutionary innovation in 1984. Frequently, the α-amino group of the amino acid building blocks is protected with a Fmoc group, which is base-labile, while all other reactive functional groups over the side-chains are protected with acid-labile groups. Normally, polystyrene

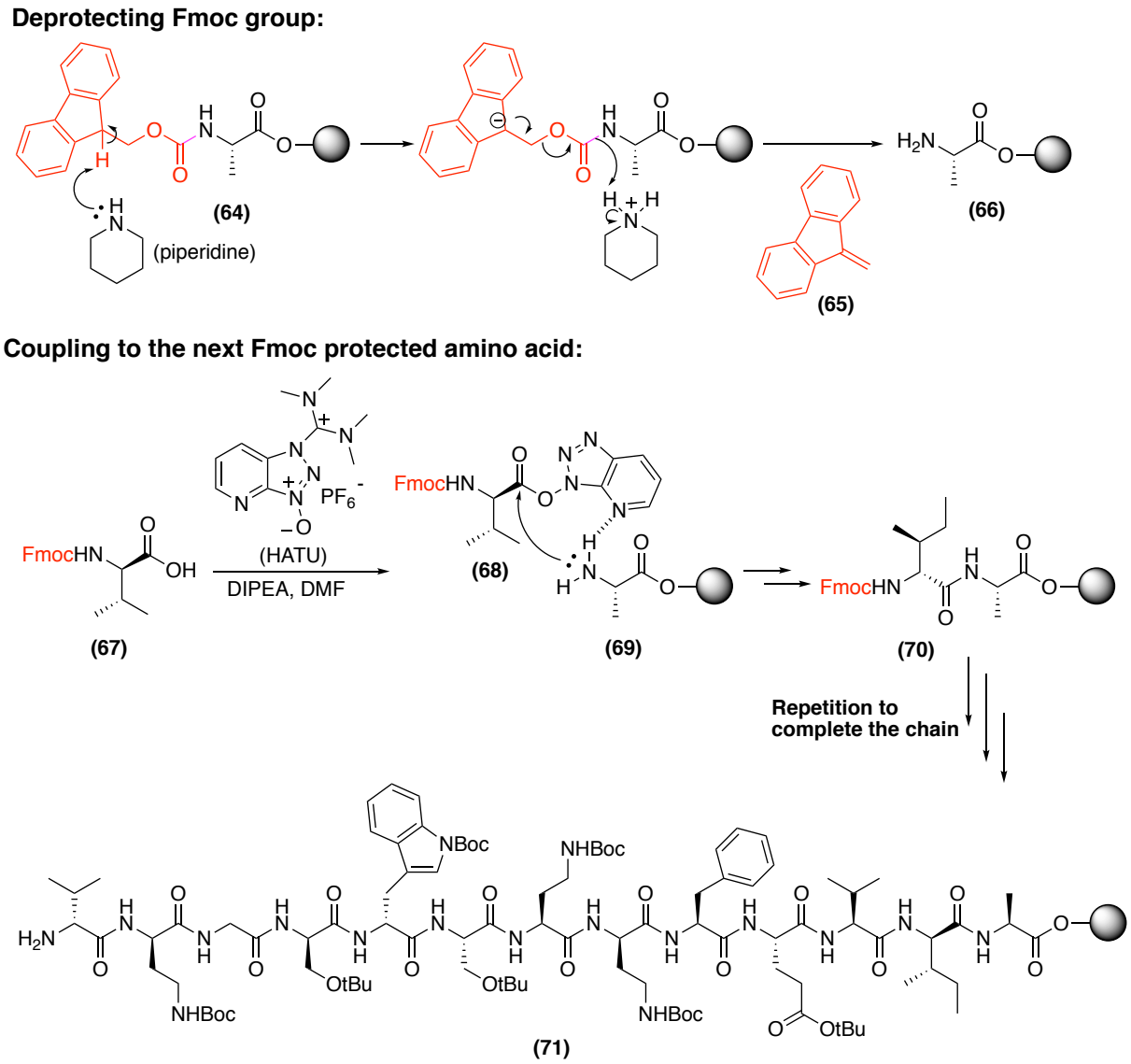

Scheme 3.1. General approach in solid phase peptide synthesis.

beads are loaded with the C-terminal amino acid in the peptide chain, allowing sequential elongation of the peptide toward the N-terminal, with purification at each step by simple washing and filtering of the resin. These quick steps will remove all the excess reagents and side products conveniently.

The synthesis of tridecaptin A1 analogs was performed by loading Fmoc

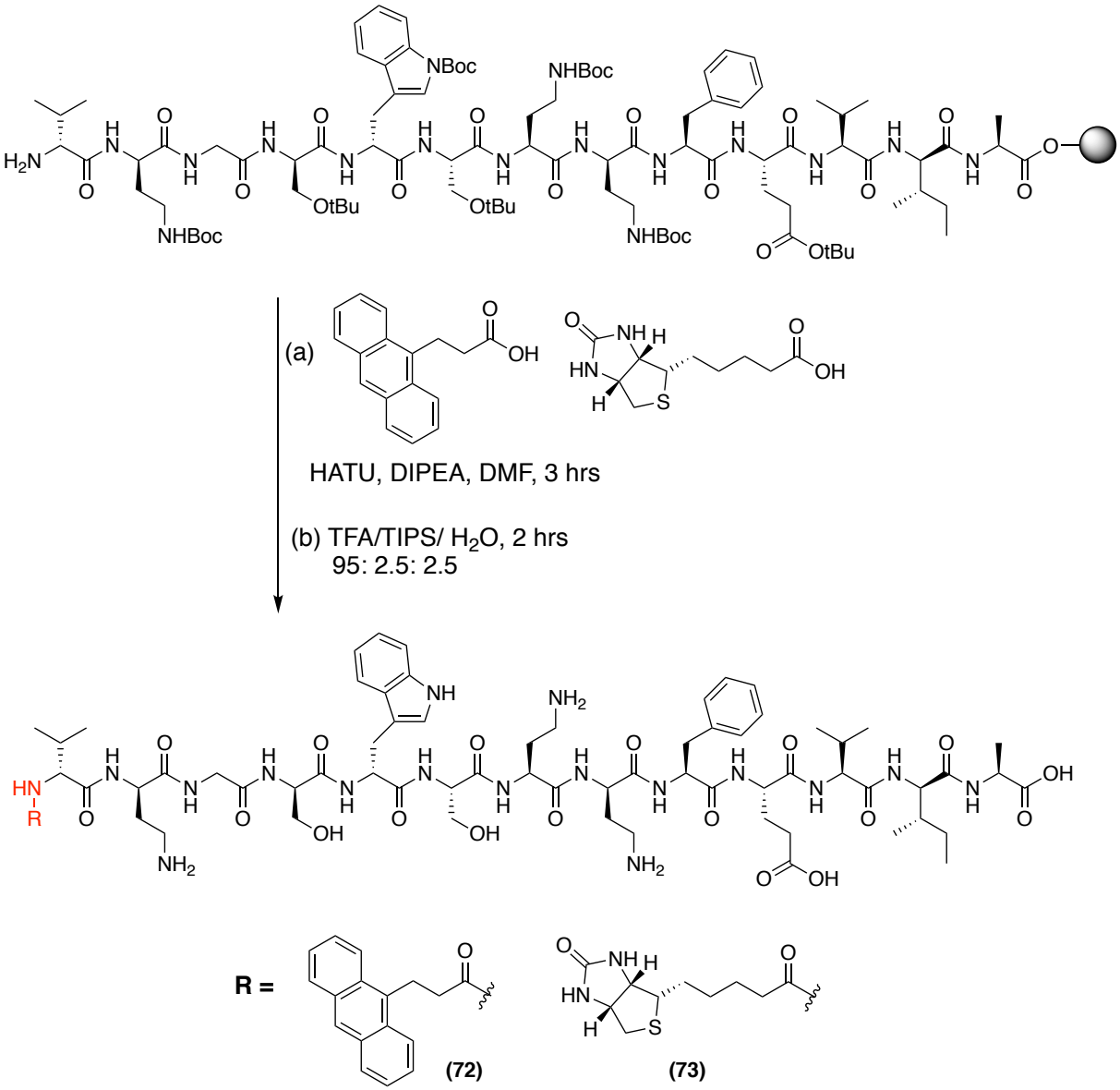

Scheme 3.2. Coupling of biotin/anthracene to the N-terminal of tridecaptin A1.

protected alanine over trityl resin. In the following step, the Fmoc protecting group was removed from the amine functionality by treating the resin-bound alanine with a 20% solution of piperidine in dimethylformamide (DMF) (Scheme 3.1). The result of this deprotection was the formation of amine (66) and fulvene (65) as a side product. The latter compound absorbs under UV light, which can be used to monitor

the completion of the deprotection step of the SPPS. Then, the next amino acid Fmoc-d-allo-Ile-OH (67) was pre-activated with HATU, a coupling reagent used to make an activated ester (68). To perform the next coupling step, the formation of a new peptide bond, the solution of the activated ester was added to amine (69) to give a dipeptide (70). This sequence of deprotection and coupling was repeated until the full peptide chain was synthesized.

Next, to finalize the synthesis of the tridecaptin A1 analog, the tail of interest, for example anthracene (72) or biotin (73), can be coupled to the peptide while it is still bound to the resin. To perform this step, the Fmoc protecting group on the N-terminal amino acid was removed, and then, either anthracene or biotin was converted to an activated ester using the coupling reagent HATU. Gentle stirring of the resin bound tridecaptin A1 with five equivalents of the activated tail of interest for 3 hours in DMF yielded the N-terminally acylated peptide (Scheme 3.2). The resin bound peptide was then treated with a cleavage solution (TFA: TIPS: H_2O; 95: 2.5: 2.5) to release the deprotected peptide from the resin. The crude peptide was precipitated from a cold solution of diethyl ether. The peptide was re-dissolved in a mixed solution of H_2O:ACN (50:50) and purified using HPLC to yield the final pure product.

3.4.2 Mechanistic studies on tridecaptin A1

3.4.2.1 Bacterial growth kinetic study

An effective approach for studying antibiotic mechanism is to measure the time taken by the compounds to exert its activity.[18] If an antibiotic compound halts cell

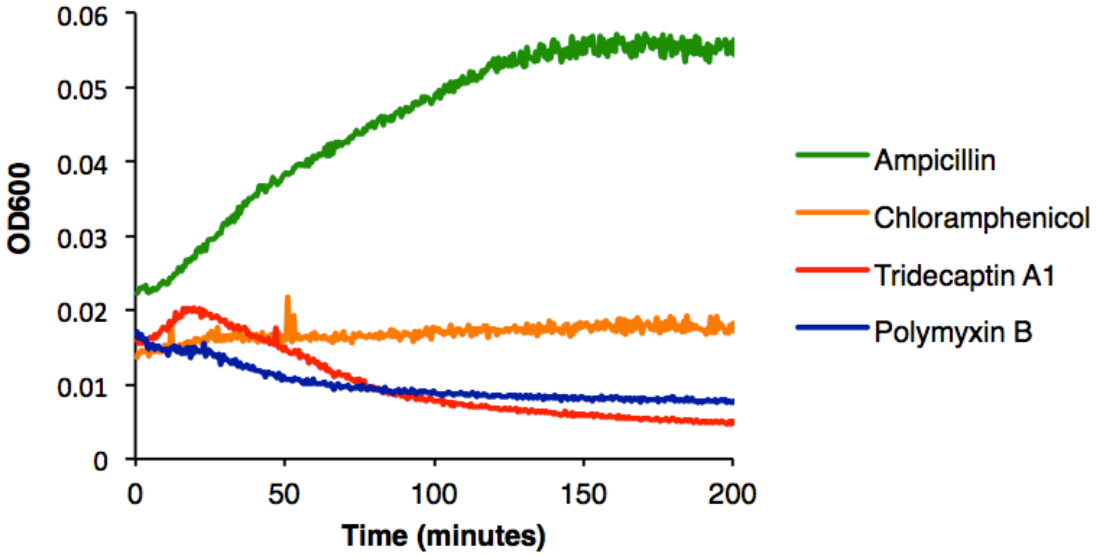

Figure 3.4. Bacterial growth kinetics comparing the activity of tridecapin A1 with other antibiotics with a known mechanism of activity against *E. coli.*

division without diminishing the number of viable cells, it is classified as a bacteriostatic agent. To be effective, this class of antibiotic must work together with our bodies' immune system to kill off the microbes and clear the infection. Examples of bacteriostatic antibiotics are tetracyclins, which inhibits protein synthesis or rifampicin, which inhibits RNA synthesis.[225,226]

However, If an antibiotic is capable of diminishing the number of viable bacterial cells, it is a bactericidal agent, and measuring the time taken to exterminate the bacteria provides valuable information. β-Lactams are bactericidal antibiotics that inhibit the biosynthesis of peptidoglycan and exert their activity through binding to penicillin-binding proteins. Therefore, cells affected by these antibiotics lose the capacity to crosslink the peptidoglycan, which is crucial to sustain the cellular integrity. The time needed for β-lactams to exert their activity is in the range of 3 hours or more, but antimicrobial compounds targeting the cell membrane are

exterminating bacterial cells in a range of minutes.[72]

In this study, *E. coli* cells were exposed to tridecaptin A1 as well as other antibiotics with known mechanisms of action, and the time taken by tridecaptin A1 to kill cells was compared with that of other antibiotics. Among those, chloramphenicol is a protein-synthesis inhibitor, ampicillin is a peptidoglycan biosynthesis inhibitor and polymyxin B is a membrane targeting agent. In a period of three hours, the optical density of the cells pre-treated with these antibiotics (2 x MIC) was measured. As a result, it was found that, after being exposed to tridecaptin A_1, cells were still able to grow at a diminished rate for about 20 minutes, followed by a steady decrease in the number of cells. Ampicillin, a β-lactam antibiotic, needs an expected delay time of 3 hours to exert its activity, polymyxin B reduces the number of viable cells from the beginning and chloramphenicol, a bacteriostatic agent, does not reduce optical density (Figure 3.4). This experiment was performed by Dr. Brandon Findlay.

3.4.2.2 Time-kill assay

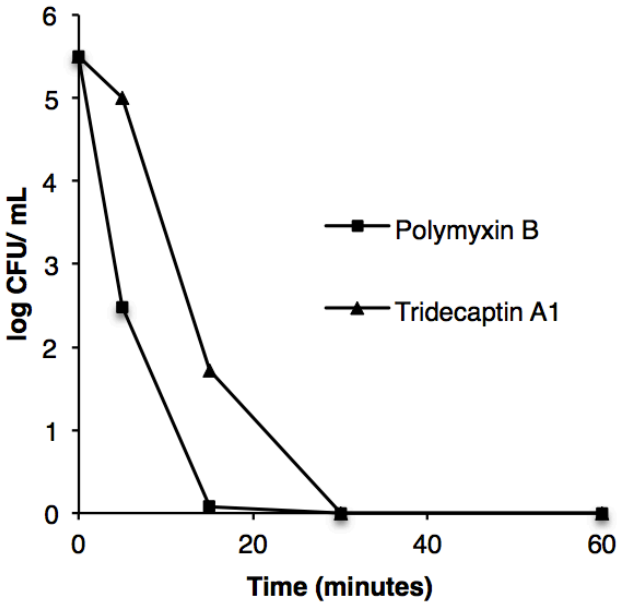

Figure 3.5. Time-kill assay comparison of tridecaptin A1 and polymyxin B activity against *E. coli*.

A similar approach to that of bacterial growth kinetics is the time-kill assay.[227] To perform this assay, an indicator strain of bacterial cells was mixed with antibiotics at a concentration ten times that of the MIC. Then, at certain time points, an aliquot of this mix of bacteria cells and antibiotic are diluted and streaked on an agar plate with no antibiotic. The bacteria cells on the plate were grown overnight, and the number of bacterial colonies was counted the next day. This experiment indicated that the time taken by the antibiotic to kill all the cells (Figure 3.5). It can be seen from the figure that polymyxin B exerts its activity much faster than tridecaptin A1; polymyxin B can exterminate the bacterial cells in a span of 30 min. The combination of growth-kinetic assays and time-kill assay suggested that the target for tridecaptin A1 is the bacterial membrane. This experiment was performed by Dr. Brandon Findlay.

3.4.2.3 Inner-membrane depolarization assay

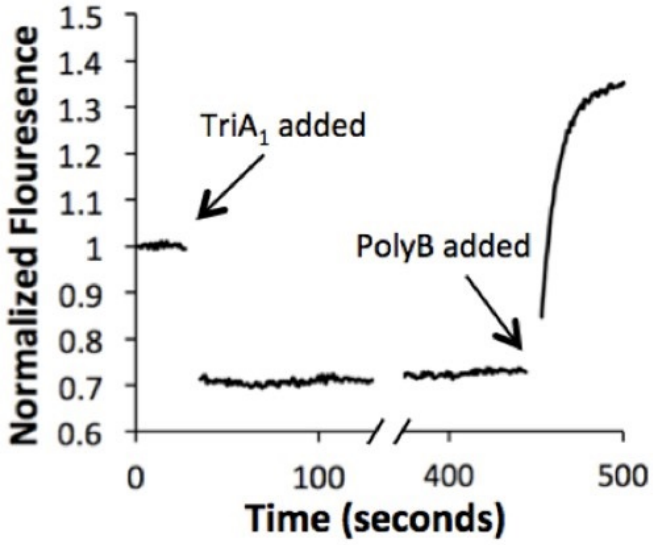

Figure 3.6. Membrane depolarization experiment with the aid of the potential sensitive dye $DiBAC_4$ (3).

The inner-membrane depolarization assay is an effective method to study the possibility of interaction between an antimicrobial compound and the membrane. $DiBAC_4$(3) is a bisoxonol dye suitable properties for bacterial membrane studies. It can be used to estimate the potassium gradient across the bacterial inner membrane using fluoroscopy.[228] There is a high concentration of potassium ions on the exterior side of the inner-membrane, so this negatively charged dye first penetrates through the outer-membrane. It then accumulates on the external part of the inner-membrane where the potassium ions are. If the inner-membrane is ruptured, for example by a membrane-damaging antibiotics, the potassium-ion gradient will disappear. At this stage, the dye molecules will enter the cytoplasm where they will bind to hydrophobic proteins leading to an increase in fluorescence signal. In this assay, *E. coli* cells were pretreated with $DiBAC_4$(3) and then exposed to tridecaptin A1 (2xMIC), which did not

cause the fluorescence to increase. As is evident from Figure 3.6, the addition of tridecaptin A1 only caused a dilution effect, which is observed as a decrease in the fluorescence signal. This result suggests that tridecaptin A1 cannot induce depolarization of the inner-membrane. However, subsequent to polymyxin B addition, depolarization of the inner membrane was observed by a fluorescence enhancement, which also shows that the dye was functional under applied experimental conditions. This experiment was performed by Dr. Brandon Findlay.

3.4.2.4 Inner-membrane disruption study

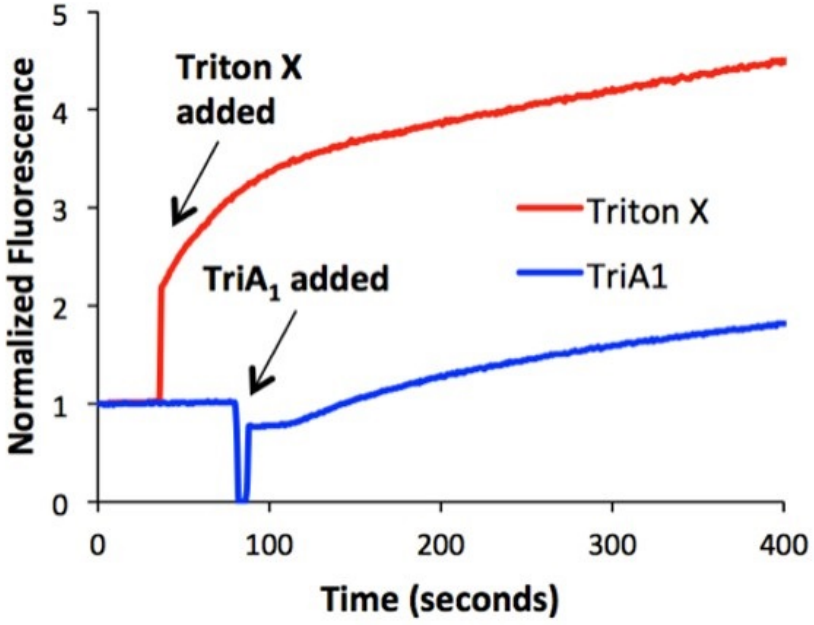

Figure 3.7. SYTOX Green dye and membrane-disruption assay.

To study whether or not tridecaptin A1 can lyse the inner-membrane, a membrane-disruption assay was used which employed SYTOX Green, a dye that shows an enhancement in fluorescent signal intensity if it crosses the inner-

membrane to bind to nucleic acids in the cytoplasm.[199] Basically, if the antibiotic induces the formation of large pores on the inner-membrane, a fluorescence signal intensification is expected. SYTOX Green is also called a “live/dead” stain because the fluorescence signaling by this dye results in the formation of large tears that cause rapid cell death. In the assay, *E. coli* cells were pretreated with SYTOX Green and then exposed to tridecaptin A1, but only very slow fluorescence signal increase was observed (Figure 3.7). As a positive control, subsequent addition of the surfactant TritonX-100 caused fluorescence signal intensification up to 6-fold. By comparison, there is correlation between the death rate in the time-kill assay and a fluorescence enhancement in SYTOX Green (approximate doubling in fluorescence over five min), from which it can be concluded that the fluorescence intensification is related to the number of dead cells. Furthermore, formation of tears over the membrane is not a prompt consequence of tridecaptin A1 exposure. This experiment was performed by Dr. Brandon Findlay.

3.4.2.5 Proton-motive force disruption assay

The results for $DiBAC_4(3)$ and SYTOX Green were in contrast to what was predicted from the time-kill assay that demonstrated rapid killing of *E. coli* cells. Inhibition of nucleic acid synthesis, protein synthesis or biosynthesis of peptidoglycan cannot be the mechanism of action of tridecaptin A1 because it can exterminate most cells within 30 min after exposure, and these mechanisms of action are acting over a much longer span of time. The rapid rate of killing is an indication that tridecaptin A1 may attack the membrane, and this is supported by the importance of the lipid tail importance for the antimicrobial activity of tridecaptin A1 and the outer-membrane

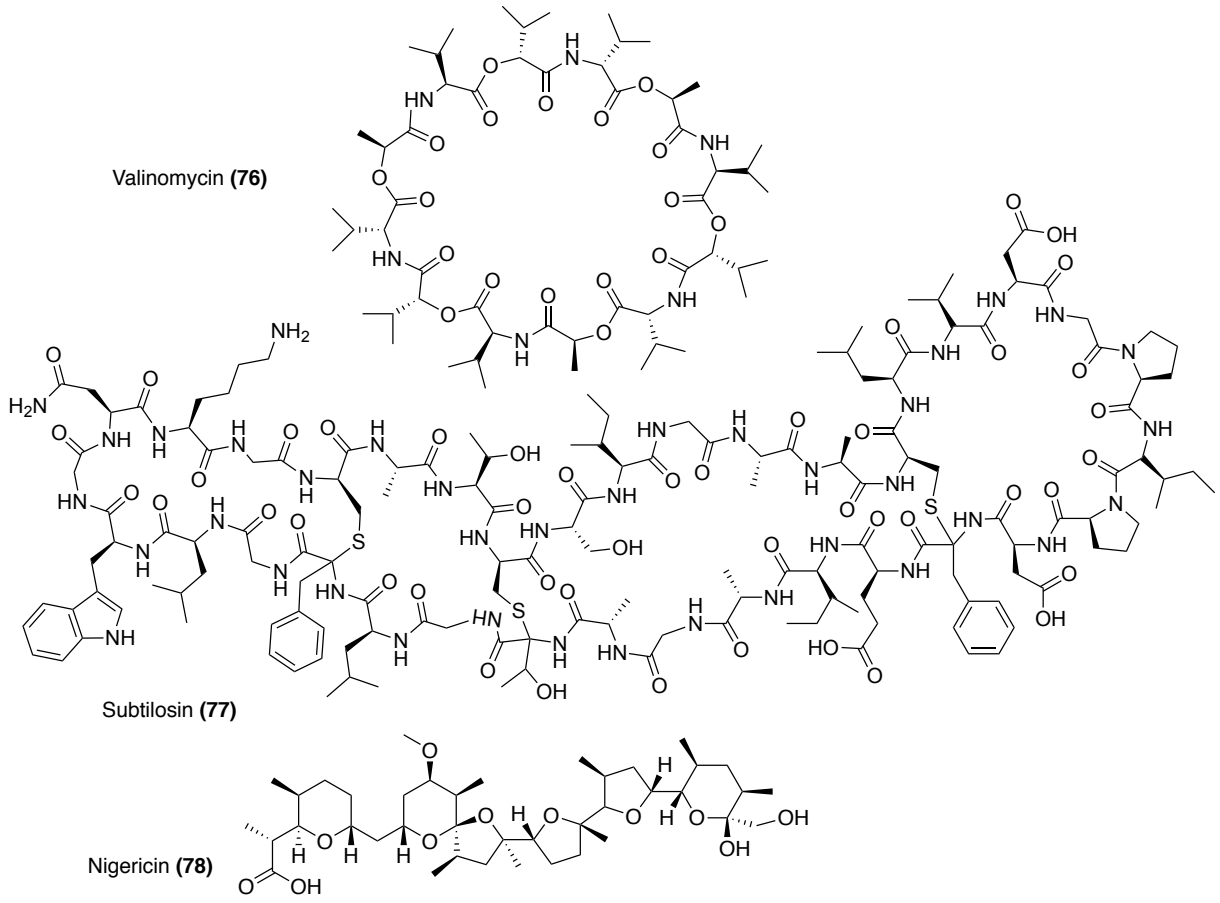

Figure 3.8. Antibiotics with proton-motive force disruption capacity.

disruption.[223] Therefore, we started to look into an alternative membrane-targeting mechanism that could be compatible with the experimental observation of a rapid kill rate.

A proton-motive force exists at the cytoplasmic membrane.[229] It is an indispensable biological phenomenon for cell growth since protons and potassium ions gradients drives the production ATP with the proton-motive force.[230] The electric potential (ΔΨ) and the pH gradient (ΔpH) are two main components of proton-motive forces, where ΔpH refers to the difference between the pH inside and outside the

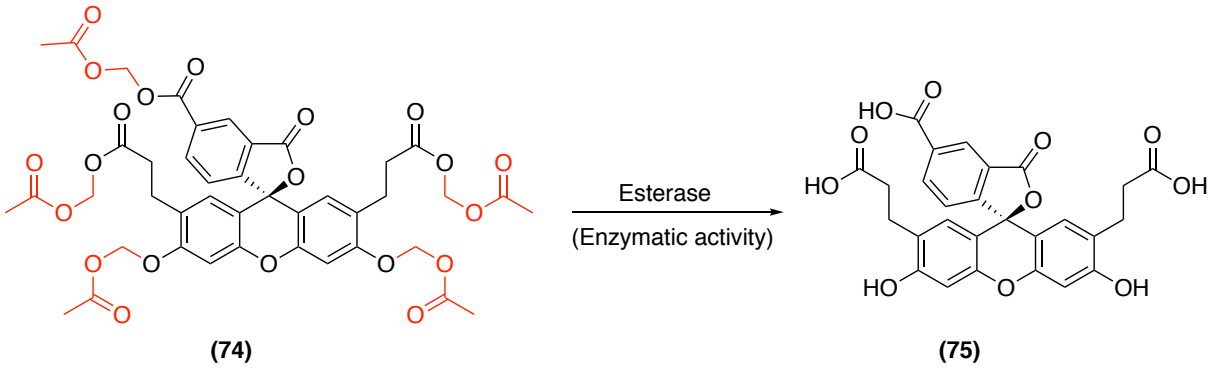

Figure 3.9. Hydrolysis of BCECF-AM in the cytoplasm.

membrane. The antibiotic nigericin (78) is known to be an antiporter of K^+ and H^+ and is able to vanish the ΔpH (Figure 3.8). The electric potential difference between outside and inside of the membrane is under the control of Na^+ and K^+ ion gradients. Valinomycin (76) has ionophore activity and can dissipate ΔΨ through selective binding to K^+ ions. The disruption of the proton-motive force has been known as a bactericidal mechanism of action by subtilosin (77), a bacteriocin acting on the Gram-positive bacterium *Gardnerella vaginalis.*[231] Subtilosin which is a cyclic lantibiotic produced by *Bacillus subtilis* KATMIRA 1933 and interact with membrane electrostatically.[232]

As an approach to elucidate the mechanism of action for tridecaptin A1, the possibility of exerting activity by disruption of the proton-motive force was studied. This idea was examined by designing an assay using of the pro-dye BCECF-AM (Figure 3.9) in Gram-negative bacteria. BCECF-AM is a pH sensitive dye that was frequently used for mammalian cell intracellular pH measurements. Within its structure, there is a fluorescein core and several acidic functionalities protected by acetoxymethyl esters. The presence of hydrophobic functionalities, including ester

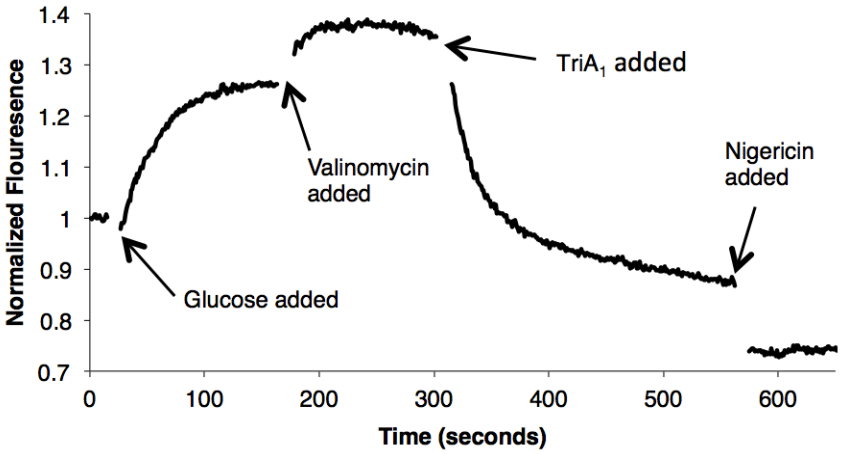

Figure 3.10. BCECF fluorescence from the cytoplasm of *E. coli* cells that are sequentially treated with glucose, valinomycin, tridecaptin A_1 and nigericin.

groups, allow the dye to cross the cytoplasmic membrane. Inside the cytoplasm, the dye is hydrolyzed by non-specific esterases to produce the active dye BCECF (75).

The pk_a for the dye is 7, and as the pH decreases from 8 to 6, the fluorescence intensity also diminishes.[233] To perform this experiment, *E. coli* were suspended in a buffer with pH 6. The cytoplasmic pH was between 7.0 – 7.4, which was different from that of the buffer. To make the *E. coli* outer membrane permeable to BCECF-AM, the cells were treated with EDTA, a divalent chelating reagent, to coordinate ions such as $Ca^{2+}$and Mg^{2+}. These ions are associated with the LPS on its phosphate groups, therefore, further coordination to EDTA causes loss of some LPS from the outer-membrane, and this exposes the phospholipids and facilitates the permeation of hydrophobic molecules.[234] Fluorescence signal enhancement was observed after the addition of glucose to the EDTA/BCECF-AM treated *E. coli* cells, which resulted from cytosolic pH elevation, signaling that the dye is functional under the applied experimental conditions (Figure 3.10).[231] To determine the net impact of

tridecaptin A1 on the proton gradient, valinomycin was added to the bacterial solution to dissipate the electric potential, and the outcome was observed as a small intensification of the fluorescence signal. This was followed by the addition of tridecaptin A1, which led to a rapid fluorescence signal fading. The latter was a result of pH alteration; protons flow from the buffer into the cytoplasm.

Upon addition of nigericin, a similar outcome of rapid decrease in the fluorescence signal was observed. Comparison between these observations from nigericin and tridecaptin A1 suggests that tridecaptin A1 disrupts the proton gradient on the inner-membrane of *E. coli* cells. Maintaining the proton gradient is vital in the cellular process to generate ATP, and we suggested that tridecaptin A1 attacks the proton-motive force to kill *E. coli.* This experiment was performed by Dr. Brandon Findlay.

3.5 Conclusions

Lipopeptides are an important class of AMPs that are showing a promising future for use as antibiotics against Gram-negative bacterial strains. This class of AMPs can be prepared with the powerful tool of solid phase synthesis, therefore, they can be enhanced structurally, and more potent members of this class of AMPs can be designed and synthesized. Tridecaptins are among the most interesting class of lipopeptides with versatile structures. Mechanistic studies have revealed that tridecaptin A1 can exert its mechanism of action through interaction with the bacterial membrane to disrupt the vital process of proton-motive force.

In summary, mechanistic studies on tridecaptin A1 and solid-phase synthesis

of tridecaptin analogues were described. The future prospect for this project involves NMR studies between tridecaptin A1 and membrane mimicking micelles: ^{13}C-labeled and/or deuterated dodecylphosphocholine (DPC). In the tridecaptin project, synthesizing the labeled DPC was the last thing that I worked on. A colleague in our group is currently continuing this project.

Chapter 4 Experimental procedures

4.1 Synthetic procedures

4.1.1 Reagents, solvents and purification

Commercially available reagents were purchased from Chem-Impex International, Sigma-Aldrich Canada Ltd., Fisher Scientific Ltd., Alfa Aesar Ltd., Caledon and ANA Spec. They were used without further purification unless otherwise stated. Solvents were of American Chemical Society (ACS) grade quality, and were used without further purification unless otherwise stated. Water-sensitive reactions were conducted in flame-dried glassware under a positive pressure of argon. The solvents used for water sensitive reactions were distilled prior to use: diethyl ether and tetrahydrofuran (THF) were distilled over sodium with benzophenone as an indicator, and methanol was distilled over magnesium. Hexanes, methanol, acetonitrile, *N,N*-dimethylforamide (DMF) and 2-propanol (IPA) of HPLC grade quality were used with no further purification. ACS grade solvents (>99.0% purity) were purchased commercially and used for column chromatography without further purification. A Milli-Q reagent water system (Millipore Co., Milford, MA) was the source of deionized water. Glass plate thin layer chromatography (TLC) with an ultraviolet (UV) fluorescent indicator (normal SiO_2, Merck 60 F254) was used to monitor the progress of reactions and to check the fractions from column chromatography. The following techniques were employed for TLC visualization: staining with phosphomolybdic acid in ethanol (10 g/ 100 mL), permanganate ($KMnO_4$:K_2CO_3:NaOH:H_2O with ratios of 1.5 g:10 g:0.12 g:200 mL) or ninhydrin (ninhydrin:acetic acid:*n*-butanol with ratios of 0.6 g:6 mL:200 mL) and UV absorption by fluorescence quenching. Purifications by flash chromatography were performed

using Merck type 60, 230–400 mesh silica gel. A Büchi rotary evaporator was used in order to remove solvents under reduced pressure. High performance liquid chromatography (HPLC) on an analytical scale was performed on a Gilson chromatograph equipped with model 322 pump heads, model 171 diode array detector, FC 203B fraction collector and a Rheodyne 7725*i* injector fitted with 1000 µL sample loop. Preparative and semi preparative scale HPLC was performed on a Gilson chromatograph equipped with model 322 pump heads, model UV/VIS-156 detector, a GX-271 liquid handler and a Vydac C_{18} (5 µm, 4.6 x 250 mm) or Phenomenex C_{18} column (5 µm, 21.2 x 250 mm). HPLC solvents were filtered and degassed prior to use.

4.1.2 Synthetic product characterization

A Perkin Elmer 241 Polarimeter with a microcell (10 cm, 1 mL) was used to measure optical rotations at ambient temperature, and the results were reported in units of 10^{-1} deg cm^2 g^{-1}. All the reported optical rotations were referenced against air and measured at the sodium D line (λ = 589.3 nm). A Nicolet Magna 750 FT-IR spectrometer or Nic-Plan FT-IR microscope were used to measure infrared spectra (IR). The term ‘’cast’’ was applied when sample loading was done by evaporation of a solution on a NaCl plate. Varian Inova 600, Inova 500, Inova 400, Inova 300 or Unity 500 spectrometer machines were used to record the nuclear magnetic resonance (NMR) spectra at 27 °C. For recording ^{1}HNMR spectra (300, 400, 500 or 600 MHz), chemical shift values (δ) were referenced to $CDCl_3$ (7.26 ppm), D_2O (4.79 ppm), CD_3OH (3.30 ppm), CD_2Cl_2 (5.32 ppm) or DMSO-d_6 (2.50 ppm) and for ^{13}C spectra

(75, 100, 125 or 150 MHz), chemical shift values were referenced to $CDCl_3$ (77.0 ppm), CD_3OH (49.0 ppm), CD_2Cl_2 (53.8 ppm) or DMSO-d_6 (39.5 ppm). Splitting patterns are reported using the following abbreviations: s = singlet, d = doublet, t = triplet, q = quartet, m = multiplet. Mass spectra (MS) were recorded on Applied BioSystems Mariner BioSpectrometry Workstation, Kratos AEIMS-50, Agilent Technologies 6220 oaTOF and Perspective Biosystems VoyagerTM Elite MALDI-TOF MS using either 3,5-dimethoxy-4-hydroxycinnamic acid (sinapinic acid) or α-cyano-4-hydroxycinnamic acid (CHCA) as a matrix. Waters (Micromass) Q-TOF Premier was used to perform LC MS/MS. To perform MALDI-TOF MS, the sample was prepared according to the following procedure. A peptide solution (1 µL) in 0.1% TFA (aq.) was mixed with a solution of sinapinic acid (10 mg/mL) in 50% acetonitrile containing 0.1% TFA (aq.) in a 1:1 ratio (vol/vol). In order to prepare the sample over the plate, a sinapinic acid layer was spread over a MALDI plate using a pipette. After the solvent was evaporated, a layer of sinapinic acid was left on the surface of the plate. Then, the sample matrix solution (1 µL) was spotted onto the dried layer of sinapinic acid, which was left to dry.

4.1.3 HPLC purification method

Lacticin 3147 HPLC purification (73, 75): on a Gilson, preparative HPLC system equipped with a model 322 HPLC pump, GX-271 liquid handler, 156 UV/vis detector and a 10-mL sample loop. Method: GraceVydac Protein and Peptide C18 100 mm column 10 micron; flow-rate 10 mL/min, UV = 220 nm, Gradient = water/acetonitrile (70:30) for 5 min, then the acetonitrile percentage was ramped up

to 95% over 45 min, kept at this ratio for 5 min, then the ratio of acetonitrile was lowered to 30 % over 3 min and maintained at this ratio for 5 min.

Nisin HPLC purification (21): GraceVydac Protein and Peptide C_{18} 100 mm column 10 micron; flow rate 10 mL/min, UV = 220 nm, Gradient = water/acetonitrile (85:15) for 5 min, then the acetonitrile ratio was ramped up to 60% over 30 min, kept at this ratio for 10 s, then, quickly the acetonitrile ratio was reduced to 15% over 30 s. This ratio was maintained for 5 min.

Lipid II HPLC purification (63): GraceVydac Protein and Peptide C_{18} 100 mm column 10 micron; flow rate 10 mL/min, UV = 220 nm, Gradient = 100 % 50 mM NH_4HCO_3 (aq) to 100% MeOH over 30 min.

Tridecaptin HPLC purification (72, 73, 95): Gilson preparative system, Phenomenex C_{18} column; flow rate 10 mL/min, UV= 220 nm. Gradient: started from 20% ACN (0.1% TFA) and 80% water (0.1% TFA) for 5 min, ramped up to 55% ACN over 30 min, then ramped up to 95% ACN over 3 min, stayed at 95% ACN for 3 min, ramped down to 20% ACN over 2 min and then kept at 20% ACN for 5 min.

4.2 General microbiology procedures

4.2.1 Isolation of lacticin 3147 A1 and A2

Isolation of the lacticin 3147 peptides was performed by following a previously reported literature procedure with modifications.[66] A glycerol stock of *Lactococcus lactis* subsp. *lactis DPC3147* was used to inoculate a 50 mL culture of Difco M17 broth, which was incubated overnight at 30 °C without shaking. Then, the overnight

culture was used to inoculate 4 x 1 L (1% inoculum) culture flasks containing liquid media that were prepared as follows: per 800 mL; yeast extract 5.0 g, tryptone 2.5 g, D/L-methionine 1.5 g, $MnSo_4 \cdot 4H_2O$ 50 mg and $MgSO_4$ 125 mg. This media contained hydrophobic components, that would interfere with the isolation of the hydrophobic peptides. To clarify the media of any hydrophobic constituents, the solution media was passed through an Amberlite XAD-16 resin (Aldrich), and about 60 g of the resin was packed in a glass column (2.5 x 40 cm). This was followed by sterilization of the media. Next, per 800 mL of the prepared media, 100 mL sterilized solutions of D-glucose (100 g/L) and β-glycerophosphate (190 g/L) were added. The resulting cultures were incubated at 30 °C for 24 h. The cell pellets were collected by centrifugation (4 °C, 25 min, 6000 rpm) and re-suspended in 7:3 isopropanol: water + 0.1% trifluoroacetic acid. This suspension was stirred for 4 h at 4 °C, and the cells were removed by centrifugation (4 °C, 20 min, 8000 rpm). The resulting supernatant was concentrated to ~50 mL with a rotary evaporator. A disposable C18 column (Strata C18-E, 10 g/60 mL, 55 µm, 70A) was pre-equilibrated by washing with 50 mL methanol, followed by 100 mL of Milli-Q water. The supernatant was then loaded onto the column at 2 mL/min, followed by sequential washes of the column with 60 mL of water, 60 mL of 30% ethanol and 40 mL of 25% isopropanol. The peptides were then eluted from the column by washing the column with 4:1 isopropanol:water + 0.1% trifluoroacetic acid. The volume of this fraction was reduced to ~ 15 mL and further purified by Reversed-Phase High Performance Liquid Chromatography (RP-HPLC) on a Gilson preparative HPLC system equipped with a model 322 HPLC pump, GX-271 liquid handler, 156 UV/vis detector and a 10 mL sample loop. Method:

GraceVydac Protein and Peptide C18 100 mm column 10 micron; flow-rate = 10 mL/min, UV = 220 nm, Gradient = water/acetonitrile (70:30) for 5 min, then the acetonitrile ratio was ramped up to 95% over 45 min, kept at this ratio for 5 min, then the acetonitrile ratio was lowered to 30 % over 3 min and maintained this percentage for 5 min.

4.2.2 Purification of nisin

Nisin is commercially available (Alfa Aesar), but it also contains sodium chloride and other small peptides. To purify nisin efficiently, 500 mg of the commercial material was suspended in 10 mL of 35% acetonitrile (0.1% TFA) followed by sonication for 5 min. The insoluble material was separated through centrifugation, and the supernatant was used for HPLC purification (see 4.1.3).

4.2.3 Fluoroscopy Experiments

Measurements were performed on a 75 XE PTI Fluorescence spectrophotometer, with all slits open 1 mm and measurements taken every second. Results were visualized in Felix32 analysis software, and analyzed in Microsoft Excel.

4.2.4 BCECF Containing LUV Preparation

BCECF containing LUVs were prepared as previously described.2 1,2-Dioleoyl-sn-glycero-3-phosphoethanolamine (DOPE) (16 mg) and 1,2-dioleoyl-sn-glycero-3-phospho-(1'-rac-glycerol) (DOPG) (4 mg) were dissolved in chloroform (2

mL). If necessary Gram-positive lipid II (obtained from the BaCWAN synthetic facility at the University of Warwick, United Kingdom) was then added as a solution in 2:3:1 $CHCl_3$:MeOH:H_2O to 1 mol%. The solution was thoroughly mixed by shaking, then the solvent was removed under reduced pressure and the film dried in the dark under high vacuum overnight. The desiccated lipids were rehydrated with potassium phosphate buffer (50 mM, pH 8, 2 mL) and BCECF acid (2 mM, 10 µL). In dim light the solution was shaken thoroughly, vortexed and transferred to a 5 mL cryovial. The vial was frozen in liquid nitrogen, and thawed at 37 ^{o}C. The lipids were shaken thoroughly until finely suspended (vortexing was insufficient) and re-frozen. This process was repeated five times in total. The finely dispersed vesicles were extruded 21 times (back and forth 10.5 times) through a lipid extruder (Avanti Polar Lipids) containing a 100 nm pore. Non-encapsulated dye was removed by passing the pale-yellow solution through a Sephadex G-50 size exclusion column (50 mM potassium phosphate buffer as eluent, pH 8). The vesicles were then stored in the dark on ice at 4 ^{o}C for further use.

4.2.5 Preparation of Lipid II LUVs for ITC studies

LUVs were prepared as previously described.2 DOPE (16 mg) and DOPG (4 mg) were dissolved in chloroform (2 mL). Gram-positive lipid II was then added as a solution in 2:3:1 $CHCl_3$:MeOH:H_2O to 1 mol%. The solution was thoroughly mixed by shaking, then the solvent was removed under reduced pressure and the film dried in the dark under high vacuum overnight. The desiccated lipids were rehydrated with potassium phosphate buffer (50 mM, pH 6.7, 2 mL). The solution was shaken thoroughly, vortexed and transferred to a 5 mL cryovial. The vial was frozen in liquid

nitrogen and thawed at 37 ^{o}C. The lipids were shaken thoroughly until finely suspended and re-frozen. This process was repeated five times in total. The finely dispersed vesicles were extruded 21 times (back and forth 10.5 times) through a lipid extruder (Avanti Polar Lipids, AL) containing a 100 nm pore.

4.2.6 ITC Binding Study

The binding experiments were performed on an MCS isothermal titration calorimeter (Microcal, Northampton, MA) at 25 °C. Lipid II containing LUVs were injected into the cell containing 20 μM (or 100 μM depending on quality of the purified peptides) of the desired peptide/peptide mixture in the same buffer system. We found that peptide aggregating in solution is a major obstacle for ITC binding detection. To overcome this issue, several cycles of dissolving the peptide in acetonitrile and water, and sonication followed by lyophilization and passing the peptides through an antistatic device were helpful. Furthermore, we found that a small quantity of oxidized peptide also triggers peptide aggregation, therefore, peptides should be kept cold and under argon for each experiment. The applied experiment conditions include temperature = 25 °C, reference power = 17 μalcal/s, syringe-stirring speed = 300 rpm, number of injections = 29, injection volume = 5 μL and time between injections = 240 s. Heat change during the experiment was recorded in real time and raw data was processed using the Origin® 7 software. For controls, LUVs were injected into buffer, and buffer was injected into peptide solutions. In all cases the heats of dilution were significantly lower in comparison with ligand-receptor bindings.

4.2.7 *In vitro* assay using BCECF LUVs

For BCECF experiments, the excitation and emission wavelengths on the fluorescence spectrometer were set to 500 nm and 522 nm, respectively. Freshly prepared lipid vesicles (50 µL) were added to potassium phosphate buffer (50 mM, pH 6, 2 mL), and a small stir bar was used to properly disperse the vesicles. The fluorescence was monitored for approximately 100 s to establish a baseline. BCECF LUVs with no lipid II or 1 mol % Gram-positive lipid II were treated with the desired peptide/peptide mixture (to a final concentration of 5 µM or 100 nM), and fluorescence was monitored for another 100 s. The experiments shown are representative of results from three technical replicates.

4.2.8 Time-kill assay

This assay was performed according to a previously reported literature procedure.[72] *Lactococcus lactis* subsp*. cremoris HP* was grown overnight (OD600 = 1.1) and then diluted with Difco M17 broth to a concentration of 1x 10^6 CFU/mL. This suspension was mixed 1:1 with either 500 nM LtnA1, 2 µM LtnA1, 500 nM LtnA2 or 500 nM LtnA1 + 500 nM LtnA2. The resulting cultures were incubated at ambient temperature. At desired time points, 25 µL of culture was streaked onto an agar plate. Cells not treated with peptides were used as a negative control. Plates were incubated at 30 °C for 24 h, and the remaining colonies were counted. Agar plates were prepared using sterilized Difco M17 media containing 10% lactose and 1.5% agarose.

4.2.9 Peptide-membrane interaction study using SYTOX Green

The excitation and emission wavelengths on the fluorescence spectrophotometer were adjusted to 488 nm and 523 nm, respectively. *Lactococcus lactis* subsp*. cremoris HP* was grown to an OD_{600} = 0.38. To this cell suspension, SYTOX Green (2.5 µM, 37 µL) was added and incubated for 5 min. Peptides were added to a final concentration of 100 nM. Fluorescence was monitored for 10 min, with the peptide/peptides mixtures added after ~60 s.

4.2.10 Membrane depolarization assay

Measurements were performed over a 75 XE PTI Fluorescence spectrophotometer. All slits were open 1 mm, and data collection was done every second. Data were visualized using the Felix32 analysis software and analyzed in Microsoft Excel. For DiBAC4 experiments, the excitation and emission wavelengths were adjusted to 492 nm and 515 nm, respectively. *Lactococcus lactis* subsp*. cremoris HP* was grown overnight to OD_{600} = 0.5 using Difco M17 broth. This cell suspension (70 µL) was mixed with DiBAC4 (3 mg/L, 30 µL) and incubated at room temperature for 5 min. The mixture was transferred to a 0.2 mL cuvette, and individual or a mixture of desired peptides was added to a final concentration of 100 nM.

4.3 CD spectroscopy

CD spectra were recorded on OLIS SpectralWorks (V. 5.0.54) using the

following parameters: collection mode; Scan, number of points: 66, Monochromator = 250 to 185 nm, timing mode = as Fxn of HVs, reduction mode = Circular Dichroism, average scans mode = 5 scans averaged, scan mode = fixed bandwidth (bandwidth = 2 nm), total elapsed time for each sample = 14 min. Peptide solutions with a concentration of 1 mg/mL were used to perform the experiments.

4.4 NMR spectroscopy

Lacticin 3147 A1 lantibiotic peptide and (*E,E*)-farnesyl lipid II were dissolved in 1:1:1 CD_3OH:CD_3CN:H_2O (phosphate buffer 25 mM, pH 6.7) to a final concentration of 1 mM each. All spectra were referenced to 1% DSS (4,4-dimethyl-4-silapentane-1-sulfonic acid).[235] 1D ^{1}H-NMR and 2D homonuclear ^{1}H-^{1}H correlation spectroscopy (COSY), total correlation spectroscopy with excitation sculpting and zero quantum artifact suppression (ZTOCSY-ES),[236,237] Nuclear Overhauser Effect Spectroscopy with excitation sculpting (NOESY-ES) and Rotating Frame Nuclear Overhauser Effect experiments with excitation sculpting (ROESY-ES)[238] were acquired at 27 °C on a four-channel 700-MHz Varian VNMRS spectrometer with a z-gradient HCN cold probe. The acquisition software used by the spectrometer was VNMRJ 4.2A. NMRPipe[239] and NMRview[240] were used to process and analyze the NMR data. Manual assignment of chemical shifts was performed as previously described.[212] The NMR spectrometer parameters for experiments are described in Table 4.6.

4.4.1 CYANA structural calculation

The structure of the complex between synthetic lipid II and LtnA1 was calculated using CYANA 2.1.[213] Seven cycles were done with 10000 steps per cycle producing 100 structures. NOESY cross peaks were assigned automatically. A total number of 271 NOE distance restraints were kept and used by CYANA in the final structure cycle (193 short-range, 33 medium-range, 45 long-range). Structural statistics are provided in Table 4.5.

The determination of the solution structure of the complex necessitated custom additions to the standard cyana library for all non-conventional amino acids. The PDB structure of 1WCO was used as a starting point and was followed by additional modifications using PyMOL.[241] The definition of non-standard residues was carried out in agreement with cyana's library format.[242] Furthermore, the farnesyl pyrophosphate and MurNAc moieties on lipid II were defined and integrated as part of a single custom residue to comply with cyana's requirement that all residues be part of a single linear chain. For support in nmrviewJ,[243] topology files were manually built according to the requirements described in the program's manual.[244] Based on observed ^{31}P chemical shift perturbations and detected intermolecular NOEs following the lipid II interactions with lacticin 3147 A1 and earlier work of Sahl et al,[38] four loose artificial NOE restraints were introduced involving residues E24 and K30 with both phosphate atoms for relative anchoring of lacticin 3147 A1 and lipid II.

4.5 General procedure for manual Fmoc solid phase peptide synthesis

A scale of 0.5 mmol of the first amino acid was loaded over a trityl resin (Chem-Impex). Reactions were performed in a custom-built 20 mL glass fritted column fitted with a T-joint and a three-way T-bore teflon stopcock. After transferring the resin into the vessel, it was pre-swollen in DMF (10 mL, 15 min), and this was accompanied with agitation of the solution using an argon flow from the bottom of the vessel. In the following step, Fmoc deprotection was performed using 20% piperidine in DMF (3 x 10 mL x 5 min). Between deprotections and couplings, the vessel was drained under argon pressure and washed with DMF (3 x 5 mL). The completion of the deprotection was followed by UV measurement. For the coupling step, Fmoc protected amino acid (5 equivalents) was pre-activated using HATU (5 equivalents) and DIPEA (5 equivalents) in DMF (5 mL) for 5 min. The solution of pre-activated amino acid was transferred into the vessel containing the resin-loaded amino acid with continuous argon bubbling for 3 h. Upon completion of the coupling step, the vessel was drained, and the resin was washed with dried DMF (3 x 10 mL). The sequence of deprotections and couplings was continued until the last desired amino acid was incorporated into the peptide chain. CH_2Cl_2 (3 x 10 mL) was used to wash the resin-bound peptide, which was followed by drying under a house vacuum line overnight. To cleave the peptide from the resin, it was transferred to a screw top vial and treated with a solution of TFA:TIPS:H_2O (95:2.5:2.5, 5 mL), then stirred 2 h. The solution was filtered and evaporated using argon flow, the crude peptide was precipitated from Et_2O and the precipitate was separated after centrifugation. Lastly, HPLC purification of the crude peptide was performed after it was dissolved in a

solution of H_2O:ACN (1:1, 5 mL). The product containing fractions was lyophilized to yield pure products.

4.6 General procedure for Fmoc solid phase peptide synthesis using a peptide synthesizer

Standard and non canonical amino acids were purchased from Chem-Impex. The peptide synthesizer Prelude X was used for this purpose. The first amino acid was loaded manually over a trityl resin, and the loading rate was determined using UV measurement of the solution resulting from the Fmoc cleavage of a pre-measured loaded resin. 200 mM solutions of amino acids, N,N-diisopropylethylamine (DIPEA), HATU in dimethylformamide (DMF) were prepared and transferred to the peptide synthesizer. Fmoc deprotection was performed over the peptide synthesizer using a 20 % solution of piperidine in DMF (3 x 5 min), and coupling steps were performed by loading the DMF solution amino acids into the reactor containing the resin pre-loaded with the first amino acid. This was followed by sequential addition of HATU, base (DIPEA) and a 15 min shaking with argon flow agitation at room temperature for each coupling step. Then, the peptide cleavage and HPLC purification steps were followed, as has been explained already in the manual SPPS section, to obtain the pure peptide.

4.7 General procedure for coupling a lipid tail to resin-bound tridecaptin A1

A HATU activated solution of desired tail (5 mmol), either 3-anthracen-9yl-

propionic acid or biotin, was stirred in a suspension of Fmoc deprotected resin-bound tridecaptin A1 (1 mmol) in CH_2Cl_2 (5 mL) at ambient temperature under argon for 24 h. The suspension was then filtered, washed with CH_2Cl_2 (3 x 8 mL) and dried under house vacuum for 5 min. To cleave the peptide from the resin and deprotect its side chains, the resin was transferred to a screw-top vial with a premixed solution of TFA:TIPS:H_2O (95:2.5:2.5, 1 mL) and stirred for 2 h. The resin beads were filtred through glass wool, and the solution was concentrated under an argon flow. The crude mixture of peptide was precipitated from cold Et_2O. To purify the final compound by HPLC, the crude peptide was re-dissolved in H_2O/ACN (1:1) containing 0.1 % TFA (aq) and purified.

4.8 Synthesis and characterization of compounds

Benzyl 2-Acetamido-2-deoxy-α-D-glucopyranoside (98)

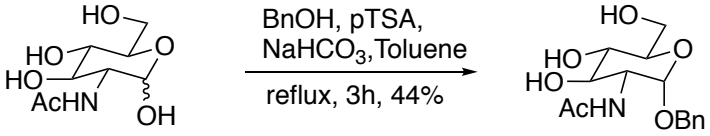

(79) **(98)**

N-Acetyl-D-glucosamine (79) (20.3, 91.8 mmol) and p-toluenesulfonic acid (1.75 g, 9.18 mmol) were suspended in toluene (240 mL) and benzyl alcohol (140 mL), refluxed for three hours and cooled to room temperature. This was followed by addition of $NaHCO_3$ (1.27g, 15.0 mmol) dissolved in water. Toluene was removed under reduced pressure, Et_2O-hexane (2:1, 800 mL) was added, and the reaction mixture stirred vigorously for one hour. The precipitate was filtered and recrystallized

from ethanol (150 mL) overnight at -18 °C. The product was filtered off, washed with cold EtOH (30 mL) and Et_2O (100 mL) and dried to yield an off-white solid (12.56 g, 44%). $[\alpha]^{D}_{25}$ = 166.94 (*c* = 0.410 g/100 mL, DMSO); IR (CH_2Cl_2 cast) 3294, 3089, 3031, 2935, 2899, 1648, 1549, 1497, 1453, 1413, 1375 cm^{-1}; ^1H NMR (500 MHz, d_6-DMSO) δ 7.81 (*d*, *J* = 8.1 Hz, 1H, AcNH), 7.39 – 7.25 (m, 5H, ArH), 5.01 (d, *J* = 5.6 Hz, 1H, OH), 4.73 (d, *J* = 5.6 Hz, 1H, OH), 4.70 (d, *J* = 3.6 Hz, 1H, H1), 4.66 (d, *J* = 12.5 Hz, 1H, PhCHH), 4.53 (t, *J* = 5.8 Hz, 1H, OH), 4.41 (d, *J* = 12.5 Hz, 1H, PhCHH), 3.70 – 3.63 (m, 2H, H2+H6), 3.56 – 3.43 (m, 3H, H3+H5+H6), 3.15 (ddd, *J* = 9.7, 8.5, 5.6 Hz, 1H, H4), 1.83 (s, 3H, CH_3). ^{13}C NMR (126 MHz, d_6-DMSO) δ 169.9, 138.4, 128.6, 128.0, 127.9, 96.4, 73.6, 71.4, 71.0, 68.1, 61.3, 54.2, 23.0. HRMS (ES) Calcd for $C_{15}H_{21}NNaO_6$ $[M+Na]^+$ 334.1261, found 334.1262.[201, 245]

Benzyl 2-acetamido-4,6-O-benzylidene-2-deoxy-α-D-glucopyranoside (48)

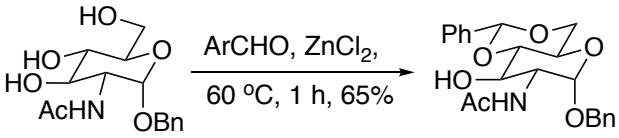

(98) **(48)**

Benzyl-2-acetamido-2-deoxy-α-D-glucopyranoside (98) (12.0 g, 38.5 mmol) was co-evaporated with toluene to dry it, and then it was added to a suspension of $ZnCl_2$ (12.3 g, 90.0 mmol) in benzaldehyde (50 mL, 490 mmol) under an argon atmosphere. The reaction mixture was heated to 60 °C (to reach a clear solution) and stirred at that temperature for one hour. The reaction mixture was cooled to room temperature, and a mixture of ice-water was poured over the solution. The precipitate was collected by filtration and washed with cooled H_2O (20 mL), Et_2O (50 mL). The

resulting powder was dried in a vacuum oven at 50 °C (10.6 g, 65%). $[\alpha]^{D}_{25}$ = 108.90 (*c* = 0.545 g/100mL, DMSO); IR (CH_2Cl_2 cast) 3447, 3284, 3090, 3062, 3035, 2978, 2918, 2869, 1956, 1816, 1649, 1557, 1497cm^{-1}; ^{1}H NMR (500 MHz, d_6-DMSO) δ 7.98 (d, *J* = 8.3 Hz, 1H, AcNH), 7.49 – 7.25 (m, 10H, ArH), 5.61 (s, 1H, CH- benzylidene acetal), 5.17 (d, *J* = 5.9 Hz, 1H, 3-OH), 4.79 (d, *J* = 3.7 Hz, 1H, H1), 4.70 (d, *J* = 12.6 Hz, 1H, PhCHH), 4.49 (d, *J* = 12.6 Hz, 1H, PhCHH), 4.14 (dd, *J* = 9.2, 4.1 Hz, 1H, H6), 3.88 – 3.80 (m, 1H, H2), 3.78 – 3.65 (m, 3H, H3+H5+H6), 3.50 (t, *J* = 9.0 Hz, 1H, H4), 1.84 (s, 3H, CH_3);^{13}C NMR (126 MHz, d_6-DMSO) δ 169.9, 138.2, 129.3, 128.7, 128.5, 128.1, 128.0, 126.8, 101.3, 97.4, 82.6, 69.0, 68.5, 67.7, 63.3, 54.6, 23.0; HRMS (ES) Calcd for $C_{22}H_{25}NNaO_6$ $[M+Na]^+$ 422.1574, found 422.1575.[201, 245]

1,3,4,6-Tetra-O-acetyl-2-deoxy-2-[(2,2,2-trichloroethoxy)carbonylamino]-(α,β)-D-glucopyranoside (52)

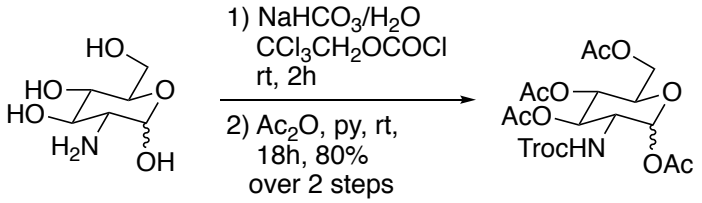

(51) **(52)**

D-Glucosamine (51) (10.0 g, 46.4 mmol) and $NaHCO_3$ (7.80 g, 92.8 mmol) were dissolved in water (120 mL) and stirred vigorously for five minutes. 2,2,2-Trichloroethoxycarbonyl chloride (7.65 mL, 55.6 mmol) was added dropwise and the solution was stirred at ambient temperature for two hours, over which time a white precipitate formed. The precipitate was filtered, washed with water and dried by lyophilization (24 h) to give a white flocculent solid. This solid was dissolved in dry

pyridine (100 mL) and acetic anhydride (50 mL) and stirred at ambient temperature for 18 h. The reaction mixture was concentrated *in vacuo* and co-evaporated with toluene (3 x 50 mL). The resulting oily residue was dissolved in chloroform (100 mL) and washed with 1M hydrochloric acid (100 mL). The aqueous phase was back extracted with chloroform (2 x 100 mL), and the combined organic extracts washed with brine (50 mL). Then, the organic phase was dried over anhydrous sodium sulfate and concentrated *in vacuo* to yield 1,3,4,6-tetra-*O*-acetyl-2-troc-d-glucosamine (19.42 g, 80%) as a white solid. $[\alpha]^{D}_{25}$ = 64.73 (*c* = 1.13 g/100mL, $CHCl_3$); IR ($CHCl_3$ cast) 3328, 3024, 2959, 1754, 1538, 1369 cm^{-1}; ^{1}H NMR (500 MHz, $CDCl_3$) δ 6.28 (d, *J* = 3.7 Hz, 1H, AcNH), 5.32 (dd, *J* = 10.8, 9.5 Hz, 1H, H1), 5.24 (t, *J* = 9.8 Hz, 1H, H3), 5.14 (d, *J* = 9.3 Hz, 1H, H4), 4.86 (d, *J* = 12.0 Hz, 1H, Troc-CH_2), 4.66 (d, *J* = 12.1 Hz, 1H, Troc-CH_2), 4.32 (dd, *J* = 12.5, 4.1 Hz, 1H, H6), 4.28 – 4.22 (m, 1H, H2), 4.10 (dd, *J* = 12.5, 2.4 Hz, 1H, H6), 4.05 (ddd, J = 10.1, 4.1, 2.4 Hz, 1H, H5), 2.24 (s, 3H, Ac), 2.13 (s, 3H), 2.09 (s, 6H, Ac); ^{13}C NMR (126 MHz, $CDCl_3$) δ 171.3, 170.6, 169.2, 168.6, 154.0, 95.2, 90.4, 77.3, 77.2, 77.0, 76.8, 74.7, 70.4, 69.8, 67.5, 61.5, 53.3, 20.9, 20.7, 20.6; HRMS (ES) Calcd for $C_{17}H_{22}Cl_3NNaO_{11}$ $[M+Na]^+$ 544.0151, found 544.0146.[201, 245]

Synthesis of 3,4,6-tris-O-acetyl-1-α-trichloroacetimido-2-troc-D-glucosamine (glycosyl acceptor) (53)

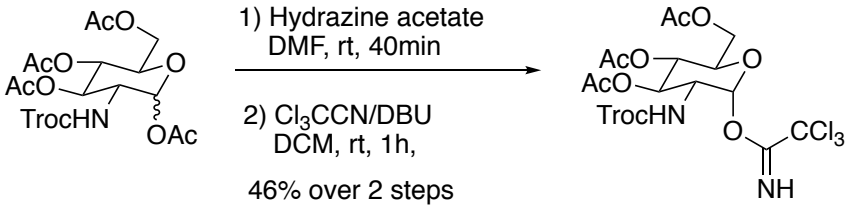

(52) **(53)**

Sugar compound (52) (10.0 g, 19.3 mmol) was dissolved in dry dimethylformamide (100 mL), and this was followed by addition of hydrazine acetate (2.11 g, 23.0 mmol). The reaction mixture was stirred at room temperature for 45 min, diluted with ethyl acetate (100 mL) and washed with water (100 mL), saturated sodium bicarbonate (100 mL) and water (100 mL). The aqueous phases were combined to be back extracted with ethyl acetate (100 mL), and the combined organic phases were washed with brine, dried over anhydrous sodium sulfate and concentrated *in vacuo*. The resultant yellow oil was re-dissolved in dichloromethane (100 mL) to which trichloroacetonitrile (19.2 mL, 191.3 mmol) was added, and this was followed by addition of 1,8-Diazabicycloundec-7-ene (0.570 mL, 3.83 mmol). The reaction mixture was stirred at room temperature for 95 min and concentrated *in vacuo*. The crude reaction mixture was purified by flash column chromatography (silica, 2:1 hexanes:ethyl acetate + 0.1% triethylamine) to yield 3,4,6-tris-O-acetyl-1-α-trichloroacetimido-2-troc-d-glucosamine (53) as a white foam (5.5 g, 46%). $[\alpha]_D^{25}$ = 54.32 (*c* = 0.90 g/100mL, $CHCl_3$); IR ($CHCl_3$ cast) 3429, 3316, 3022, 2956, 2854, 1748, 1677, 1368 cm^{-1}; 1H NMR (500 MHz, $CDCl_3$) δ 8.82 (s, 1H, acetimidate-NH), 6.45 (d, 1H, *J* = 3.6 Hz, H1), 5.37 (dd, 1H, *J* = 10.9, 9.4 Hz, H3), 5.27 (t, 1H, *J* = 9.9

Hz, H4), 5.21 (d, 1H, *J* = 9.3 Hz, Troc-NH), 4.79 – 4.69 (m, 2H, Troc-CH_2), 4.35 – 4.26 (m, 2H, H2 + H6), 4.20 – 4.11 (m, 2H, H5 + H6), 2.10 (m, 3H, 1 x Ac), 2.08 (m, 6H, 2 x Ac); ^{13}C NMR (126 MHz, $CDCl_3$) δ 171.1, 170.5, 169.2, 160.4, 154.1, 95.2, 94.6, 90.7, 74.7, 70.3, 67.4, 61.4, 60.4, 53.9, 21.1, 20.7, 20.6; HRMS (ES) Calcd for $C_{17}H_{20}Cl_6N_2NaO_{10}$ $[M+Na]^+$ 644.9141, found 644.9136.[201, 245]

Synthesis of Alanine-2-(phenylsulfonyl)-ethyl ester (80)

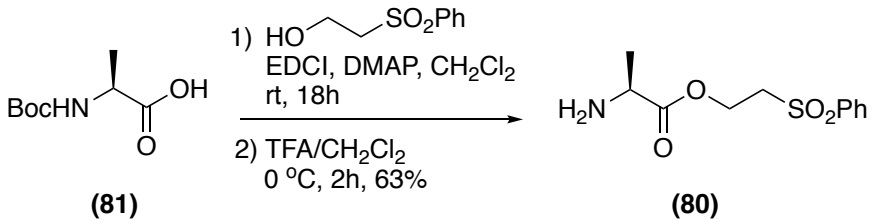

(81) **(80)**

Boc-l-alanine (80) (5.08 g, 26.8 mmol), 2-phenylsulfonylethanol (5.00 g, 26.8 mmol), 1-(3-Dimethylaminopropyl)-3-ethylcarbodiimide hydrochloride (5.20 g, 26.8 mmol) and 4-dimethylaminopyridine (0.330 g, 2.68 mmol) were dissolved in dry dichloromethane (150 mL) and stirred at ambient temperature under an argon atmosphere for 18 h. Next, the reaction mixture was washed with 0.5 M hydrochloric acid (100 mL) and saturated sodium bicarbonate (100 mL). Each aqueous phase was back extracted with dichloromethane (50 mL), the combined organic extracts washed with brine (100 mL), then dried over anhydrous sodium sulfate and concentrated *in vacuo*. The resulting orange oil was dissolved in dichloromethane (30 mL) and cooled to 0 °C. Trifluoroacetic acid (30 mL) was added slowly, then the solution was warmed to ambient temperature and stirred for two hours. The resulting orange solution was concentrated *in vacuo*, dissolved in water (50 mL) and basified to pH 8.0 with 3M

NaOH. This solution was extracted with dichloromethane (5 x 50 mL), and the combined organic extracts dried over anhydrous sodium sulfate and concentrated *in vacuo* to yield the product as a clear oil (4.30 g, 63%). $[\alpha]_D^{25}$ = -106.7 (*c* = 0.55 g/100mL, CH_2Cl_2); IR (EtOAc cast) 3378, 3312, 3064, 2978, 2934, 1739 cm^{-1}; ^1H NMR (500 MHz, $CDCl_3$) δ 7.95 – 7.90 (m, 2H, *O*-ArH), 7.70 – 7.65 (m, 1H, *p*-ArH), 7.61 – 7.56 (m, 2H, *m*-ArH), 4.50 – 4.41 (m, 2H, O-CH_2), 3.52 – 3.42 (m, 2H, S-CH_2), 3.30 (q, *J* = 7.0 Hz, 1H, Hα), 1.17 (d, *J* = 7.0 Hz, 3H, Hβ); ^{13}C NMR (125 MHz, $CDCl_3$) δ 175.92, 139.53, 134.18, 129.59, 129.54, 129.45, 128.09, 56.37, 55.20, 49.95, 20.33; HRMS (ES) Calcd for $C_{11}H_{15}NO_4S$ $[M+H]^+$ 258.0795, found 258.0794.[201, 245]

Benzyl 2-Acetamido-4,6-*O*-benzylidene-2-deoxy-3-*O*-(D-1-carboxyethyl)-α-D-glucopyranoside (82)

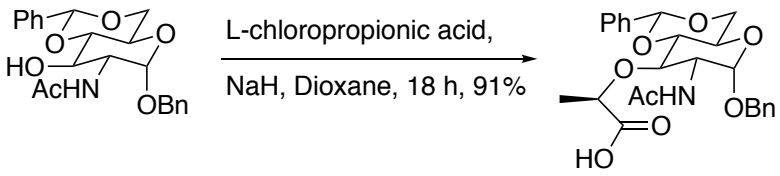

(48) **(82)**

Glycol (48) (7.00 g, 17.5 mmol) was added to dry dioxane (100 mL), and sodium hydride reagent (60% dispersion in mineral oil, 4.90 g, 122.5 mmol) was added in portions at room temperature. The cloudy suspension was stirred at 50 °C for 1 h and cooled to 0 °C. It is important that the temperature of the reaction mixture be reduced to 0 °C to prevent epimerization of l-chloropropionic acid. Next, a solution of L-chloropropionic acid (5.00 g, 46.1 mmol) in dry dioxane (20 mL) was added dropwise over 10 min. Then, the temperature of the reaction mixture was increased to

ambient temperature and stirred for 18 hours. The reaction solvents were removed using a rotary evaporator, and the resulting solid stirred in brine (100 mL) at 4 °C for 1 h. Next, the suspension was filtered and the solid washed using cold water. The solid was dried overnight in a vacuum oven at 50 °C, followed by re-suspension in 60:39:1 methanol:dichloromethane: triethylamine (200 mL) and stirring for 10 min. Then, the mixture was filtered through celite and concentrated *in vacuo* to yield the muramic acid ammonium salt as a white foam (9.11 g, 91%), which was used directly without further purification in the next step. $[\alpha]_D^{25}$ = 81.61 (*c* = 0.762 g/100 mL, DMSO); IR (CH_2Cl_2 cast) 3418, 3286, 3064, 3033, 2974, 2926, 2868, 1953, 1890, 1812, 1597, 1497 cm^{-1}; ^1H NMR (500 MHz, d_6-DMSO) δ 10.82 (d, *J* = 3.0 Hz, 1H, -COOH), 7.43 – 7.25 (m, 11H, ArH + AcNH), 5.66 (s, 1H, O_2CH), 5.35 (d, *J* = 3.5 Hz, 1H, H1), 4.64 (d, *J* = 12.4 Hz, 1H, PhCHH), 4.43 (d, *J* = 12.4 Hz, 1H, PhCHH), 4.13 – 4.06 (m, 1H, H3), 3.96 (q, *J* = 6.9 Hz, 1H, MurNAc-CH), 3.74 – 3.62 (m, 4H, H2+H4+H6), 3.45 (dt, *J* = 10.4, 3.3 Hz, 1H, H5), 1.84 (s, 3H, Ac), 1.17 (d, *J* = 6.9 Hz, 3H, MurNAc-CH_3); ^{13}C NMR (126 MHz, d_6-DMSO) δ 177.6, 170.1, 138.3, 138.3, 129.2, 128.7, 128.6, 128.0, 128.0, 126.3, 100.7, 97.1, 83.0, 78.5, 73.7, 69.5, 68.4, 63.5, 55.4, 23.1, 20.2; HRMS(ES) Calcd for $C_{25}H_{29}NNaO_8$ $[M+Na]^+$ 494.1785, found 494.1781.[201, 245]

(2S)-2-(Phenylsulfonyl)ethyl-2-((2R)-2-(7-acetamido-6-(benzyloxy)-2-phenylhexahydropyrano[3,2-d][1,3]dioxin-8-yloxy)propanamido)propanoate (49)

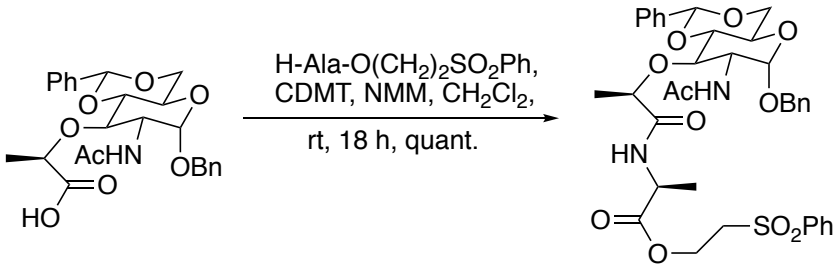

(82) **(49)**

The muramic acid derivative (82) (3.00 g, 5.24 mmol) was dissolved in dichloromethane (40 mL), and the temperature of the reaction mixture was reduced to 0 °C. 2-Chloro-4,6-dimethoxy-1,3,5-triazine (1.10 g, 6.29 mmol) and N-methylmorpholine (0.580 mL, 5.24 mmol) reagents were added, and the reaction mixture stirred at 0 °C for 50 min. Next, alanine-2-(phenylsulfonyl)-ethyl ester (1.62 g, 6.29 mmol) was added, and the temperature of the reaction mixture was increased to ambient temperature and stirred for 18 h. The resultant cloudy solution was diluted with dichloromethane (30 mL) and washed with 1M hydrochloric acid (100 mL) and brine (100 mL). Lastly, the organic phase was dried over anhydrous sodium sulfate and concentrated *in vacuo* to yield (49) as a white solid (3.90 g, quant.). $[\alpha]_D^{25}$ = 51.54 (*c* = 0.4 g/100mL, CH_3OH); IR (CH_3OH cast) 3295, 3065, 3031, 2950, 2923, 2869, 1744, 1652 cm^{-1}; ^1H NMR (500 MHz, $CDCl_3$) δ 7.96 – 7.93 (m, 2H, ArH), 7.72 – 7.67 (m, 1H, ArH), 7.59 (t, *J* = 7.8 Hz, 2H, ArH), 7.50 (dd, *J* = 7.1, 2.5 Hz, 2H, ArH), 7.42 – 7.33 (m, 8H, ArH), 6.97 (d, *J* = 7.1 Hz, 1H, Ala1-NH), 6.20 (d, *J* = 8.9 Hz, 1H, AcNH), 5.60 (s, 1H, O2CH), 4.99 (d, *J* = 3.8 Hz, 1H, H1), 4.75 (d, *J* = 11.8 Hz, 1H, PhCHH), 4.40-4.53 (m, 3H, PhCHH + OCH_2), 4.33 (dt, *J* = 9.3, 4.7 Hz, 1H, H2), 4.28

(dd, *J* = 10.2, 4.8 Hz, 1H, H6), 4.20 (t, *J* = 7.2 Hz, 1H, Ala1-Hα), 4.11 (q, J = 6.7 Hz, 1H, OCH), 3.91 (dt, J = 9.2, 4.9 Hz, 1H, H5), 3.80 (t, *J* = 10.2 Hz, 1H, H6), 3.75 – 3.67 (m, 2H, H3 + H4), 3.46 (qdd, *J* = 14.7, 6.6, 5.5 Hz, 2H, SCH_2), 1.97 (s, 3H, Ac), 1.41 (d, *J* = 6.7 Hz, 3H, MurNAc-CH3), 1.33 (d, *J* = 7.2 Hz, 3H, Ala1-Hβ);^{13}C NMR (126 MHz, $CDCl_3$) δ 173.0, 171.8, 170.5, 139.2, 137.1, 136.7, 134.1, 129.5, 129.1, 128.7, 128.4, 128.3, 128.2, 128.1, 125.9, 101.5, 97.5, 81.5, 78.5, 78.2, 70.2, 68.9, 63.2, 58.0, 55.0, 53.0, 48.0, 23.5, 19.4, 17.2; HRMS (ES) Calcd for $C_{36}H_{42}N_2NaO_{11}S$ $[M+Na]^+$ 733.2402, found 733.2392.[201]

Benzyl N-acetyl-6-benzylmuramic acid monopeptide ester (glycosyl donor) (50)

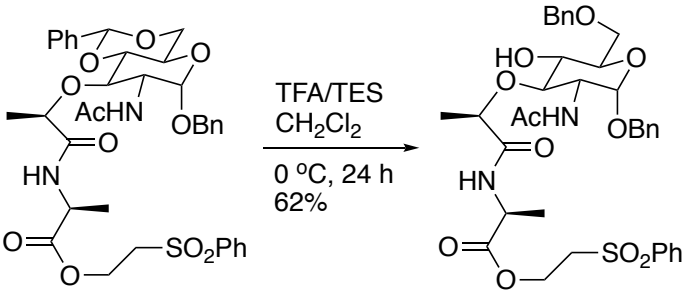

(49) **(50)**

Benzylidene (49) (3.46 g, 4.87 mmol) was dissolved in dichloromethane (50 mL), and the temperature of the reaction mixture was reduced to 0 °C. Next, triethylsilane (3.63 mL, 24.3 mmol) was added, and this was followed by the dropwise addition of trifluoroacetic acid (1.86 mL, 24.34 mmol) to carry out the reduction reaction. After stirring the reaction mixture for five hours at 0 °C, another portion of trifluoroacetic acid (1.12 mL, 14.6 mmol) was added. The reaction mixture was stirred for 19 more hours at 0 °C and then diluted with dichloromethane (50 mL). To perform the workup, saturated sodium bicarbonate (50 mL) was slowly added, and the

aqueous layer was extracted with dichloromethane (50 mL). The combined organic phases were washed with brine (50 mL), dried over anhydrous sodium sulfate and concentrated *in vacuo*. The crude product was purified by column chromatography (silica, gradient: 0%–3% MeOH in CH_2Cl_2) to yield the product (50) as a white foam (2.0 g, 62%). $[\alpha]_D^{25}$ = 58.90 (c = 0.90 g/mL, $CHCl_3$); IR ($CHCl_3$ cast) 3370, 3063, 3031, 2983, 2928, 1748, 1659 cm^{-1}; ^1H NMR (500 MHz, $CDCl_3$) δ 7.98 – 7.92 (m, 2H, ArH), 7.74 – 7.67 (m, 1H, ArH), 7.65 – 7.57 (m, 3H, ArH), 7.42 – 7.29 (m, 9H, ArH), 6.93 (d, *J* = 7.2 Hz, 1H, Ala1-NH), 6.08 (d, *J* = 9.0 Hz, 1H, MurNAc-NH), 4.94 (d, *J* = 3.6 Hz, 1H, H1), 4.72 (d, *J* = 11.7 Hz, 1H, PhCHH), 4.67 – 4.56 (m, 2H, $PhCH_2$), 4.50 – 4.39 (m, 3H, PhCHH + OCH_2), 4.29 – 4.22 (m, 2H, H2 + Ala1-Hα), 4.16 (q, *J* = 6.7 Hz, 1H, MurNAc-OCH), 3.84 (dt, *J* = 9.2, 4.4 Hz, 1H, H5), 3.77 (dd, *J* = 10.2, 4.5 Hz, 1H, H6), 3.74 – 3.69 (m, 2H, H3 + H4), 3.56 (dd, *J* = 10.5, 8.7 Hz, 1H, H6), 3.46 – 3.38 (m, 2H, SCH_2), 2.99 (d, *J* = 3.1 Hz, 1H, OH), 1.93 (s, 3H, Ac), 1.43 (d, *J* = 6.7 Hz, 3H, MurNAc-CH_3), 1.33 (d, *J* = 7.2 Hz, 3H, Ala1-Hβ);^{13}C NMR (126 MHz, $CDCl_3$) δ 172.9, 171.9, 170.3, 139.2, 139.0, 137.8, 137.0, 134.1, 134.0, 129.5, 128.6, 128.5, 128.2, 128.1, 128.0, 127.8, 127.7, 97.1, 80.5, 77.9, 73.7, 71.6, 70.4, 70.2, 69.9, 58.3, 58.0, 56.4, 55.0, 52.5, 47.9, 23.4, 19.0, 17.1; HRMS (ES) Calcd for $C_{36}H_{44}N_2NaO_{11}S$ $[M+Na]^+$ 735.2558, found 735.2547.[201]

N-Trichloroethoxycarbonyl-(2-deoxy-2-aminoglucopyranosyl)-β-[1,4]-N-acetyl-muramyl monopeptide ester (57)

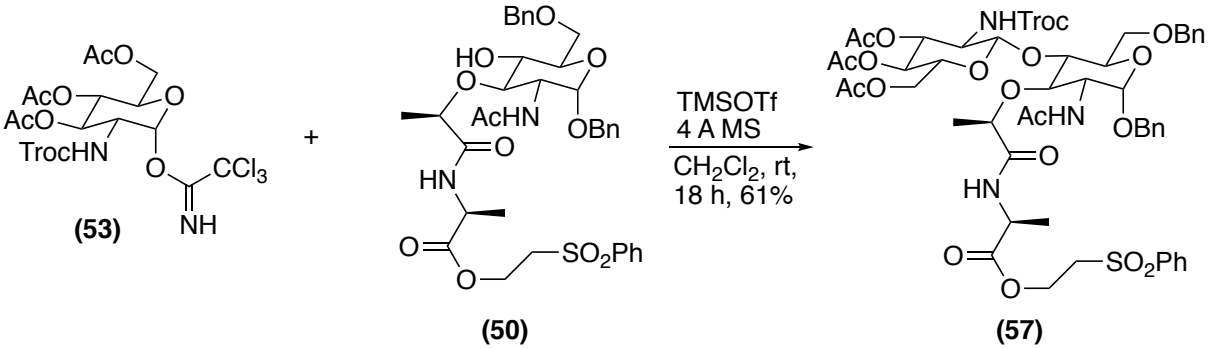

Glycol (50) (2.00 g, 2.81 mmol) was dissolved in dry dichloromethane (30 mL), added to a round-bottomed flask already containing activated 4 Å molecular sieves (MS) (20 g) under argon, and the reaction mixture stirred gently. This was followed by the addition of trimethylsilyl triflate (0.300 mL, 2.81 mmol) and the solution of acetimidate (53) (5.26 g, 8.42 mmol) already dissolved in dry dichloromethane (30 mL). At this point, the reaction mixture was stirred at room temperature overnight. Next, the reaction mixture was decanted and the solution diluted with dichloromethane (50 mL). To perform the work up, the organic solution was washed with saturated sodium bicarbonate (80 mL) and brine (100 mL) and dried over anhydrous sodium sulfate. The solution was concentrated *in vacuo* and purified by flash column chromatography (silica, gradient: 1:1 EtOAc:hexane to ethyl acetate to 19:1 EtOAc:MeOH) to yield the product as a white foam (2.00 g, 61%). $[\alpha]_D^{25}$ = 37.73 (0.30 g/100mL, CH_2Cl_2); IR 3351, 3281, 3064, 3032, 2984, 2932, 1749, 1659, 1536, 1448, 1368, 1322, 1293 cm^{-1}; ^1H NMR (500 MHz, $CDCl_3$) δ 7.97 – 7.92 (m, 2H, ArH), 7.71 – 7.67 (m, 1H, ArH), 7.62 – 7.47 (m, 6H, ArH), 7.42 – 7.30 (m, 6H, ArH), 6.87 (d, *J* = 7.5 Hz, 1H, Ala1NH), 6.57 (d, *J* = 7.4 Hz, 1H, MurNAc-NH), 5.13 (d, *J* = 3.6 Hz,

1H, MurNAc-H1), 5.01 (t, *J* = 9.6 Hz, 1H, GlcNAc-H4), 4.91 (d, *J* = 12.0 Hz, 1H, MurNAc-1-CHHPh), 4.80 (dd, *J* = 11.2, 8.6 Hz, 2H, GlcNAc-H3 + Troc-CHH), 4.63 (t, *J* = 11.5 Hz, 2H, Troc-CHH + MurNAc-6-CHHPh), 4.51 – 4.44 (m, 2H, OCHH + MurNAc-6-CHHPh), 4.39 (dd, *J* = 12.1, 5.6 Hz, 2H, OCHH + MurNAc-1-CHHPh), 4.29 – 4.14 (m, 5H, MurNAc-H2 + MurNAc-CHO + GlcNAc-H1 + GlcNAc-H6 + Ala1Hα), 4.02 (dd, *J* = 12.4, 2.2 Hz, 1H, GlcNAc-H6), 3.95 (t, *J* = 9.5 Hz, 1H, MurNAc-H3), 3.72 (dd, *J* = 10.9, 2.4 Hz, 1H, MurNAc-H6), 3.66 (dt, *J* = 10.1, 2.3 Hz, 1H, MurNAc-H4), 3.59 (td, J = 10.2, 8.4 Hz, 1H, MurNAc-H5), 3.49 – 3.41 (m, 4H, CH_2S + GlcNAc-H2 + GlcNAc-H5), 2.07 – 2.00 (m, 9H, 3 x Ac), 1.93 (s, 3H, Ac), 1.37 (d, *J* = 6.7 Hz, 3H, Ala1Hβ), 1.28 (dd, *J* = 7.2, 2.6 Hz, 3H, MurNAc-CH_3); ^{13}C NMR ($CDCl_3$, 125 MHz) δ 173.47, 171.93, 170.79, 170.54, 170.41, 169.53, 154.25, 139.37, 137.45, 137.27, 134.18, 129.54, 129.24, 128.67, 128.26, 128.23, 100.13, 97.26, 95.74, 77.73, 75.78, 74.60, 73.89, 72.28, 71.32, 70.53, 70.40, 68.42, 67.27, 61.58, 58.24, 56.31, 55.04, 53.75, 47.83, 23.38, 20.75, 18.44, 17.63; HRMS (ES) Calcd for $C_{51}H_{62}Cl_3N_3NaO_{20}S$ $[M+Na]^+$ 1196.2605, found 1196.2614.[201]

N-Acetyl-(2-deoxy-2-aminoglucopyranosyl)-β-[1,4]-N-acetylmuramyl monopeptide ester (58)

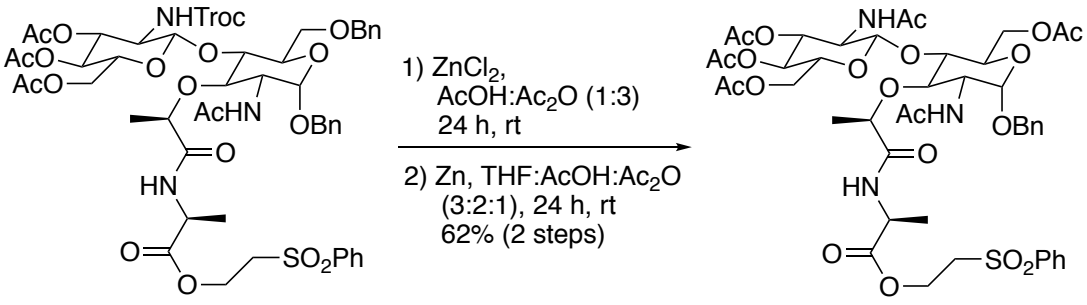

(57) **(58)**

Acetic anhydride and acetic acid, (3:1, 23 mL) were used to dissolve troc-disaccharide (57) (4.0 g, 3.4 mmol). This was followed by the addition of an anhydrous solution of $ZnCl_2$ (4.60 g, 34.0 mmol) in Ac_2O and AcOH (3:1, 11 mL). The reaction mixture was stirred at room temperature for 24 h, and this was followed by addition of zinc dust (8.9 g, 136.0 mmol) plus a mixture of THF, Ac_2O and AcOH (3:2:1, 54 mL). At this point, the reaction mixture was again stirred for 24 more hours at ambient temperature and filtered through celite, washed with EtOAc and concentrated *in vacuo*. The final residue was co-evaporated with toluene (2 x 30 mL) and re-dissolved in EtOAc (100 mL). Next, the organic layer was washed with saturated sodium bicarbonate (2 x 50 mL), water (2 x 50 mL) and brine (50 mL), dried over anhydrous sodium sulfate and concentrated *in vacuo*. The crude product was purified by flash column chromotography (silica, 2% MeOH in EtOAc) to yield the product as a white foam (2.13 g, 63%). $[\alpha]_D^{25}$ = 16.50 (c = 0.2 g/100mL, $CHCl_3$); IR ($CHCl_3$ cast) 3280, 3067, 2986, 2934, 1745, 1664, 1539, 1448, 1370 cm^{-1}; ^1H NMR ($CDCl_3$, 500 MHz) δ 7.97 – 7.86 (m, 2H, *o*-ArH), 7.72 – 7.63 (m, 1H, *p*-ArH), 7.57 (m,

2H, *m*-ArH), 7.38 – 7.24 (m, 5H, Bn-ArH), 7.16 (d, *J* = 7.6 Hz, 1H, MurNAc-NH), 6.84 (d, *J* = 6.8 Hz, 1H, Ala1NH), 6.02 (d, *J* = 9.5 Hz, 1H, GlcNAc-NH), 5.17 – 5.06 (m, 2H, MurNAc-H1 + GlcNAc-H3), 4.64 (d, *J* = 12.1 Hz, 1H, MurNAc-1-CHHPh), 4.49 (d, *J* = 12.1 Hz, 1H, MurNAc-1-CHHPh), 4.46 – 4.22 (m, 6H, OCH_2 + MurNAc-CHO + GlcNAc-H1 + GlcNAc-H6 + MurNAc-H6), 4.19 – 4.14 (m, 1H, MurNAc-H6), 4.12 (q, *J* = 7.1 Hz, 1H, GlcNAc-H6), 4.09 – 3.97 (m, 3H, GlcNAc-H2 + MurNAc-H2 + MurNAc-H3), 3.78 (d, *J* = 5.2 Hz, MurNAc-H5), 3.62 - 3.54 (m, 2H, GlcNAc-H5 + MurNAc-H4), 3.36 (m, 2H, CH_2S), 2.14 (s, 3H), 2.05 – 1.97 (m, 6H), 1.95 (s, 3H), 1.93 (s, 3H), 1.37 (d, *J* = 6.7 Hz, 3H, MurNAc-CH_3), 1.29 (d, *J* = 7.2 Hz, 3H, Ala1Hβ); ^{13}C NMR ($CDCl_3$, 500 MHz) δ 173.8, 172.0, 171.3, 171.06, 170.9, 170.73, 170.7, 169.4, 139.2, 137.4, 134.2, 129.5, 128.6, 128.2, 128.1, 128.01, 100.4, 97.08, 76.1, 75.7, 72.6, 71.9, 70.4, 69.6, 68.2, 62.4, 61.7, 60.5, 58.1, 55.03, 54.7, 53.7, 47.9, 23.38, 23.32, 21.1, 20.77, 20.75, 20.74, 18.49, 17.47; HRMS (ES) Calcd for $C_{45}H_{59}N_3NaO_{20}S$ $[M+Na]^+$ 1016.3305, found 1016.3292.[201]

Phosphate (59)

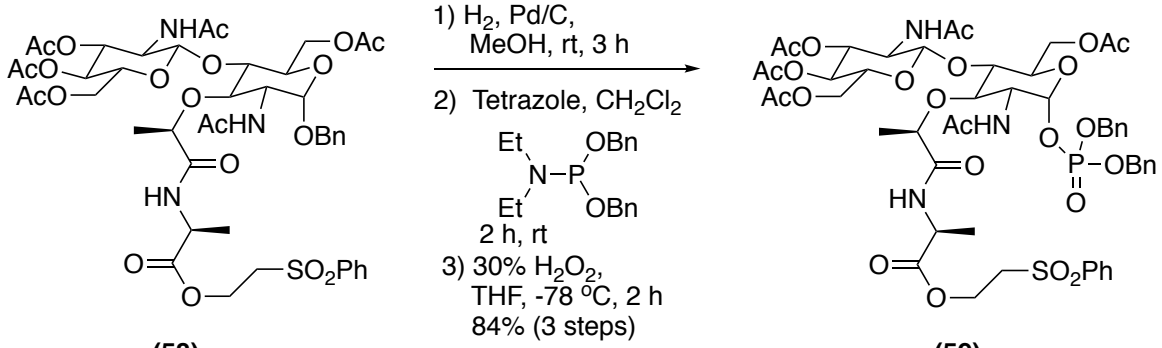

Benzyl ether (58) (1.50 g, 1.51 mmol) was dissolved in MeOH and THF (1:4, 45 mL), and this was followed by the addition of a suspension of 10% palladium on charcoal (2.70 g, 2.54 mmol) in the same solvent (30 mL). After stirring for 3 h under hydrogen atmosphere, the reaction mixture was filtered through a thin layer of Celite. The celite was also washed with CH_2Cl_2 (150 mL) to collect most of the compound. The filtrate was concentrated *in vacuo*, and the resultant oil was precipitated from hexanes and ether (1:1, 35 mL). The precipitate was collected by filtration and dried to yield the lactol as a white solid (1.35 g, 99%). Anhydrous CH_2Cl_2 (8 mL) was used to re-dissolve the lactol, which was added rapidly to a stirring suspension of tetrazole (0.53 g, 7.5 mmol) and dibenzyl N,N′-diethylphosphoramidite (1.35 mL, 4.50 mmol) in anhydrous CH_2Cl_2 (8 mL) under argon at room temperature. After stirring for 2 h, the reaction mixture was worked up by diluting it with CH_2Cl_2 (8 mL) and washing it with saturated sodium bicarbonate (7 mL), water (7mL) and brine (7 mL). The organic phase was dried over anhydrous Na_2SO_4 and concentrated *in vacuo* to obtain a colourless oil, which was precipitated through treating with hexanes and ether (1:1, 40 mL) to yield the phosphite, a white solid. To perform the chemical transformation

of phosphite to phosphate, the phosphite product was dissolved in THF (25 mL) and kept at -78 °C. Hydrogen peroxide (30%, 1.63 mL) was added dropwise to the stirring solution of the reaction mixture using a syringe. On completion of the hydrogen peroxide addition, the ice bath was removed, and the mixture was allowed to warm to room temperature over two hours. At this point, ice-cold saturated sodium sulfite (6 mL) was added to dilute the reaction mixture, and this was followed by addition of EtOAc (10 mL) and stirring for 10 min. The organic layer was dried over anhydrous sodium sulfate and concentrated *in vacuo* to obtain phosphate (59) as a white solid (1.46 g, 84%). $[\alpha]_D^{25}$ = 1.89 (*c* = 1.75 g/100mL, $CHCl_3$); IR ($CHCl_3$ cast) 3280, 3065, 2956, 1747, 1666, 1544, 1498, 1455, 1371, 1322 cm^{-1}; ^1H NMR (DMSO-d_6, 500 MHz) δ 8.67 (d, *J* = 4.6 Hz, 1H, NHAc), 8.40 (d, *J* = 7.0 Hz, 1H, NHAc), 8.07 (d, *J* = 9.0 Hz, 1H, NHAc), 7.92 – 7.80 (m, 2H, *o*-ArH), 7.76 – 7.72 (m, 1H, *p*-ArH), 7.67 – 7.59 (m, 2H, *m*-ArH), 7.44 – 7.27 (m, 10H, 2 x Bn-ArH), 5.81 (dd, *J* = 6.4, 3.1 Hz, H1, MurNAc-H1), 5.24 (t, *J* = 9.9 Hz, 1H, GlcNAc-H3), 5.13 – 4.95 (m, 4H, 2 x CH_2Ph), 4.91 (t, *J* = 9.8 Hz, 1H, GlcNAc-H4), 4.72 (dd, *J* = 16.2, 7.5 Hz, 1H, GlcNAc-H1), 4.60 (d, *J* = 6.7 Hz, 1H, MurNAc-CHO), 4.40 – 4.18 (m, 3H, MurNAc-H6 + GlcNAc-H6 + OCHH), 4.13 – 3.95 (m, 4H, MurNAc-H6 + GlcNAc-H6 + OCHH + Ala1Hα), 3.87 – 3.71 (m, 4H, GlcNAc-H2 + GlcNAc-H5 + MurNAc-H3 + MurNAc-H5), 3.65 – 3.56 (m, 3H, MurNAc-H2 + SCH_2), 3.42 (dd, *J* = 10.9, 8.7 Hz, 1H, MurNAc-H4), 2.03 – 1.87 (m, 12H, 4 x Ac), 1.75 (s, 3H, Ac), 1.69 (s, 3H, Ac), 1.29 (d, *J* = 6.7 Hz, 3H, MurNAc-CH_3), 1.11 (d, *J* = 7.3 Hz, 3H, AlaHβ); ^{13}C NMR (DMSO-d_6, 125 MHz) δ 174.48, 171.35, 169.91, 169.83, 169.56, 169.30, 139.26, 135.76, 133.93, 129.39, 128.43, 128.38, 128.36, 128.33, 127.93, 127.84, 127.70, 127.65, 127.62, 99.60, 75.97, 75.75, 73.89, 72.34,

70.74, 70.43, 68.69, 68.46, 68.42, 68.30, 66.36, 61.63, 57.92, 53.65, 47.35, 40.02, 39.95, 39.85, 39.78, 39.69, 39.61, 39.52, 39.44, 39.35, 39.19, 39.02, 22.61, 22.38, 20.53, 20.38, 20.27, 18.96, 16.52; HRMS (ES) Calcd for $C_{52}H_{66}N_3NaO_{23}PS$ $[M+Na]^+$ 1186.3438, found 1186.3415.[201]

Boc-D-Ala-D-Ala-OMe (54)

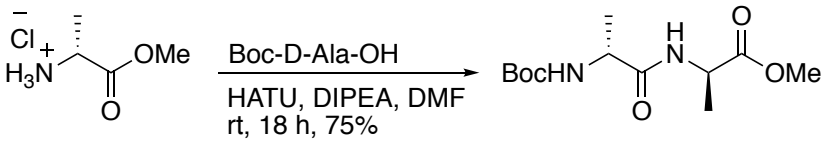

(84) **(54)**

H-D-Ala-OMe.HCl (84) (5.00 g, 35.8 mmol), Boc-D-Ala-OH (6.78 g, 35.8 mmol) and HATU (13.60 g, 35.8 mmol) were all dissolved in dry DMF as solvent (175 mL), and the temperature of the reaction flask was reduced to 0 °C. DIPEA (6.25 mL, 107.4 mmol) was added, and the reaction mixture was stirred at ambient temperature for 18 h. After the solution was concentrated *in vacuo*, it was re-dissolved in EtOAc (200 mL) that was washed with 0.5 M HCl (100 mL), saturated sodium bicarbonate (100 mL) and brine (100 mL), respectively. Next, the organic phase was dired over anhydrous sodium sulfate and concentrated *in vacuo* to obtain Boc-dipeptide (54), a white foam (7.37 g, 75%). $[\alpha]_D^{25}$ = 69.56 (*c* = 0.675 g/100mL, H_2O); IR (H_2O cast) 3309, 3066, 2980, 2980, 2937, 1747 cm^{-1}; ^1H NMR ($CDCl_3$, 400 MHz) δ 6.67 (m, 1H, D-Ala5NH), 5.03 (m, 1H, D-Ala4NH), 4.56 (pentet, *J* = 7.2 Hz, 1H, D-Ala5Hα), 4.17 (m, 1H, D-Ala4Hα), 3.74 (s, 3H, D-Ala5-OMe), 1.44 (m, 9H, Boc), 1.39 (d, *J* = 7.1 Hz, 3H, D-Ala5Hβ), 1.35 (d, *J* = 7.1 Hz, 3H, D-Ala4Hβ); ^{13}C NMR ($CDCl_3$, 125 MHz) δ 173.32,

172.30, 52.59, 48.15, 28.43, 18.50, 18.41; HRMS (ES) Calcd for $C_{12}H_{22}N_2NaO_5$ $[M+Na]^+$ 297.1421, found 297.142.[201, 245]

Boc-Lys(TFA)-D-Ala-D-Ala-OMe (55)

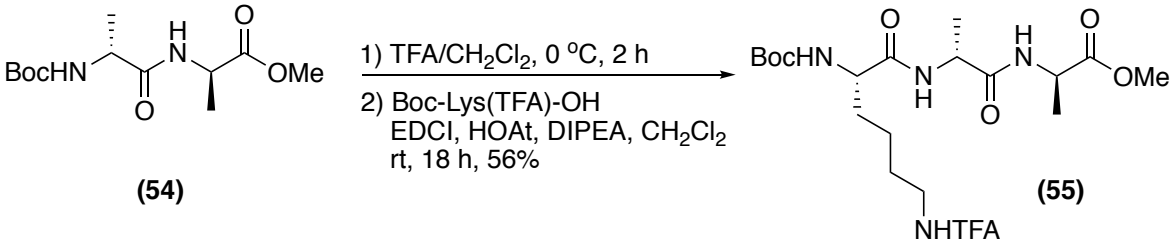

(54) **(55)**

Boc-D-Ala-D-Ala-OMe (54) (3.2 g, 11.7 mmol) was dissolved in CH_2Cl_2 (50 mL) and cooled to 0 °C. TFA (50 mL) was added, and the reaction was stirred at 0 °C for 2 h. The reaction mixture was concentrated *in vacuo* and co-evaporated with toluene (3 x 20 mL). In a separate flask, Boc-Lys(TFA)-OH (4.00 g, 11.7 mmol) was dissolved in CH_2Cl_2 (50 mL) and cooled to 0 °C. DIPEA (6 mL, 35 mmol), EDCI.HCl (2.24 g, 11.7 mmol) and a 0.6 M solution of HOAt in DMF (19.5 ml, 11.7 mmol) were added, and the reaction was stirred for 15 min. Then, a solution of the freshly deprotected dipeptide in CH_2Cl_2 (50 mL) and DIPEA (4 mL) was added, and the solution stirred at ambient temperature overnight. The reaction mixture was concentrated *in vacuo* and re-dissolved in EtOAc (150 mL). The organic phase was washed with 0.5 M HCl solution (100 mL), which was then extracted with EtOAc (100 mL). The combined organic phases were washed with a solution of saturated $NaHCO_3$ (100 mL), which was also extracted with EtOAc (100 mL). Then, the combined organic phase was washed with brine (2 x 100 mL), dried over Na_2SO_4 and concentrated *in vacuo*. The oil was precipitated from Et_2O (200 mL) and filtered to yield the product as a white

powder (3.20 g, 56%). $[\alpha]_D^{25}$ = 38.82 (*c* = 0.445 g/100 mL, H_2O); IR (cast) 3305, 3086, 2979, 2940, 2869, 1711, 1656, 1529, 1455 cm^{-1}; ^{1}H-NMR (500 MHz, $CDCl_3$) δ 6.95 (s, 1H, Lys3-NHTFA), 6.90 (s, 1H, D-Ala4-NH), 6.80 (d, *J* = 7.5 Hz, 1H, D-Ala5-NH), 5.21 (d, *J* = 7.7 Hz, 1H, Lys3-NH), 4.57 – 4.47 (m, 2H, D-Ala4-Hα + D-Ala5-Hα), 4.11 (dd, *J* = 14.0, 7.0 Hz, 1H, Lys3-Hα), 3.75 (s, 3H, -OMe), 3.37 (app. q, *J* = 6.8 Hz, 2H, Lys3Hε), 1.85 (m, 1H, Lys3-Hβ), 1.74 (m, 2H, Lys3-Hδ), 1.71 – 1.56 (m, 3H, Lys3-Hβ + Hγ), 1.44 (s, 9H, Boc), 1.40 (m, 6H, D-Ala4-Hβ + D-Ala5-Hβ); ^{13}C-NMR (126 MHz, $CDCl_3$) δ 173.1, 171.9, 171.6, 157.3, 116, 80.4, 60.4, 54.3, 52.5, 48.8, 48.2, 39.4, 31.7, 28.31, 28.3, 28.29, 22.4, 18.1, 17.9; ^{19}F-NMR (376 MHz, $CDCl_3$) δ -75.8; HRMS (ESI) Calcd for $C_{20}H_{34}F_3N_4O_7$ $(M+H)^+$ 499.2374, found 499.2386.

Boc-D-γ-Glu(α-amide)-Lys(TFA)-D-Ala-D-Ala-OMe (56)

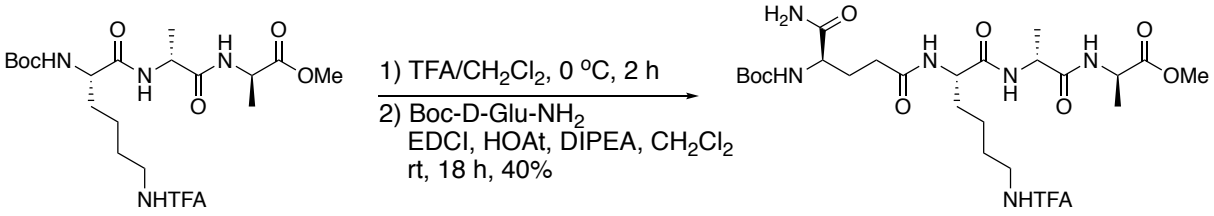

(55) **(56)**

Boc-tripeptide (55) (3.00 g, 6.02 mmol) was suspended in CH_2Cl_2 (30 mL) and cooled to 0 °C. TFA (30 mL) was added, at which point all the solid dissolved, and the resulting solution was stirred at 0 °C for two hours. Then, the reaction mixture was concentrated *in vacuo* and co-evaporated with toluene (2 x 40 mL). The colorless oil was re-dissolved in CH_2Cl_2 (50mL) and DIPEA (2 equivalents) so that the final pH

was ~8. This solution was added to a stirring solution of Boc-D-γ-Glu-NH2 (1.48 g, 6.02 mmol), EDCI (1.15 g, 6.02 mmol), 0.6 M HOAt (10 mL, 6.02 mmol) and DIPEA (1.05 mL, 6.02 mmol) in CH_2Cl_2 (50 mL) at 0 °C. The resulting yellow solution was stirred at ambient temperature overnight. The reaction mixture was concentrated *in vacuo* and re-dissolved in EtOAc (150 mL). The organic phase was washed with 0.5 M HCl solution (100 mL), which was then extracted with EtOAc (100 mL). The combined organic phases were washed with a solution of saturated $NaHCO_3$ (100 mL), which was then extracted with EtOAc (100 mL). Then, the combined organic phase was washed with brine (2 x 100 mL), dried over Na_2SO_4 and concentrated *in vacuo*. The oil was precipitated from Et_2O (200 mL) and filtered to yield the product as a white powder (1.64 g, 40%). $[\alpha]^{D}_{25}$ = 15.87 (*c* = 0.65 g/100 mL, MeOH); IR (cast) 3314, 3089, 2977, 2935, 1699, 1669; ^{1}H-NMR (500 MHz, DMSO-d_6) δ 9.34 (t, *J* = 5.7 Hz, 1H, Lys3-NHTFA), 8.16 (d, *J* = 7.1 Hz, 1H, D-Ala5-NH), 8.12 (d, *J* = 8.0 Hz, 1H, D-Ala4-NH), 7.96 (d, *J* = 7.4 Hz, 1H, Lys3-NH), 7.19 (s, 1H, D-γ-Glu2-NH_2), 6.94 (s, 1H, D-γ-Glu2-NH_2), 6.67 (d, *J* = 8.2 Hz, 1H, D-γ-Glu2-NH), 4.29 – 4.24 (m, 1H, D-Ala4-Hα), 4.24 – 4.20 (m, 1H, D-Ala5-Hα), 4.14 (app. q, *J* = 7.4 Hz, 1H, Lys3-Hα), 3.80 (m, 1H, D-γ-Glu2-Hα), 3.58 (s, 3H, -OMe), 3.12 (app. q, *J* = 6.8 Hz, 2H, Lys3-Hε), 2.12 (m, 2H, D-γ-Glu2-Hγ), 1.78 (m, 1H, D-γ-Glu2-Hβ), 1.70 – 1.60 (m, 1H, D-γ-Glu2-Hβ), 1.56 (m, 1H, Lys3-Hβ), 1.50 – 1.39 (m, 4H, L-Lys3-Hδ + Lys3-Hβ + Lys3-Hγ), 1.35 (s, 9H, Boc), 1.27 (d, *J* = 7.3 Hz, 3H, D-Ala5-Hβ), 1.23-1.20 (m, 1H, L-Lys3-Hγ), 1.16 (d, *J* = 7.1 Hz, 3H, D-Ala4-Hβ); ^{13}C-NMR (126 MHz, DMSO-d_6) δ 173.7, 172.8, 171.9, 171.8, 171.3, 156.1, 155.1, 115.8, 78.0, 53.8, 52.6, 51.8, 47.5, 47.5, 31.8, 31.3, 28.1, 28.1, 27.9, 22.5, 17.9, 16.7; ^{19}F NMR (376 MHz, $(CD_3)_2SO$) δ -74.4;

HRMS (ESI) Calcd for $C_{25}H_{42}F_3N_6O_9$ $(M+H)^+$ 627.296, found 627.2957.

Synthesis of pentapeptidyl disaccharide (61)

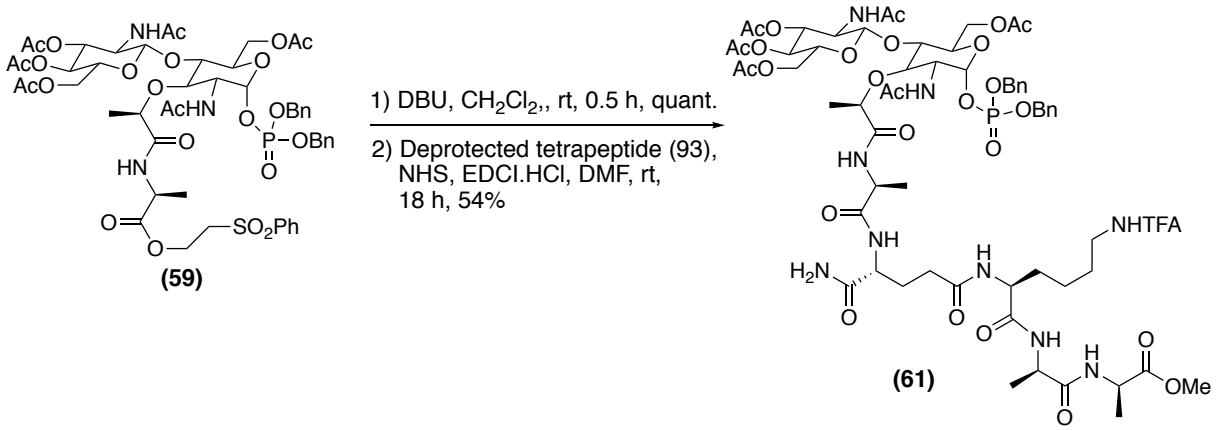

Phosphate (59) (430 mg, 0.370 mmol) was dissolved in dry CH_2Cl_2 (5 mL) and stirred under an argon atmosphere. 1,8-Diazabicyclo[5.4.0]undec-7-ene (DBU) (50 µL, 0.37 mmol) was added, and the resulting solution was stirred for 30 min at ambient temperature. Next, the reaction mixture was diluted with CH_2Cl_2 (10 mL) and washed with 1M HCl (10 mL) and brine (6 mL). The organic phase was dried over Na_2SO_4, concentrated *in vacuo* and precipitated from Et_2O (10 mL). The resulting white solid was dried under high vacuum for one hour to give acid (60) (322 mg, 0.32 mmol). Acid (60) (322 mg, 0.32 mmol) was dissolved in anhydrous DMF (4 mL) and cooled to 0 ^oC. EDCI.HCl (93 mg, 0.49 mmol) and N-hydroxysuccinimide (NHS) (60 mg, 0.49 mmol) were added, and the resulting solution stirred under argon for 18 h. Next, the reaction mixture was diluted with EtOAc (20 mL), washed with water (10 mL) (which was back-extracted with EtOAc (4 mL)), washed with brine (10 mL), dried over Na_2SO_4 and concentrated *in vacuo* to yield the NHS ester as an oil (292 mg, 0.27 mmol). In a separate flask, Boc-tetrapeptide (56) (170 mg, 0.28 mmol) was

suspended in CH_2Cl_2 (5 mL) and cooled to 0 ^oC. TFA (5 mL) was added, and the reaction mixture stirred at 0 ^oC for two hours, concentrated *in vacuo* and co-evaporated with toluene. The NHS ester (292 mg, 0.27 mmol), tetrapeptide TFA salt (0.28 mmol) and DIPEA (161 µL, 0.924 mmol) were dissolved in dry DMF (3 mL) and stirred under argon for 18 h. The reaction mixture was concentrated *in vacuo*, re-dissolved in $CHCl_3$:IPA (9:1), washed with brine (3 x 5 mL), dried over Na_2SO_4, filtered and concentrated *in vacuo*. The resulting oil was precipitated from Et_2O and dried under high vacuum for 1 h to yield pentapeptidyl disaccharide (61) as a white powder (301 mg, 54% from disaccharide ester). This compound was used in the next step without further purification; HRMS (ES) Calcd for $C_{64}H_{89}F_3\ N_9O_{27}PNa\ [M+Na]^+$ 1526.545, found 1526.5457.

Synthesis of bis ammonium (*E,E*)-farnesyl phosphate (88)

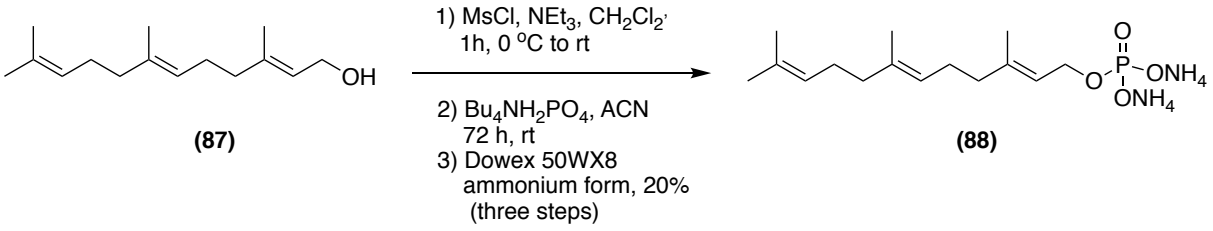

(87) **(88)**

Methansulfonyl chloride (93 µL, 1.2 mmol) was added dropwise at 0 °C to a solution of Farenesol (87) (222 mg, 1.00 mmol) and triethylamine (210 µL, 1.5 mmol) in CH_2Cl_2 (10 mL). The reaction was allowed to reach ambient temperature, stirred for 45 min, and then diluted with CH_2Cl_2 (3 x 5 mL). The combined organic extracts were washed with HCl solution (1 M, 10 mL) and brine (10 mL), dried over anhydrous Na_2SO_4 and concentrated in vacuo to yield the crude mesylate. To another flame-dried flask under argon was added tetrabutylammonium dihydrogen phosphate (1 g, 3.0 mmol) and dry acetonitrile (6 mL). A solution of the crude mesylate in acetonitrile (3mL) was added dropwise to the phosphate solution, and the resulting mixture stirred at ambient temperature for 72 h. The ion-exchange resin was prepared in the following way: Dowex 50W-X8,100-200 mesh (30 g, Acros Organics) was added to a 2.5 x 25 cm fritted glass column. The resin was washed with concentrated NH_4OH (4 x 40 mL), followed by H_2O to reach pH 7 and buffer (2x 40mL, 25 mM NH_4HCO_3 in 49:1 H_2O: IPA). The reaction mixture was concentrated in vacuo, dissolved in buffer (2mL) and loaded on to the ion exchange column. The column was eluted with buffer, and 5 mL fractions were collected. These fractions were combined and concentrated in vacuo. The resulting residue was dissolved in 4:2:1 ethyl acetate: IPA: H_2O (7 mL) and purified by silica flash chromatography column using the same eluent. The product containing fractions were concentrated to 10 mL, frozen and lyophilized to

yield bisammonium farnesyl phosphate as a solid white powder. The product containing fractions were determined using ESI-MS $[M-H]^-$ = 301.1 (50 mg, 20%).[201]

Synthesis of (*E*, *E*)-farnesyl lipid II (63)

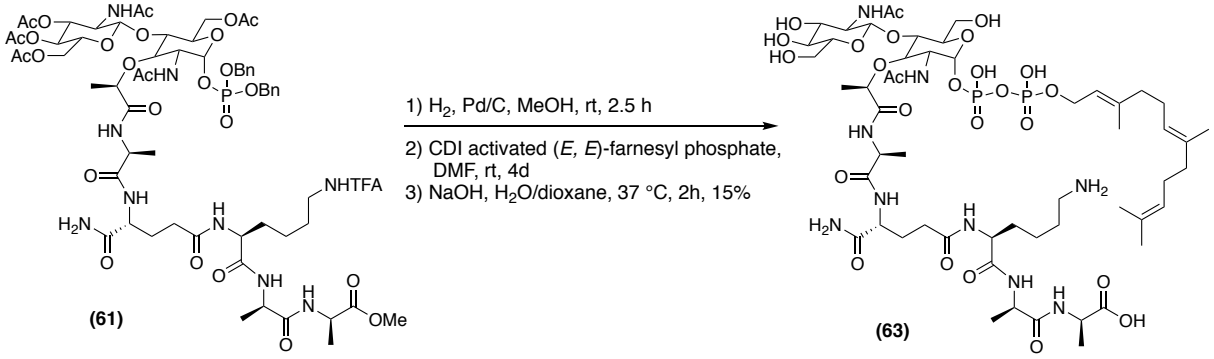

Disaccharide (61) (53 mg, 0.04 mmol) was dissolved in anhydrous MeOH (6 mL) and degassed with argon. Palladium on activated charcoal (10%, 0.094 mmol, 100 mg) was added, and the suspension stirred under H_2 pressure for two and a half hours. Then, the reaction mixture was filtered through celite, which was washed with MeOH, and concentrated *in vacuo*. The resulting phosphate was dried under high vacuum overnight to give a white solid. In a separate flask, (*E,E*)-Farnesyl phosphate (10 mg, 0.03 mmol) and carbonyl diimidazole (CDI) (25.0 mg, 0.153 mmol) were dissolved in anhydrous DMF (0.5 mL) and stirred at room temperature for 2 h. Farnesyl phosphate formed a cloudy mixture in DMF, which turned to a clear solution upon addition of CDI. Anhydrous MeOH (4 equivalents) was added, and the solution was stirred for 45 min. Excess MeOH was removed carefully by rotary evaporation. Then, the disaccharide phosphate was dissolved in anhydrous DMF (0.5 mL) and added to this CDI-activated farnesyl phosphate solution. The resulting solution was

stirred for 4 days at ambient temperature and then concentrated *in vacuo* to yield a clear oil. This was dissolved in H_2O:Dioxane (1:1, 2 mL), to which a solution of 1M NaOH (0.3 mL, 0.3 mmol, 10 equivalents) was added, and the resulting solution was stirred for 2 h at 37 ^oC . The reaction mixture changed from a clear solution to a cloudy one over this time period. The reaction mixture was filtered through a millipore filter disc, which was also washed with H_2O (1 mL). Next, the crude reaction mixture was purified by RP-HPLC: GraceVydac Protein and Peptide C_{18} 100 mm column 10 micron; flow rate 10 mL/min, UV= 220 nm, method = 100 % 50 mM NH_4HCO_3 (aq) to 100% MeOH over 30 min. Fractions that contained product were determined by ESI-MS, pooled, concentrated and lyophilized to give (*E,E*)-farnesyl lipid ll as a white powder (6 mg, 14.7%); ^{13}C-NMR (126 MHz, CD_3OH) δ 179.3, 175.4, 174.5, 174.3, 173.8, 141.9, 136.2, 132.5, 125, 121.2, 101, 75.2, 74.9, 73.5, 71.7, 63.5, 62.4, 40.2, 32.7, 31.6, 28.6, 28.3, 27.5, 27.2, 25.7, 23.5, 23.1, 20.2, 19.3, 19.0, 17.7, 17.5, 16.5, 16.3, 16.0; ^1H-NMR (Table 4.3).

6-O-Benzylbromohexane (91)

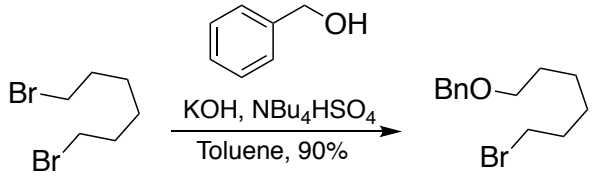

(90) **(91)**

To a solution of benzylalcohol (1.44 mL, 12.8 mmol) and 1,6-dibromohexane (11.0 mL, 72 mmol, 5.5 eq) in toluene (70 mL) was added ground potassium hydroxide (3.17 g, 56.8 mmol, 4.4 eq) and tetrabutylammonium hydrogen sulfate (0.47 g, 0.10 eq). The mixture was stirred rapidly for 3.5 h at room temperature, then quenched with saturated aqueous sodium bicarbonate. The resulting solution was diluted with water, then extracted with water and brine. The organic layer was dried with sodium sulfate, and the toluene was removed under reduced pressure to give a clear oil (15.5516 g). This oil was distilled under house vacuum to 100 °C, and the residue that did not distill was collected. This residue was the title compound (3.3338 g, 90%). $[\alpha]^{D}_{25}$ = 0.16 (*c* = 1.00 g/100mL, CH_2Cl_2); IR (CH_2Cl_2 cast) 3061, 3031, 3004, 2936, 2857, 2793, 1495; ^{1}H-NMR (500 MHz, $CDCl_3$) δ 7.37 – 7.31 (m, 4H), 7.31 – 7.27 (m, 1H), 4.50 (s, 2H), 3.47 (t, *J* = 6.5 Hz, 2H), 3.40 (t, *J* = 6.8 Hz, 2H), 1.92 – 1.81 (m, 2H), 1.69 – 1.59 (m, 2H), 1.51 – 1.36 (m, 4H);^{13}C-NMR (126 MHz, $CDCl_3$) δ 38.8, 128.5, 127.8, 127.6, 73.1, 70.3, 34.0, 32.9, 29.7, 28.1, 25.6.[246]

6-O-Benzyl-hexyltriphenylphosphonium bromide (92)

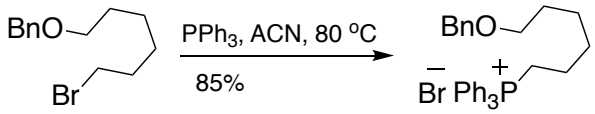

(91) **(92)**

To a solution of 6-O-benzylhexylbromide (2.11 g, 7.75 mmol) in dry acetonitrile (20 mL) was added triphenylphosphine (4.06 g, 15.5 mmol, 2 eq). The mixture was heated overnight at 80 °C, then the solvent was removed under reduced pressure to give a clear oil (7.09 g). Purification using flash chromatography (8% MeOH in DCM eluent) gave the title compound as a clear oil (3.76 g, 91%). $[\alpha]^{D}_{25}$ = -0.22 (*c* = 1.00 g/100mL, $CHCl_3$); IR ($CHCl_3$ cast) 3281, 3054, 2928, 2858, 2791, 2458, 1649, 1586, 1542; ^{1}H NMR (700 MHz, $CDCl_3$) δ 7.9 – 7.8 (m, 6H), 7.8 – 7.7 (m, 3H), 7.7 – 7.6 (m, 6H), 7.3 (m, 4H), 7.2 (m, 1H), 4.4 (s, 2H), 3.9 – 3.7 (m, 2H), 3.5 (d, *J* = 4.8 Hz, 2H), 3.4 (t, *J* = 6.4 Hz, 2H), 1.7 – 1.6 (m, 1H), 1.6 (m, 2H), 1.6 – 1.5 (m, 1H), 1.4 – 1.3 (m, 2H); ^{13}C NMR (176 MHz, $CDCl_3$) δ 138.7, 135.0, 135.0, 133.9, 133.8, 130.6, 130.5, 128.4, 127.8, 127.6, 118.9, 118.4, 73.0, 70.4, 30.3, 30.2, 29.4, 26.0, 23.1, 22.8, 22.7; HRMS (ES) Calcd for $C_{31}H_{34}OP$ $[M]^{\cdot+}$ 453.2347, found 453.2334.[247]

1-^{13}C-Hexanal (94)

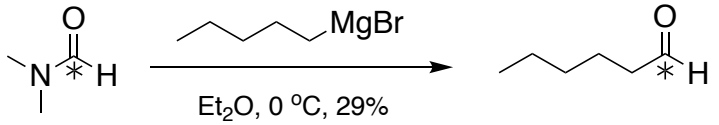

(93) **(94)**

To a solution of pentylmagnesium bromide (1.75 M in diethyl ether, 4.1 mL, 0.97 eq) in diethyl ether (7 mL) at 0 °C, was added 1-^{13}C-dimethylformamide (0.55 mL in 7.0 mL diethyl ether) over 25 min. The DMF was then rinsed down with diethyl ether (2 x 2 mL) over 10 min, allowed to react for a further 5 min, then quenched with the addition of hydrochloric acid (2 M, 10 mL). The organic layer was removed, and the aqueous layer was extracted three times with diethyl ether. All organic layers were combined, washed once with brine, dried with magnesium sulfate, filtered and concentrated at room temperature under a weak vacuum (~100 mmHg) to give a light-yellow liquid (1.1639 mL). Then, this liquid was purified via distillation (kugelrohr) to give the title compound as a clear oil (0.200 g, 29%). $[\alpha]^{D}_{25}$ = 0.58 (*c* = 1.00 g/100mL, CH_2Cl_2); IR (CH_2Cl_2 cast) 3399, 2956, 2930, 2859, 1722, 1670, 1466, 1378; ^{1}H NMR (600 MHz, $CDCl_3$) δ 9.76 (dt, *J* = 169.8, 1.9 Hz, 1H), 2.46 – 2.38 (m, 2H), 1.64 (td, *J* = 7.3, 4.6 Hz, 2H), 1.36 – 1.29 (m, 4H), 0.93 – 0.88 (m, 2H); ^{13}C NMR (150 MHz, $CDCl_3$) δ 205.8, 203.07, 98.6, 93.4, 66.4, 65.8, 63.1, 22.4, 15.2; HRMS (ES) Calcd for C_6H_{12} $[M]^+$ 100.0888, found 100.0889.[248]

Anthracene-tridecaptin A1 (72)

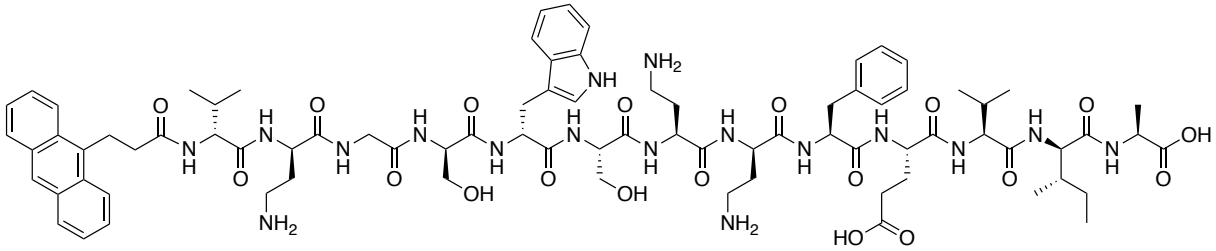

(72)

Peptide (72) was isolated as a single peak using C18 RP-HPLC (5.5 mg, 25 %). Retention time = 39 min. ^{1}H NMR (D_2O + 10 % CD_3OD, 600 MHz): δ 7.51 – 7.02 (m,18H, Trp5-ArH + Phe9-ArH + Anth-ArH), 4.65 – 4.61 (m, 1H, Phe9-Hα), 4.55 (t, 1H, *J* =7.3 Hz, Trp5-Hα), 4.39 – 4.18 (m, 7H, D-Ser4-Hα + D-Dab2-Hα + D-*allo*-Ile12-Hα +Dab7-Hα + Glu10-Hα + D-Dab8-Hα + Ala13-Hα), 4.09 – 4.06 (m, 2H, Val11-Hα + Ser6-Hα), 3.89 – 3.86 (m, 3H, D-Val1-Hα + Gly3-Hα), 3.70 – 3.63 (m, 2H, D-Ser4-Hβ), 3.56 – 3.53 (m, 1H, Ser6-Hβ), 3.30 – 3.10 overlapped by MeOH (m, 4H, Ser6-Hβ + D-Trp5-Hβ + Phe9-Hβ), 3.01 – 2.91 (m, 4H, D-Dab2-Hγ + Dab7-Hγ), 2.87 – 2.79 (m, 1H, Phe9-Hβ), 2.70-2.64(m, D-Dab8-Hγ), 2.59 – 2.54 (m, 1H, D-Dab8-Hγ), 2.28 – 2.10 (m, 6H, Glu10-Hγ + D-Dab2-Hβ + D-Dab2-Hβ + Dab7-Hβ + Anth-Hα), 2.01 – 1.75 (m, 9H, D-Val1-Hβ + Dab7-Hβ + D-Dab8-Hβ + Glu10-Hβ + Val11-Hβ + D-*allo*-Ile12-Hβ + Glu10-Hγ), 1.29 – 1.12 (m, 5H, Ala13-Hβ + D-*allo*-Ile12-Hγ), 0.90 – 0.80 (m, 18H, D-Val1-Hγ + Val11-Hγ + D-*allo*-Ile12-Hγ, Hδ); HRMS (ESI) Calcd for $C_{81}H_{111}N_{17}O_{19}$ $(M+2H)^{+2}$ 813.9194, found 813.9182.[223]

Biotin-tridecaptin A1 (73)

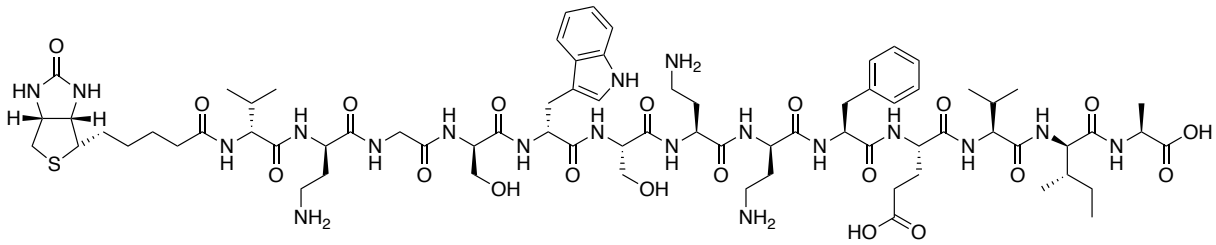

(73)

Peptide (73) was isolated as a single peak using C18 RP-HPLC (8.3 mg, 50.0 %). Retention time = 22.87 min. ^{1}H NMR (D_2O, 600 MHz): δ 7.57 (d, 1H, *J* = 8.5 Hz,Trp5-ArH), 7.46 (d, 1H, *J* = 8.2 Hz, Trp5-ArH), 7.32 – 7.25 (m, 3H, Trp5-ArH + Phe9-ArH), 7.21 – 7.19 (m, 4H, Trp5-ArH + Phe9-ArH), 7.11 (t, 1H, *J* = 7.5 Hz, Trp5-ArH),4.67 (dd, 1H, *J* = 9.5, 5.3 Hz, Phe9-Hα), 4.62 (t, 1H, *J* = 7.1 Hz, Trp5-Hα), 4.50 – 4.48 (m, 1H, Biotin-NHC*H*CH2-) 4.45 – 4.41 (m, 2H, D-Ser4-Hα + D-Dab2-Hα), 4.35 – 4.26 (m, 5H,D-*allo*-Ile12-Hα + Dab7-Hα + Glu10-Hα + D-Dab8-Hα + Biotin-NHC*H*CH-), 4.22 – 4.18 (m, 1H, Ala13-Hα), 4.13 – 4.10 (m, 2H, Val11-Hα + Ser6-Hα), 4.01 (d, 1H, *J* = 7.5 Hz, D-Val1-Hα), 3.89 (s, 2H, Gly3-Hα), 3.75 (app. qd, 2H, *J* = 12.0, 5.4 Hz, D-Ser4-Hβ), 3.55 (dd, 1H, *J* = 11.5, 6.2 Hz, Ser6-Hβ), 3.31 (dd, 1H, *J* = 11.2, 5.3 Hz, Ser6-Hβ), 3.25 (d, 2H, *J* = 6.9 Hz, D-Trp5-Hβ), 3.19 – 3.16 (m, 2H, Phe9-Hβ + Biotin-NHCHC*H*), 3.07 – 2.97 (m, 4H, D-Dab2-Hγ + Dab7-Hγ), 2.90 – 2.85 (m, 2H, Phe9-Hβ + Biotin-NHCHC*H*H), 2.73 – 2.68 (m, 2H, D-Dab8-Hγ + Biotin-NHCHCH*H*), 2.61 – 2.56 (m, 1H, D-Dab8-Hγ), 2.32 – 1.78 (m, 14H, Glu10-Hγ + D-Dab2-Hβ + Dab7-Hβ + D-Val1-Hβ + D-Dab8-Hβ +Glu10-Hβ + D-*allo*-Ile12-Hβ + Biotin-NHC(O)*CH$_2$*-), 1.64 – 1.44 (m, 4H, Biotin-NHC(O)CH$_2$CH$_2$CH$_2$C*H$_2$*-), 1.34 – 1.19 (m, 7H, Ala13-Hβ + D-*allo*-Ile12-Hγ + Biotin-NHC(O)CH$_2$CH$_2$C*H$_2$*-), 0.96 – 0.84 (m, 18H, D-Val1-Hγ + Val11-Hγ + D-*allo*-Ile12-Hγ,Hδ); HRMS (ESI) Calcd for

$C_{74}H_{113}N_{19}O_{20}S$ $(M+2H)^{+2}$ 810.9138, found 810.9129.[223]

Fmoc-tridecaptin A1 (95)

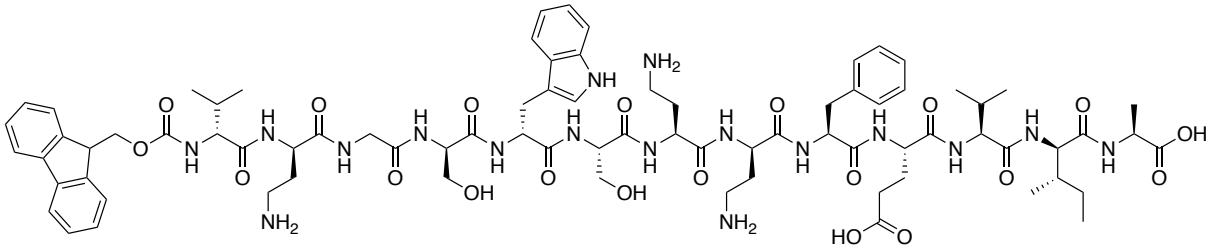

(95)

Peptide (95) was isolated as a single peak using C18 RP-HPLC (10 mg, 20 %). Retention time = 38 min. MS/MS: m/z 203.1 (y2), 302.2 (y3), 431.2 (y4), 578.3 (y5), 678.3 (y6), 778.4 (y7), 865.4 (y8), 1051.4 (y9), 1138.4 (y10), 1195.5 (y11), 1295.5 (y12), 422.2 (b2), 479.2 (b3), 566.2 (b4), 752.3 (b5), 839.3 (b6), 1039.4 (b8), 1186.5 (b9), 1315.5 (b10), 1414.6 (b11), 294.2 (a1), 538.2 (a4), 724.3 (a5), 1386.5 (a11). MW calculated for $C_{79}H_{110}N_{17}O_{20}$ 1616.8108, found high resolution (FTICR-ESI-MS)1616.8088 $(M+H)^{+}$.[223]

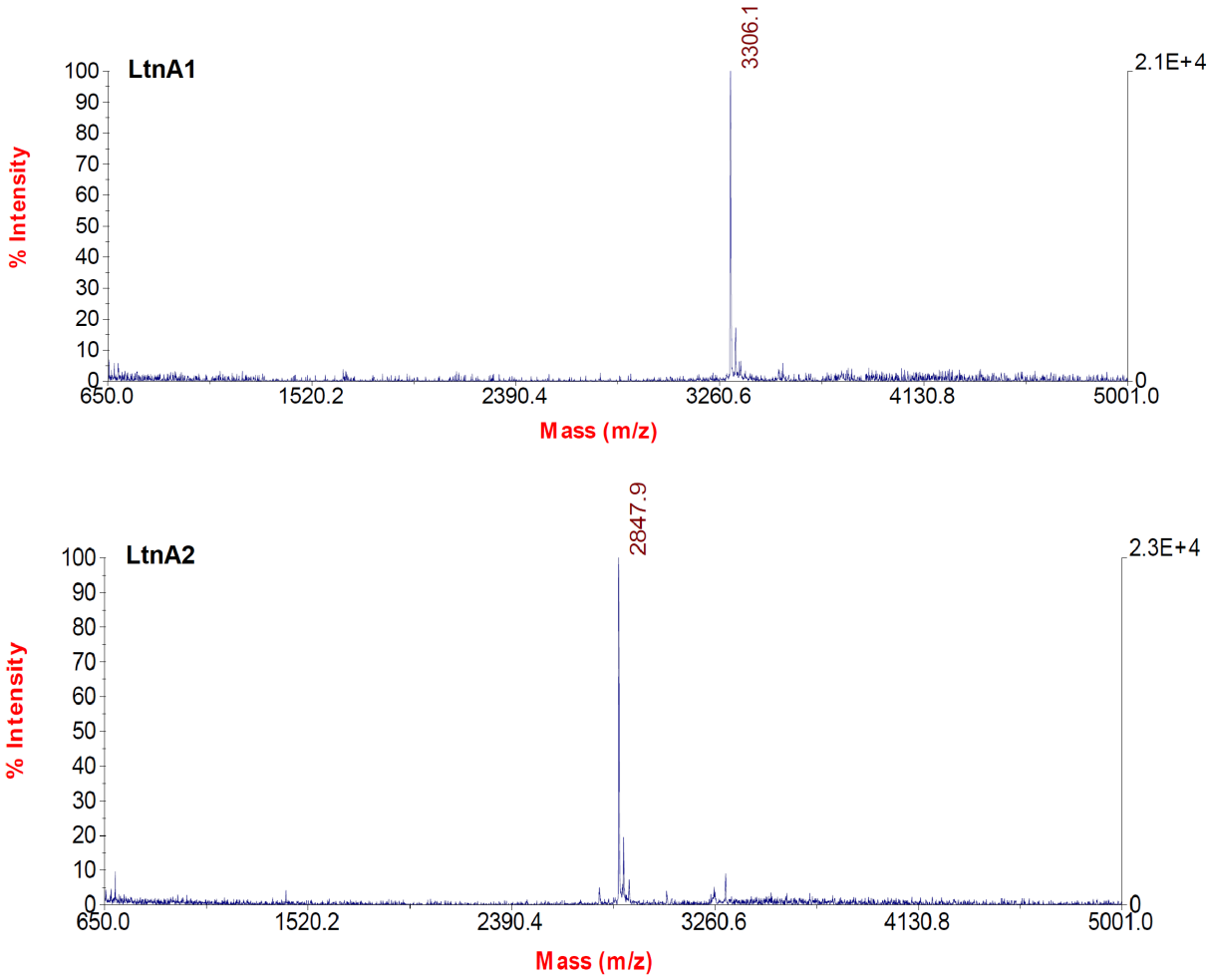

Figure 4.1. MALDI-TOF detection of lacticin 3147 peptides

Residue	Chemical Shifts (ppm)				
	NH	Hα	Hβ	Hγ	Other
Lan1	Not found	Not found	Not found	NA	NA
Lan2	7.935	4.687	3.111 3.329	NA	NA
Dhb3	Not found	NA	Not found	Not found	NA
Asn4	8.092	4.767	2.883	NA	HD1 = 7.549, HD2 = 6.877
Dhb5	Not found	NA	Not found	Not found	NA
Phe6	7.862	4.525	3.174 2.992	NA	HD1 = 7.209, HE1= 7.267
D-Ala7	7.868	4.233	1.215	NA	NA
Leu8	7.823	4.345	1.572	1.217	HD1 = 0.835, HD2 = 0.821
Lan9	8.176	4.560	2.784 3.133	NA	NA
Asp10	8.241	4.587	2.731 2.643	NA	NA
Tyr11	7.974	4.101	2.592 2.524	NA	HD1 = 6.562, HE1 = 6.5
Trp12	7.923	4.553	3.441 3.116	NA	HD1 = 7.231, HE1 = 10.101, HZ2 = 7.428, HH2 = 7.639, HZ3 = 7.173, HE3 = 7.107
Gly13	7.936	3.989 3.804	NA	NA	NA
Asn14	8.473	4.722	2.777 2.775	NA	HD1 = 7.827, HD2 = 6.727
Asn15	8.342	4.771	2.718 2.820	NA	HD1 = 6.694, HD2 = 7.408
Gly16	8.186	3.756 3.849	NA	NA	NA
Ala17	8.100	4.075	1.123	NA	NA
Trp18	7.767	4.566	3.369 3.121	NA	HD1 = 7.14, HE1 = 10.029, HZ2 = 7.375, HH2 = 7.12, HE3 = 7.562, HZ3 = 7.023
Lan19	7.784	4.518	2.878 2.834	NA	NA
Abu20	7.425	4.772	3.645	1.245	NA

Leu21	7.85	4.743	1.636 1.564	1.509	HD1 = 0.839, HD2 = 0.828
Abu22	8.421	4.622	3.658	1.234	NA
His23	8.699	4.512	3.236 3.191	NA	HD2 = 7.057, HE1 = 7.979
Glu24	8.771	3.938	1.909	2.189 2.112	NA
Lan25	7.118	4.550	2.873	NA	NA
Met26	7.786	4.324	1.573 1.487	2.239 2.354	NA
Ala27	8.254	4.003	1.239	NA	NA
Trp28	7.244	4.563	3.275 3.333	NA	HD1 = 7.153, HE1 = 10.117, HZ2 = 7.434, HH2 = 7.173, HZ3 = 7.101, HE3 = 7.553
Lan29	7.428	4.269	2.720 2.369	NA	NA
Lys30	7.742	4.199	1.829, 1.720	1.391	HD2 = 1.644, HE2 = 2.364, HE3 = 2.931

Table 4.1. Chemical shift assignment of lacticin 3147 A1 alone. Some N-terminal residues were not observed. NA = not applicable.

Residue	Chemical Shifts (ppm)				
	Amide NH	Hα	Hβ	Hγ	Other
Lan1	Not found	Not found	Not found	NA	NA
Lan2	7.885	4.675	3.094 3.316	NA	NA
Dhb3	Not found	NA	Not found	Not found	NA
Asn4	8.101	4.767	2.879	NA	HD1 = 7.555, HD2 = 6.879
Dhb5	Not found	NA	Not found	Not found	NA
Phe6	7.865	4.521	3.179 2.996	NA	HD1 = 7.212, HE1 = 7.267
D-Ala7	7.865	4.239	1.218	NA	NA
Leu8	7.820	4.348	1.579	1.199	HD1 = 0.851, HD2 = 0.821
Lan9	8.168	4.573	2.782 3.140	NA	NA
Asp10	8.235	4.595	2.749 2.642	NA	NA
Tyr11	7.977	4.103	2.581 2.524	NA	HD1 = 6.565, HE1 = 6.499
Trp12	7.935	4.554	3.442 3.119	NA	HD1 = 7.236, HE1 = 10.114, HZ2 = 7.423, HZ3 = 7.169, HE3 = 7.109, HH2 = 7.644
Gly13	7.945	3.997 3.800	NA	NA	NA
Asn14	8.49	4.725	2.766 2.794	NA	HD1 = 7.859, HD2 = 6.725
Asn15	8.34	4.781	2.714 2.816	NA	HD1 = 6.695, HD2 = 7.411
Gly16	8.194	3.753 3.852	NA	NA	NA
Ala17	8.117	4.076	1.121	NA	NA
Trp18	7.765	4.563	3.370 3.128	NA	HD1 = 7.141, HE1 = 10.029, HZ2 = 7.368, HH2 = 7.119, HE3 = 7.568, HZ3 = 7.023
Lan19	7.786	4.523	2.889 2.838	NA	NA
Abu20	7.429	4.782	3.611	1.242	NA

Leu21	7.858	4.746	1.640 1.567	1.509	HD1 = 0.858, HD2 = 0.828
Abu22	8.447	4.628	3.661	1.233	NA
His23	8.674	4.514	3.205 3.180	NA	HD1 = 9.155, HD2 = 7.023, HE1 = 7.872
Glu24	8.793	3.944	1.902	2.187 2.108	NA
Lan25	7.119	4.553	2.875	NA	NA
Met26	7.801	4.323	1.598 1.519	2.255 2.362	NA
Ala27	8.237	4.017	1.235	NA	NA
Trp28	7.278	4.562	3.281 3.322	NA	HD1 = 7.15, HE1 = 10.112, HZ2 = 7.434, HH2 = 7.169, HZ3 = 7.097, HE3 = 7.557
Lan29	7.452	4.261	2.714 2.382	NA	NA
Lys30	7.711	4.207	1.834 1.713	1.387	HD2 = 1.643, HE2 = 2.365, HE3 = 2.928

Table 4.2. Chemical shift assignment of lacticin 3147 A1 with lipid II. Some N-terminal residues were not observed. NA = not applicable**.**

Residue	Chemical Shifts (ppm)				
	Amide NH	**Hα**	**Hβ**	**Hγ**	**Other**
GlcNAc	8.05	NA	NA	NA	H1 = 4.54, H2 = 3.67, H3 = 3.88, H4 = 3.51, H5 = 3.29, H6 = 4.225, Ac = 2.01
MurNAc	8.40	NA	NA	NA	H1 = 5.46, H2 = 4.06, H3 = 4.09, H4 = 3.77, H5 = 3.85, H6 = 3.70, Ac = 1.98, O*CH* = 4.33, CH_3 = 1.38
Ala1	7.92	4.217	1.406	NA	NA
Glu2	8.181	4.401	2.155 1.910	2.344	NA
Lys3	8.169	4.215	1.640 1.751	1.407	HD = 1.407, HE = 2.946
Ala4	8.087	4.312	1.312	NA	NA
Ala5	7.582	4.071	1.266	NA	NA
Farnesyl	NA	NA	NA	NA	C1-H = 4.446, C2-H = 5.385, C3-CH3 = 1.685, C4-H = 2.014, C5-H = 2.097, C6-H = 5.105, C7-CH3 = 1.591, C8-H = 1.973, C9-H = 2.059, C10-H = 5.10, C11-CH3 = 1.663, 1.593

Table 4.3. Chemical shift assignment of lipid II. NA = not applicable**.**

Residue	Chemical Shifts (ppm)				
	Amide NH	**Hα**	**Hβ**	**Hγ**	**Other**
GlcNAc	8.09	NA	NA	NA	H1 = 4.540, H2 = 3.666, H3 = 3.890, H4 = 3.507, H5 = 3.292, H6 = 4.22, Ac = 2.031
MurNAc	8.45	NA	NA	NA	H1 = 5.467, H2 = 4.05, H3 = 4.09, H4 = 3.762, H5 = 3.880, H6 = 3.71, Ac = 1.99, O*CH* = 4.345, CH_3 = 1.383
Ala1	7.935	4.242	1.417	NA	NA
Glu2	8.175	4.304	2.170 1.922	2.377	NA
Lys3	8.17	4.236	1.661 1.777	1.411	HD = 1.437, HE = 2.951
Ala4	8.087	4.312	1.346	NA	NA
Ala5	7.584	4.084	1.301	NA	NA
Farnesyl	NA	NA	NA	NA	C1-H = 4.444, C2-H = 5.393, C3-CH3 = 1.685, C4-H = 2.031, C5-H = 2.097, C6-H = 5.133, C7-CH3 = 1.60, C8-H = 1.973, C9-H = 2.059, C10-H = 5.10, C11-CH3 = 1.663, 1.593

Table 4.4. Chemical shift assignment of lipid II with lacticin 3147A1. NA = not applicable.

	Full Complex	A1 res. 8-30 – lipid II structure
RMSD Backbone atoms (Å)	2.87	0.83 ± 0.20
RMSD heavy atoms (Å)	3.14	1.44 ± 0.23

Table 4.5. CYANA RMSD outputs.

LtnA1	Sweep width (Hz) (direct, indirect)	ni	np	nt	Mix time (ms)	γB_1 (Hz)
ZTOCSY-ES	10000, 10000	512	10000	24	80	7054
NOESY-ES	10000, 10000	512	10000	32	100	NA
COSY	10000, 10000	512	10000	96	NA	NA
Lipid II						
ZTOCSY-ES	8389.26, 8389.26	256	8192	32	100	6582
ROESY-ES	8389.26, 8389.26	320	8192	48	150	3300
COSY	8389.26, 8389.26	256	8192	96	NA	NA
Complex						
ZTOCSY-ES	10000, 10000	512	10000	24	80	7054
NOESY-ES	10000, 10000	512	10000	32	100	NA
COSY	10000, 10000	512	10000	96	NA	NA

Table 4.6. NMR experiment details. ni = number of complex points collected for the indirectly detected dimension; np = number of real plus imaginary points for the directly detected dimension; nt = number of cumulative scans collected for each point of acquisition; γB_1 = the induced B_1 field for spin lock sequences.

References

(1) Barrington, W. T.; Lusis, A. J. *Nat. Rev. Cardiol.* **2017**.

(2) Lynch, D. B.; Jeffery, I. B.; Cusack, S.; O'Connor, E. M.; O'Toole, P. W. *Interdiscip. Top. Gerontol.* **2015**, *40*, 141–154.

(3) Chaudet, M. M.; Allen, J.-L.; Rose, D. R. *Protein Expr. Purif.* **2012**, *86*, 135–141.

(4) Cotter, P. D.; Hill, C.; Ross, R. P. *Nat. Rev. Microbiol.* **2005**, *3*, 777–788.

(5) Martens, E.; Demain, A. L. *J. Antibiot. (Tokyo).* **2017**, *70* (5), 520–526.

(6) Wu, H.; Moser, C.; Wang, H.-Z.; Høiby, N.; Song, Z.-J. *Int. J. Oral Sci.* **2014**, *7*, 1–7.

(7) Jevons, M. P. *BMJ* **1961**, *1*, 124–125.

(8) Piddock, L. J. V. *Lancet Infect. Dis.* **2016**, *16*, 767–768.

(9) Dulaney, E. L. *Ann. N. Y. Acad. Sci.* **1954**, *60*, 155–163.

(10) Sköld, O. *Antibiotics and Antibiotic Resistance*, First.; John Wiley & Sons, Inc.: Hoboken, NJ, USA, 2011.

(11) Butler, M. S.; Blaskovich, M. A.; Cooper, M. A. *J. Antibiot. (Tokyo).* **2013**, *66*, 571–591.

(12) Sauermann, R.; Rothenburger, M.; Graninger, W.; Joukhadar, C. *Pharmacology* **2008**, *81*, 79–91.

(13) Houghton, J. L.; Green, K. D.; Chen, W.; Garneau-Tsodikova, S. *ChemBioChem* **2010**, *11*, 880–902.

(14) Endimiani, A.; Hujer, K. M.; Hujer, A. M.; Armstrong, E. S.; Choudhary, Y.;

Aggen, J. B.; Bonomo, R. A. *Antimicrob. Agents Chemother.* **2009**, *53*, 4504–4507.

(15) Sutcliffe, J. A. *Ann. N. Y. Acad. Sci.* **2011**, *1241*, 122–152.

(16) Cuddy, P. G. *Crit. Care Nurs. Q.* **1997**, *20*, 89–102.

(17) Epand, R. F.; Schmitt, M. A.; Gellman, S. H.; Epand, R. M. *Biochim. Biophys. Acta - Biomembr.* **2006**, *1758*, 1343–1350.

(18) Schneider, T.; Kruse, T.; Wimmer, R.; Wiedemann, I.; Sass, V.; Pag, U.; Jansen, A.; Nielsen, A. K.; Mygind, P. H.; Raventos, D. S.; Neve, S.; Ravn, B.; Bonvin, A. M.; De Maria, L.; Andersen, A. S.; Gammelgaard, L. K.; Sahl, H. G.; Kristensen, H. H. *Science (80-.).* **2010**, *328*, 1168–1172.

(19) O'Shea, R.; Moser, H. E. *J. Med. Chem.* **2008**, *51*, 2871–2878.

(20) Silver, L. L. *Expert Opin. Drug Discov.* **2008**, *3*, 487–500.

(21) Silver, L. L. *Clin. Microbiol. Rev.* **2011**, *24*, 71–109.

(22) Münch, D.; Sahl, H.-G. *Biochim. Biophys. Acta - Biomembr.* **2015**, *1848*, 3062–3071.

(23) Typas, A.; Banzhaf, M.; Gross, C. A.; Vollmer, W. *Nat. Rev. Microbiol.* **2011**, *10*, 123–136.

(24) Fleming, A. *Bull. World Health Organ.* **2001**, *79*, 780–790.

(25) Bycroft, B. W.; Shute, R. E. *Pharm. Res.* **1985**, *2*, 3–14.

(26) Spratt, B. G. *Proc. Natl. Acad. Sci. U. S. A.* **1975**, *72*, 2999–3003.

(27) von Nussbaum, F.; Brands, M.; Hinzen, B.; Weigand, S.; Häbich, D. *Angew. Chemie Int. Ed.* **2006**, *45*, 5072–5129.

(28) Taneja, N.; Kaur, H. *Microbiol. insights* **2016**, *9*, 9–19.

(29) Llarrull, L. I.; Testero, S. A.; Fisher, J. F.; Mobashery, S. *Curr. Opin. Microbiol.* **2010**, *13*, 551–557.

(30) Stachyra, T.; Levasseur, P.; Pechereau, M.-C.; Girard, A.-M.; Claudon, M.; Miossec, C.; Black, M. T. *J. Antimicrob. Chemother.* **2009**, *64*, 326–329.

(31) Sohlenkamp, C.; Geiger, O. *FEMS Microbiol. Rev.* **2016**, *8*, 133–159.

(32) Koch, L. A. *The Bacteria: Their Origin, Structure, Function and Antibiosis*, 1st ed.; Springer Netherlands: Dordrecht, 2007.

(33) Silhavy, T. J.; Kahne, D.; Walker, S. *Cold Spring Harb. Perspect. Biol.* **2010**, *2*, a000414.

(34) Zhang, Y.-M.; Rock, C. O. *J. Lipid Res.* **2008**, *50*, S115–S119.

(35) Coates, A. R. M.; Hu, Y. *Trends Pharmacol. Sci.* **2008**, *29*, 143–150.

(36) Epand, R. M.; Epand, R. F.; Rasko, D. A.; Chapman, G. D.; Chute, M. D.; Marston, C. K.; De, B. K.; Sacchi, C. T.; Fitzgerald, C.; Mayer, L. W.; Maiden, M. C.; Priest, F. G.; Barker, M.; Jiang, L.; Cer, R. Z.; Rilstone, J.; Peterson, S. N.; Weyant, R. S.; Galloway, D. R.; Read, T. D.; Popovic, T.; Fraser, C. M. *Mol. Biosyst.* **2009**, *5*, 580.

(37) *Antibiotics*; Gualerzi, C. O., Brandi, L., Fabbretti, A., Pon, C. L., Eds.; Wiley-VCH Verlag GmbH & Co. KGaA: Weinheim, Germany, 2013.

(38) Hsu, S.-T. D.; Breukink, E.; Tischenko, E.; Lutters, M. A. G.; de Kruijff, B.; Kaptein, R.; Bonvin, A. M. J. J.; van Nuland, N. A. J. *Nat. Struct. Mol. Biol.* **2004**, *11*, 963–967.

(39) Biswas, S.; Brunel, J.-M.; Dubus, J.-C.; Reynaud-Gaubert, M.; Rolain, J.-M. *Expert Rev. Anti. Infect. Ther.* **2012**, *10*, 917–934.

(40) Velkov, T.; Thompson, P. E.; Nation, R. L.; Li, J. *J. Med. Chem.* **2010**, *53*, 1898–1916.

(41) Rogers, L. A.; Whittier, E. O. *J. Bacteriol.* **1928**, *16*, 211–229.

(42) Yount, N. Y.; Yeaman, M. R. *Ann. N. Y. Acad. Sci.* **2013**, *1277*, 127–138.

(43) Müller, A.; Ulm, H.; Reder-Christ, K.; Sahl, H.-G.; Schneider, T. *Microb. Drug Resist.* **2012**, *18*, 261–270.

(44) Bierbaum, G.; Sahl, H. G. *J. Bacteriol.* **1987**, *169*, 5452–5458.

(45) Dathe, M.; Wieprecht, T. *Biochim. Biophys. Acta - Biomembr.* **1999**, *1462*, 71–87.

(46) Lohner, K. *Gen. Physiol. Biophys.* **2009**, *28*, 105–116.

(47) Brogden, K. A. *Nat. Rev. Microbiol.* **2005**, *3*, 238–250.

(48) Matsuzaki, K. *Biochim. Biophys. Acta - Biomembr.* **1999**, *1462*, 1–10.

(49) Breukink, E.; De Kruijff, B. *Biochim. Biophys. Acta - Biomembr.* **1999**, *1462*, 223–234.

(50) Sengupta, D.; Leontiadou, H.; Mark, A. E.; Marrink, S.-J. *Biochim. Biophys. Acta - Biomembr.* **2008**, *1778*, 2308–2317.

(51) Rotem, S.; Mor, A. *Biochim. Biophys. Acta - Biomembr.* **2009**, *1788*, 1582–1592.

(52) Jean-François, F.; Elezgaray, J.; Berson, P.; Vacher, P.; Dufourc, E. J. *Biophys. J.* **2008**, *95*, 5748–5756.

(53) Matsuzaki, K.; Murase, O.; Fujii, N.; Miyajima, K. *Biochemistry* **1996**, *35*, 11361–11368.

(54) Casteels, P.; Tempst, P. *Biochem. Biophys. Res. Commun.* **1994**, *199*, 339–345.

(55) Yan, L. Z.; Gibbs, A. C.; Stiles, M. E.; Wishart, D. S.; Vederas, J. C. *J. Med. Chem.* **2000**, *43*, 4579–4581.

(56) Jenssen, H.; Hamill, P.; Hancock, R. E. W. *Clin. Microbiol. Rev.* **2006**, *19*, 491–

511.

(57) Malik, E.; Dennison, S.; Harris, F.; Phoenix, D. *Pharmaceuticals* **2016**, *9*, 67.

(58) Cotter, P. D.; Ross, R. P.; Hill, C. *Nat. Rev. Microbiol.* **2013**, *11*, 95–105.

(59) de Kruijff, B.; van Dam, V.; Breukink, E. *Prostaglandins Leukot. Essent. Fat. Acids* **2008**, *79*, 117–121.

(60) Arnison, P. G.; Bibb, M. J.; Bierbaum, G.; Bowers, A. A.; Bugni, T. S.; Bulaj, G.; Camarero, J. A.; Campopiano, D. J.; Challis, G. L.; Clardy, J.; Cotter, P. D.; Craik, D. J.; Dawson, M.; Dittmann, E.; Donadio, S.; Dorrestein, P. C.; Entian, K.-D.; Fischbach, M. A.; Garavelli, J. S.; Göransson, U.; Gruber, C. W.; Haft, D. H.; Hemscheidt, T. K.; Hertweck, C.; Hill, C.; Horswill, A. R.; Jaspars, M.; Kelly, W. L.; Klinman, J. P.; Kuipers, O. P.; Link, A. J.; Liu, W.; Marahiel, M. A.; Mitchell, D. A.; Moll, G. N.; Moore, B. S.; Müller, R.; Nair, S. K.; Nes, I. F.; Norris, G. E.; Olivera, B. M.; Onaka, H.; Patchett, M. L.; Piel, J.; Reaney, M. J. T.; Rebuffat, S.; Ross, R. P.; Sahl, H.-G.; Schmidt, E. W.; Selsted, M. E.; Severinov, K.; Shen, B.; Sivonen, K.; Smith, L.; Stein, T.; Süssmuth, R. D.; Tagg, J. R.; Tang, G.-L.; Truman, A. W.; Vederas, J. C.; Walsh, C. T.; Walton, J. D.; Wenzel, S. C.; Willey, J. M.; van der Donk, W. A. *Nat. Prod. Rep.* **2013**, *30*, 108–160.

(61) Islam, M. R.; Nagao, J.; Zendo, T.; Sonomoto, K. *Biochem. Soc. Trans.* **2012**, *40*, 1528–1533.

(62) Kruszewska, D.; Sahl, H. G.; Bierbaum, G.; Pag, U.; Hynes, S. O.; Ljungh, Å. *J. Antimicrob. Chemother.* **2004**, *54*, 648–653.

(63) Hsu, S.-T. D.; Breukink, E.; Tischenko, E.; Lutters, M. A. G.; de Kruijff, B.; Kaptein, R.; Bonvin, A. M. J. J.; van Nuland, N. A. J. *Nat. Struct. Mol. Biol.* **2004**, *11*, 963–967.

(64) Hsu, S. T. D.; Breukink, E.; Bierbaum, G.; Sahl, H. G.; De Kruijff, B.; Kaptein, R.; Van Nuland, N. A. J.; Bonvin, A. M. J. J. *J. Biol. Chem.* **2003**, *278*, 13110–13117.

(65) Brotz, H.; Bierbaum, G.; Leopold, K.; Reynolds, P. E.; Sahl, H. *Antimicrob. Agents Chemother.* **1998**, *42*, 154–160.

(66) Martin, N. I.; Sprules, T.; Carpenter, M. R.; Cotter, P. D.; Hill, C.; Ross, R. P.; Vederas, J. C. *Biochemistry* **2004**, *43*, 3049–3056.

(67) Wiedemann, I.; Bottiger, T.; Bonelli, R. R.; Schneider, T.; Sahl, H.-G.; Martinez, B. *Appl. Environ. Microbiol.* **2006**, *72*, 2809–2814.

(68) Turner, D. L.; Brennan, L.; Meyer, H. E.; Lohaus, C.; Siethoff, C.; Costa, H. S.; Gonzalez, B.; Santos, H.; Suárez, J. E. *Eur. J. Biochem.* **1999**, *264*, 833–839.

(69) McClerren, A. L.; Cooper, L. E.; Quan, C.; Thomas, P. M.; Kelleher, N. L.; van der Donk, W. A. *Proc. Natl. Acad. Sci.* **2006**, *103*, 17243–17248.

(70) Navaratna, M. A.; Sahl, H. G.; Tagg, J. R. *Appl. Environ. Microbiol.* **1998**, *64*, 4803–4808.

(71) Roces, C.; Pérez, V.; Campelo, A. B.; Blanco, D.; Kok, J.; Kuipers, O. P.; Rodríguez, A.; Martínez, B. *Antimicrob. Agents Chemother.* **2012**, *56*, 5520–5527.

(72) Cochrane, S. A.; Findlay, B.; Bakhtiary, A.; Acedo, J. Z.; Rodriguez-Lopez, E. M.; Mercier, P.; Vederas, J. C. *Proc. Natl. Acad. Sci.* **2016**, *113*, 11561–11566.

(73) Parenti, F.; Cavalleri, B. *J. Antibiot. (Tokyo).* **1989**, *42*, 1882–1883.

(74) Cavalleri, B.; Parenti, F. *Glycopeptides (Dalbaheptides)*; John Wiley & Sons, Inc.: Hoboken, NJ, USA, 2000.

(75) MCCORMICK, M. H.; MCGUIRE, J. M.; PITTENGER, G. E.; PITTENGER, R. C.; STARK, W. M. *Antibiot. Annu.* **1956**, *3*, 606–611.

(76) Harris, C. M.; Kopecka, H.; Harris, T. M. *J. Am. Chem. Soc.* **1983**, *105*, 6915–6922.

(77) Kahne, D.; Leimkuhler, C.; Lu, W.; Walsh, C. *Chem. Rev.* **2005**, *105*, 425–448.

(78) Hojo, H.; Nakahara, Y. *Biopolymers* **2007**, *88*, 308–324.

(79) Liu, L.; Bennett, C. S.; Wong, C.-H. *Chem. Commun. (Camb).* **2006**, No. 1, 21–

33.

(80) Brocke, C. *Bioorg. Med. Chem.* **2002**, *10*, 3085–3112.

(81) Nakahara, Y.; Hojo, H. In *Experimental Glycoscience*; Springer Japan: Tokyo, 2008; pp 195–199.

(82) Pratt, M. R.; Bertozzi, C. R. *Chem. Soc. Rev.* **2005**, *34*, 58.

(83) Sitrin, R. D.; Chan, G. W.; Chapin, F.; Giovenella, A. J.; Grappel, S. F.; Jeffs, P. W.; Phillips, L.; Snader, K. M.; Nisbet, L. J. *J. Antibiot. (Tokyo).* **1986**, *39*, 68–75.

(84) Malabarba, A.; Strazzolini, P.; Depaoli, A.; Landi, M.; Berti, M.; Cavalleri, B. *J. Antibiot. (Tokyo).* **1984**, *37*, 988–999.

(85) Malabarba, A.; Ferrari, P.; Gallo, G. G.; Kettenring, J.; Cavalleri, B. *J. Antibiot. (Tokyo).* **1986**, *39*, 1430–1442.

(86) Breukink, E.; de Kruijff, B. *Nat. Rev. Drug Discov.* **2006**, *5*, 321–323.

(87) Chatterjee, C.; Miller, L. M.; Leung, Y. L.; Xie, L.; Yi, M.; Kelleher, N. L.; van der Donk, W. A. *J. Am. Chem. Soc.* **2005**, *127*, 15332–15333.

(88) Clardy, J.; Fischbach, M. A.; Walsh, C. T. *Nat. Biotechnol.* **2006**, *24*, 1541–1550.

(89) Donadio, S.; Maffioli, S.; Monciardini, P.; Sosio, M.; Jabes, D. *J. Antibiot. (Tokyo).* **2010**, *63*, 423–430.

(90) Majumdar, R.; Crum-Cianflone, N. F. *Infect. Dis. Clin. Pract.* **2017**, *25*, 176–183.

(91) Park, C. B.; Kim, H. S.; Kim, S. C. *Biochem. Biophys. Res. Commun.* **1998**, *244*, 253–257.

(92) Subbalakshmi, C.; Sitaram, N. *FEMS Microbiol. Lett.* **1998**, *160*, 91–96.

(93) Subbalakshmi, C.; Krishnakumari, V.; Nagaraj, R.; Sitaram, N. *FEBS Lett.* **1996**, *395*, 48–52.

(94) Friedrich, C. L.; Rozek, A.; Patrzykat, A.; Hancock, R. E. *J. Biol. Chem.* **2001**, *276*, 24015–24022.

(95) Haney, E. F.; Petersen, A. P.; Lau, C. K.; Jing, W.; Storey, D. G.; Vogel, H. J. *Biochim. Biophys. Acta - Biomembr.* **2013**, *1828*, 1802–1813.

(96) de Leeuw, E.; Li, C.; Zeng, P.; Li, C.; Buin, M. D.; Lu, W.-Y.; Breukink, E.; Lu, W. *FEBS Lett.* **2010**, *584*, 1543–1548.

(97) Collin, F.; Thompson, R. E.; Jolliffe, K. A.; Payne, R. J.; Maxwell, A. *PLoS One* **2013**, *8*, 1–9.

(98) Del Castillo, F. J.; Del Castillo, I. M. F. *J. Bacteriol.* **2001**, *183*, 2137–2140.

(99) Rebuffat, S. *Biochem. Soc. Trans.* **2012**, *40*, 1456–1462.

(100) Tenover, F. C. *Am. J. Infect. Control* **2006**, *34*, S1–S10.

(101) Abraham, E. P.; Chain, E. *Nature* **1940**, *146*, 837–837.

(102) Francis, J. S.; Doherty, M. C.; Lopatin, U.; Johnston, C. P.; Sinha, G.; Ross, T.; Cai, M.; Hansel, N. N.; Perl, T.; Ticehurst, J. R.; Carroll, K.; Thomas, D. L.; Nuermberger, E.; Bartlett, J. G. *Clin. Infect. Dis.* **2005**, *40*, 100–107.

(103) Tago, Y.; Imai, M.; Ihara, M.; Atofuji, H.; Nagata, Y.; Yamamoto, K. *J. Mol. Biol.* **2005**, *351*, 299–308.

(104) Azeredo da Silveira, S.; Perez, A. *Expert Rev. Anti. Infect. Ther.* **2015**, *13*, 531–533.

(105) Morar, M.; Wright, G. D. *Annu. Rev. Genet.* **2010**, *44*, 25–51.

(106) Wright, G. D. *Adv. Drug Deliv. Rev.* **2005**, *57*, 1451–1470.

(107) Massova, I.; Mobashery, S. *Antimicrob. Agents Chemother.* **1998**, *42*, 1–17.

(108) Mukhtar, T. A.; Wright, G. D. *Chem. Rev.* **2005**, *105*, 529–542.

(109) Donadio, S.; Staver, M. J.; McAlpine, J. B.; Swanson, S. J.; Katz, L. *Science* **1991**, *252*, 675–679.

(110) Ounissi, H.; Courvalin, P. *Gene* **1985**, *35*, 271–278.

(111) Arthur, M.; Autissier, D.; Courvalin, P. *Nucleic Acids Res.* **1986**, *14*, 4987–4999.

(112) Plante, I.; Centrón, D.; Roy, P. H. *J. Antimicrob. Chemother.* **2003**, *51*, 787–790.

(113) Kim, Y. H.; Cha, C. J.; Cerniglia, C. E. *FEMS Microbiol. Lett.* **2002**, *210*, 234–239.

(114) Silver, L. L. *Cold Spring Harb. Perspect. Med.* **2017**, *7*, a025262.

(115) Sahl, H.-G.; Bierbaum, G. *Annu. Rev. Microbiol.* **1998**, *52*, 41–79.

(116) Sun, Z.; Zhong, J.; Liang, X.; Liu, J.; Chen, X.; Huan, L. *Antimicrob. Agents Chemother.* **2009**, *53*, 1964–1973.

(117) Bakhtiary, A.; Cochrane, S. A.; Mercier, P.; McKay, R. T.; Miskolzie, M.; Sit, C. S.; Vederas, J. C. *J. Am. Chem. Soc.* **2017**, *139* (49), 17803–17810.

(118) Cotter, P. D.; Draper, L. A.; Lawton, E. M.; McAuliffe, O.; Hill, C.; Ross, R. P. *Appl. Environ. Microbiol.* **2006**, *72*, 4492–4496.

(119) Lazzarini, A.; Gastaldo, L.; Candiani, G.; Ciciliato, I.; Losi, D.; Marinelli, F.; Selva, E.; Parenti, F. Antibiotic 107891, its factors A1 and A2, pharmaceutically acceptable salts and compositions, and use thereof. WO 2005/014628 A1, 2003.

(120) van der Meer, J. R.; Rollema, H. S.; Siezen, R. J.; Beerthuyzen, M. M.; Kuipers, O. P.; de Vos, W. M. *J. Biol. Chem.* **1994**, *269*, 3555–3562.

(121) Xie, L.; Miller, L. M.; Chatterjee, C.; Averin, O.; Kelleher, N. L.; van der Donk, W. A. *Science* **2004**, *303*, 679–681.

(122) van der Meer, J. R.; Polman, J.; Beerthuyzen, M. M.; Siezen, R. J.; Kuipers, O. P.; De Vos, W. M. *J. Bacteriol.* **1993**, *175*, 2578–2588.

(123) Willey, J. M.; van der Donk, W. A. *Annu. Rev. Microbiol.* **2007**, *61*, 477–501.

(124) Van Kraaij, C.; De Vos, W. M.; Siezen, R. J.; Kuipers, O. P. *Nat. Prod. Rep.* **1999**, *16*, 575–578.

(125) Cotter, P. D.; Hill, C.; Ross, R. P. *Nat. Rev. Microbiol.* **2005**, *3*, 777–788.

(126) Yang, X.; van der Donk, W. A. *ACS Chem. Biol.* **2015**, *10*, 1234–1238.

(127) Donadio, S.; Maffioli, S.; Monciardini, P.; Sosio, M.; Jabes, D. *Appl. Microbiol. Biotechnol.* **2010**, *88*, 1261–1267.

(128) Crowther, G. S.; Baines, S. D.; Todhunter, S. L.; Freeman, J.; Chilton, C. H.; Wilcox, M. H. *J. Antimicrob. Chemother.* **2013**, *68*, 168–176.

(129) Jabes, D.; Donadio, S. *Methods Mol. Biol.* **2010**, *618*, 31–45.

(130) Jabés, D.; Brunati, C.; Candiani, G.; Riva, S.; Romanó, G.; Donadio, S. *Antimicrob. Agents Chemother.* **2011**, *55*, 1671–1676.

(131) Maffioli, S. I.; Potenza, D.; Vasile, F.; De Matteo, M.; Sosio, M.; Marsiglia, B.; Rizzo, V.; Scolastico, C.; Donadio, S. *J. Nat. Prod.* **2009**, *72*, 605–607.

(132) Maffioli, S.I.; Brunati, C.; Potenza, D.; Vasile, F. Lantibiotic carboxyamide derivates with enhanced antibacterial activity. WO20100058238, 2010.

(133) Wang, B.-Y.; Kuramitsu, H. K. *Appl. Environ. Microbiol.* **2005**, *71*, 354–362.

(134) Burton, J. P.; Chilcott, C. N.; Moore, C. J.; Speiser, G.; Tagg, J. R. *J. Appl. Microbiol.* **2006**, *100*, 754–764.

(135) Wescombe, P. A.; Upton, M.; Dierksen, K. P.; Ragland, N. L.; Sivabalan, S.; Wirawan, R. E.; Inglis, M. A.; Moore, C. J.; Walker, G. V; Chilcott, C. N.; Jenkinson, H. F.; Tagg, J. R. *Appl. Environ. Microbiol.* **2006**, *72*, 1459–1466.

(136) Märki, F.; Hänni, E.; Fredenhagen, A.; van Oostrum, J. *Biochem. Pharmacol.* **1991**, *42*, 2027–2035.

(137) Molina y Vedia, L. M.; Stutts, M. J. Method of treating retained pulmonary secretions. US5716931 A, 1995.

(138) Cox, C. R.; Coburn, P. S.; Gilmore, M. S. *Curr. Protein Pept. Sci.* **2005**, *6*, 77–84.

(139) Draper, L. A.; Cotter, P. D.; Hill, C.; Ross, R. P. *Microbiol. Mol. Biol. Rev.* **2015**, *79*, 171–191.

(140) Pag, U.; Sahl, H.-G. *Curr. Pharm. Des.* **2002**, *8*, 815–833.

(141) Siezen, R. J.; Kuipers, O. P.; de Vos, W. M. *Antonie Van Leeuwenhoek* **1996**, *69*, 171–184.

(142) Ross, R. P.; McAuliffe, O.; Hill, C. *Microbiology* **2000**, *146*, 2147–2154.

(143) Kodani, S.; Hudson, M. E.; Durrant, M. C.; Buttner, M. J.; Nodwell, J. R.; Willey, J. M. *Proc. Natl. Acad. Sci.* **2004**, *101*, 11448–11453.

(144) Kodani, S.; Lodato, M. A.; Durrant, M. C.; Picart, F.; Willey, J. M. *Mol. Microbiol.* **2005**, *58*, 1368–1380.

(145) Willey, J. M.; Willems, A.; Kodani, S.; Nodwell, J. R. *Mol. Microbiol.* **2006**, *59*, 731–742.

(146) Ueda, K.; Oinuma, K.-I.; Ikeda, G.; Hosono, K.; Ohnishi, Y.; Horinouchi, S.; Beppu, T. *J. Bacteriol.* **2002**, *184*, 1488–1492.

(147) Hoffmann, A.; Schneider, T.; Pag, U.; Sahl, H.-G. *Appl. Environ. Microbiol.* **2004**, *70*, 3263–3271.

(148) Peschel, A.; Götz, F. *J. Bacteriol.* **1996**, *178*, 531–536.

(149) Altena, K.; Guder, A.; Cramer, C.; Bierbaum, G. *Appl. Environ. Microbiol.* **2000**, *66*, 2565–2571.

(150) Knerr, P. J.; van der Donk, W. A. *Annu. Rev. Biochem.* **2012**, *81*, 479–505.

(151) Delves-Broughton, J.; Blackburn, P.; Evans, R. J.; Hugenholtz, J. *Antonie Van Leeuwenhoek* **1996**, *69*, 193–202.

(152) Wirawan, R. E.; Klesse, N. A.; Jack, R. W.; Tagg, J. R. *Appl. Environ. Microbiol.* **2006**, *72*, 1148–1156.

(153) Van Den Hooven, H. W.; Doeland, C. C.; Van De Kamp, M.; Konings, R. N.; Hilbers, C. W.; Van De Ven, F. J. *Eur. J. Biochem.* **1996**, *235*, 382–393.

(154) Brötz, H.; Josten, M.; Wiedemann, I.; Schneider, U.; Götz, F.; Bierbaum, G.; Sahl, H. G. *Mol. Microbiol.* **1998**, *30*, 317–327.

(155) Breukink, A. E.; Wiedemann, I.; Kraaij, C. Van; Kuipers, O. P.; Sahl, H. *Science (80-.).* **1999**, *286*, 2361–2364.

(156) Wiedemann, I.; Böttiger, T.; Bonelli, R. R.; Wiese, A.; Hagge, S. O.; Gutsmann, T.; Seydel, U.; Deegan, L.; Hill, C.; Ross, P.; Sahl, H. G. *Mol. Microbiol.* **2006**, *61*, 285–296.

(157) Hasper, H. E.; de Kruijff, B.; Breukink, E. *Biochemistry* **2004**, *43*, 11567–11575.

(158) Hsu, S.-T.; Breukink, E.; de Kruijff, B.; Kaptein, R.; Bonvin, A. M. J. J.; van Nuland, N. A. J. *Biochemistry* **2002**, *41*, 7670–7676.

(159) Bonelli, R. R.; Schneider, T.; Sahl, H. G.; Wiedemann, I. *Antimicrob. Agents Chemother.* **2006**, *50*, 1449–1457.

(160) Hasper, H. E.; Kramer, N. E.; Smith, J. L.; Hillman, J. D.; Zachariah, C.; Kuipers, O. P.; de Kruijff, B.; Breukink, E. *Science (80-.).* **2006**, *313*, 1636–1637.

(161) van Heusden, H. E.; de Kruijff, B.; Breukink, E. *Biochemistry* **2002**, *41*, 12171–12178.

(162) Wiedemann, I.; Benz, R.; Sahl, H.-G. *J. Bacteriol.* **2004**, *186*, 3259–3261.

(163) Wiedemann, I.; Breukink, E.; van Kraaij, C.; Kuipers, O. P.; Bierbaum, G.; de Kruijff, B.; Sahl, H.-G. *J. Biol. Chem.* **2001**, *276*, 1772–1779.

(164) Yuan, J.; Zhang, Z.-Z.; Chen, X.-Z.; Yang, W.; Huan, L.-D. *Appl. Microbiol. Biotechnol.* **2004**, *64*, 806–815.

(165) Tiyanont, K.; Doan, T.; Lazarus, M. B.; Fang, X.; Rudner, D. Z.; Walker, S. *Proc. Natl. Acad. Sci.* **2006**, *103*, 11033–11038.

(166) Daniel, R. A.; Errington, J. *Cell* **2003**, *113*, 767–776.

(167) Stein, T.; Borchert, S.; Conrad, B.; Feesche, J.; Hofemeister, B.; Hofemeister, J.; Entian, K.-D. *J. Bacteriol.* **2002**, *184*, 1703–1711.

(168) Dufour, A.; Hindré, T.; Haras, D.; Le Pennec, J.-P. *FEMS Microbiol. Rev.* **2007**, *31*, 134–167.

(169) Chen, P.; Novak, J.; Kirk, M.; Barnes, S.; Qi, F.; Caufield, P. W. *Appl. Environ. Microbiol.* **1998**, *64*, 2335–2340.

(170) Chatterjee, C.; Patton, G. C.; Cooper, L.; Paul, M.; van der Donk, W. A. *Chem. Biol.* **2006**, *13*, 1109–1117.

(171) Szekat, C.; Jack, R. W.; Skutlarek, D.; Färber, H.; Bierbaum, G. *Appl. Environ. Microbiol.* **2003**, *69*, 3777–3783.

(172) Widdick, D. A.; Dodd, H. M.; Barraille, P.; White, J.; Stein, T. H.; Chater, K. F.; Gasson, M. J.; Bibb, M. J. *Proc. Natl. Acad. Sci.* **2003**, *100*, 4316–4321.

(173) Wakamatsu, K.; Choung, S. Y.; Kobayashi, T.; Inoue, K.; Higashijima, T.; Miyazawa, T. *Biochemistry* **1990**, *29*, 113–118.

(174) McClerren, A. L.; Cooper, L. E.; Quan, C.; Thomas, P. M.; Kelleher, N. L.; van der Donk, W. A. *Proc. Natl. Acad. Sci. U. S. A.* **2006**, *103*, 17243–17248.

(175) Morgan, S. M.; O'Connor, P. M.; Cotter, P. D.; Ross, R. P.; Hill, C. *Antimicrob. Agents Chemother.* **2005**, *49*, 2606–2611.

(176) Cotter, P. D.; Deegan, L. H.; Lawton, E. M.; Draper, L. A.; O'Connor, P. M.; Hill, C.; Ross, R. P. *Mol. Microbiol.* **2006**, *62*, 735–747.

(177) Cox, C. R.; Coburn, P. S.; Gilmore, M. S. *Curr. Protein Pept. Sci.* **2005**, *6*, 77–84.

(178) Lohans, C. T.; Li, J. L.; Vederas, J. C. *J. Am. Chem. Soc.* **2014**, *136*, 13150–13153.

(179) Tillotson, R. D.; Wösten, H. A.; Richter, M.; Willey, J. M. *Mol. Microbiol.* **1998**, *30*, 595–602.

(180) Allison, G. E.; Fremaux, C.; Klaenhammer ', A. T. R. *J. Bacteriol.* **1994**, *176*, 2235–2241.

(181) Garneau, S.; Martin, N. I.; Vederas, J. C. *Biochimie* **2002**, *84*, 577–592.

(182) Jeknic, Z.; Holo, H.; Stevanovic, S.; Daeschel, M.; Nes, I. F. *Microbiology* **2001**, *147*, 643–651.

(183) Moll, G.; Ubbink-Kok, T.; Hildeng-Hauge, H.; Nissen-Meyer, J.; Nes, I. F.; Konings, W. N.; Driessen, A. J. *J. Bacteriol.* **1996**, *178*, 600–605.

(184) Twomey, D.; Ross, R. P.; Ryan, M.; Meaney, B.; Hill, C. *Antonie Van Leeuwenhoek* **2002**, *82*, 165–185.

(185) Brötz, H.; Bierbaum, G.; Markus, A.; Molitor, E.; Sahl, H. G. *Antimicrob. Agents Chemother.* **1995**, *39*, 714–719.

(186) Brötz, H.; Sahl, H. G. *J. Antimicrob. Chemother.* **2000**, *46*, 1–6.

(187) Cuozzo, S. A.; Castellano, P.; Sesma, F. J. M.; Vignolo, G. M.; Raya, R. R. *Curr. Microbiol.* **2003**, *46*, 180–183.

(188) Zimmermann, N.; Jung, G. *Eur. J. Biochem.* **1997**, *246*, 809–819.

(189) Galvin, M.; Hill, C.; Ross, R. P. *Lett. Appl. Microbiol.* **1999**, *28*, 355–358.

(190) Ryan, M. P.; Meaney, W. J.; Ross, R. P.; Hill, C. *Appl. Environ. Microbiol.* **1998**, *64*, 2287–2290.

(191) Twomey, D. P.; Wheelock, A. I.; Flynn, J.; Meaney, W. J.; Hill, C.; Ross, R. P. *J. Dairy Sci.* **2000**, *83*, 1981–1988.

(192) Islam, M. R.; Nishie, M.; Nagao, J. I.; Zendo, T.; Keller, S.; Nakayama, J.; Kohda, D.; Sahl, H. G.; Sonomoto, K. *J. Am. Chem. Soc.* **2012**, *134*, 3687–3690.

(193) 'T Hart, P.; Oppedijk, S. F.; Breukink, E.; Martin, N. I. *Biochemistry* **2016**, *55*, 232–237.

(194) Malvern Instruments Limited. *The Working Principle of Isothermal Titration Calorimetry*; 2015.

(195) Mohammadi, T.; van Dam, V.; Sijbrandi, R.; Vernet, T.; Zapun, A.; Bouhss, A.; Diepeveen-de Bruin, M.; Nguyen-Distèche, M.; de Kruijff, B.; Breukink, E. *EMBO J.* **2011**, *30*, 1425–1432.

(196) Pattabiraman, V. R.; McKinnie, S. M. K.; Vederas, J. C. *Angew. Chemie - Int. Ed.* **2008**, *47*, 9472–9475.

(197) Liu, H.; Pattabiraman, V. R.; Vederas, J. C. *Org. Lett.* **2009**, *11*, 5574–5577.

(198) Molenaar, D.; Abee, T.; Konings, W. N. *Biochim. Biophys. Acta - Gen. Subj.* **1991**, *1115*, 75–83.

(199) Langsrud, S.; Sundheim, G. *J. Appl. Bacteriol.* **1996**, *81*, 411–418.

(200) Li, T.; Jiang, L.; Chen, H.; Zhang, X. *J. Mol. Neurosci.* **2008**, *35*, 289–295.

(201) VanNieuwenhze, M. S.; Mauldin, S. C.; Zia-Ebrahimi, M.; Winger, B. E.; Hornback, W. J.; Saha, S. L.; Aikins, J. A.; Blaszczak, L. C. *J. Am. Chem. Soc.* **2002**, *124*, 3656–3660.

(202) Saha, S. L.; Van Nieuwenhze, M. S.; Hornback, W. J.; Aikins, J. A.; Blaszczak, L. C. *Org. Lett.* **2001**, *3*, 3575–3577.

(203) Braun, W.; Wider, G.; Lee, K. H.; Wüthrich, K. *J. Mol. Biol.* **1983**, *169*, 921–948.

(204) Gardner, K. H.; Kay, L. E. *Annu. Rev. Biophys. Biomol. Struct.* **1998**, *27*, 357–406.

(205) Gardner, K. H.; Kay, L. E. *J. Am. Chem. Soc.* **1997**, *119*, 7599–7600.

(206) Ikura, M.; Kay, L. E.; Bax, A. *Biochemistry* **1990**, *29*, 4659–4667.

(207) Sattler, M. *Prog. Nucl. Magn. Reson. Spectrosc.* **1999**, *34*, 93–158.

(208) Evans, G. A. *Cell* **1990**, *61*, 17–18.

(209) Neri, D.; Szyperski, T.; Otting, G.; Senn, H.; Wuethrich, K. *Biochemistry* **1989**, *28*, 7510–7516.

(210) Hilty, C.; Wider, G.; Fernández, C.; Wüthrich, K. *J. Biomol. NMR* **2003**, *27*, 377–382.

(211) Sailer, M.; Helms, G. L.; Henkel, T.; Niemczura, W. P.; Stiles, M. E.; Vederas, J. C. *Biochemistry* **1993**, *32*, 310–318.

(212) Wüthrich, K. *NMR of proteins and nucleic acids*; John Wiley & Sons: New York, 1986.

(213) Güntert, P.; Mumenthaler, C.; Wüthrich, K. *J. Mol. Biol.* **1997**, *273*, 283–298.

(214) Brötz, H.; Bierbaum, G.; Leopold, K.; Reynolds, P. E.; Sahl, H. G. *Antimicrob. Agents Chemother.* **1998**, *42*, 154–160.

(215) Barrett, M. S.; Wenzel, R. P.; Jones, R. N. *Diagn. Microbiol. Infect. Dis.* **1992**, *15*, 641–644.

(216) Trott, O.; Olson, A. J. *J. Comput. Chem.* **2010**, *31*, 455–461.

(217) Pirri, G.; Giuliani, A.; Nicoletto, S.; Pizzuto, L.; Rinaldi, A. *Open Life Sci.* **2009**, *4*, 258–273.

(218) Cochrane, S. A.; Vederas, J. C. *Med. Res. Rev.* **2016**, *36*, 4–31.

(219) Finking, R.; Marahiel, M. A. *Annu. Rev. Microbiol.* **2004**, *58*, 453–488.

(220) Murai, A.; Amino, Y.; Ando, T. *J. Antibiot. (Tokyo).* **1985**, *38*, 1610–1613.

(221) Kato, T.; Sakazaki, R.; Hinoo, H.; Shoji, J. *J. Antibiot. (Tokyo).* **1979**, *32*, 305–312.

(222) Kato, T.; Hinoo, H.; Shoji, J. *J. Antibiot. (Tokyo).* **1978**, *31*, 652–661.

(223) Cochrane, S. A.; Lohans, C. T.; Brandelli, J. R.; Mulvey, G.; Armstrong, G. D.; Vederas, J. C. *J. Med. Chem.* **2014**, *57*, 1127–1131.

(224) Lohans, C. T.; van Belkum, M. J.; Cochrane, S. A.; Huang, Z.; Sit, C. S.; McMullen, L. M.; Vederas, J. C. *ChemBioChem* **2014**, *15*, 243–249.

(225) Chopra, I.; Roberts, M. *Microbiol. Mol. Biol. Rev.* **2001**, *65*, 232–260.

(226) Schulz, W.; Zillig, W. *Nucleic Acids Res.* **1981**, *9*, 6889–6906.

(227) Lin, G.; Ednie, L. M.; Appelbaum, P. C. *Antimicrob. Agents Chemother.* **2010**, *54*, 2258–2261.

(228) Li, T.; Jiang, L.; Chen, H.; Zhang, X. *J. Mol. Neurosci.* **2008**, *35*, 289–295.

(229) Shikanai, T.; Yamamoto, H. *Mol. Plant* **2017**, *10*, 20–29.

(230) Mazurkiewicz, P.; Driessen, A. J. M.; Konings, W. N. *Curr. Issues Mol. Biol.* **2005**, *7*, 7–21.

(231) Sutyak Noll, K.; Sinko, P. J.; Chikindas, M. L. *Probiotics Antimicrob. Proteins* **2011**, *3*, 41–47.

(232) Algburi, A.; Zehm, S.; Netrebov, V.; Bren, A. B.; Chistyakov, V.; Chikindas, M. L. *Probiotics Antimicrob. Proteins* **2017**, *9*, 81–90.

(233) Slonczewski, J. L.; Fujisawa, M.; Dopson, M.; Krulwich, T. A. In *Advances in microbial physiology*; 2009; Vol. 55, pp 1–317.

(234) Vaara, M. *Microbiol. Rev.* **1992**, *56*, 395–411.

(235) Harris, R. K.; Becker, E. D.; De Cabral Menezes, S. M.; Granger, P.; Hoffman, R. E.; Zilm, K. W. *Magn. Reson. Chem.* **2008**, *46*, 582–598.

(236) Thrippleton, M. J.; Keeler, J. *Angew. Chemie - Int. Ed.* **2003**, *42*, 3938–3941.

(237) McKay, R. T. *Annu. Reports NMR Spectrosc.* **2009**, *66*, 33–76.

(238) Hwang, T. L.; Shaka, A. J. *J. Am. Chem. Soc.* **1992**, *114*, 3157–3159.

(239) Delaglio, F.; Grzesiek, S.; Vuister, G.; Zhu, G.; Pfeifer, J.; Bax, A. *J. Biomol. NMR* **1995**, *6*, 277–293.

(240) Johnson, B. A.; Blevins, R. A. *J. Biomol. NMR* **1994**, *4*, 603–614.

(241) PyMOL | pymol.org https://pymol.org/2/ (accessed Dec 5, 2017).

(242) Residue library file - CYANA Wiki http://www.cyana.org/wiki/index.php/Residue_library_file (accessed Dec 5, 2017).

(243) Norris, M.; Fetler, B.; Marchant, J.; Johnson, B. A. *J. Biomol. NMR* **2016**, *65*, 205–216.

(244) Molecular Topology http://www.onemoonscientific.com/nvjChunks/chap09.html (accessed Dec 5, 2017).

(245) Lioux, T.; Busson, R.; Rozenski, J.; Nguyen-Distèche, M.; Frère, J.-M.; Herdewijn, P. *Collect. Czechoslov. Chem. Commun.* **2005**, *70*, 1615–1641.

(246) Alvarez, M.; Granados, R.; Mauleón, D.; Rosell, G.; Salas, M.; Sallés, J.; Valls, N. *J. Med. Chem.* **1987**, *30* (7), 1186–1193.

(247) Tsuda, Y.; Hosoi, S.; Goto, Y. *Chem. Pharm. Bull. (Tokyo).* **1991**, *39*, 18–22.

(248) Olah, G. A.; Surya Prakash, G. K.; Arvanaghi, M. *Synthesis (Stuttg).* **1984**, *1984*, 228–230.

(249) Schneider, T.; Sahl, H.-G. *Int. J. Med. Microbiol.* **2010**, *300*, 161–169.